APPLICATION OF GEOPHYSICAL TECHNIQUES IN THE DELINEATION OF AQUIFER SYSTEMS IN THE BEAUFORT WEST AREA, WESTERN KAROO, SOUTH AFRICA

Fhatuwani Matome Adolph Sekiba

Submitted in fulfilment of the requirements for the degree

Magister Scientiae in Geohydrology

in the

Faculty of Natural and Agricultural Sciences

(Institute for Groundwater Studies)

at the

University of the Free State

Supervisor: Dr F Fourie

Co-supervisor: Dr L Chevallier

May 2019

DECLARATION

I, Fhatuwani Matome Adolph Sekiba, hereby declare that the dissertation hereby submitted by me to the Institute for Groundwater Studies in the Faculty of Natural and Agricultural Sciences at the University of the Free State, in fulfilment of the degree of Magister Scientiae, is my own independent work. It has not previously been submitted by me to any other institution of higher education. In addition, I declare that all sources cited have been acknowledged by means of a list of references.

I furthermore cede copyright of the dissertation and its contents in favour of the University of the Free State.

Fhatuwani Matome Adolph Sekiba

May 2019

ACKNOWLEDGEMENTS

Many people have contributed in variety of ways to fulfil the success of this research study. I would like to send my sincere gratitude.

Firstly I would like to thank the Lord for giving me strength and keeping me in good health through the course of my research.

I would like thank my promoter Dr Francois Fourie for his indebted knowledge and experience in this field. His kind assistance and the long discussion we had on matters concerning the research will not be forgotten.

I am very grateful to Dr Luc Chevallier my co-supervisor for his experience in the field of hydrogeology of the Karoo Supergroup. His always made time available when I needed and gave very well advises to see through the study.

My appreciation to Dr Emmanuel Sakala for always making his professional time available for any help I might request. The time he took to read through the document when it was still at its initial stage will never be forgotten.

I would like thank Dr Doug Cole for his utmost experience on the geology of the Karoo Supergroup.

Sincere appreciation to Mr Emmanuel Chirenje for directing me towards this study and his great advices are well welcomed

I would like to thank Dr Janine Cole for always having her office available for any advice that I may request.

The geophysics team of the Council for Geoscience is thanked for their assistance in acquisition of the geophysical data.

Special thanks Dr David Khoza for his utmost experience with the Magnetotelluric and gladly assisted with data acquisition.

The department of mineral resource provided funding for the research study. Their financial support will greatly be appreciated.

The Council for Geoscience is well thanked for allowing the study to proceed and funded studies through their bursary structure. Gladly appreciate support from the project manager of Karoo deep drilling project.

My Wife and my son who always motivated me to do more even through difficult time, their presence have greatly assisted me to achieve greater heights. I will always be thankful to them

Lastly but not the least, I would like thank my parents for their love and support through my life. My dad Mr N.W. Sekiba always gave me courage to become the man I am today. My mother Mrs M.G. Sekiba even if she has been called to a place of rest has always played a special role in my life (May her soul rest in peace).

TABLE OF CONTENTS

LIST OF FIGURES

LIST OF TABLES

Chapter 1:
INTRODUCTION

1.1 BACKGROUND

The Council for Geoscience (CGS) is conducting a four-year research programme funded by the Department of Mineral Resource (DMR) aimed at better understanding the geo-environmental impact of geo-resources exploratory activity on the Western Karoo aquifer systems. The possibility that exploring for shale gas in South Africa might influence the various aquifer systems and groundwater dynamics in the Main Karoo Basin has raised many environmental concerns. To address these concerns, the CGS is planning to drill a deep borehole and two monitoring boreholes (depth of 700 m) near Beaufort West to investigate the lithology, geological structures and the occurrence and quality of deep groundwater. The study involves a multidisciplinary approach in which geophysics will play a major role, especially in identifying deep aquifers. Challenges associated with the possible contamination of the shallow aquifer system by deep groundwater will also be investigated.

Aquifers are rock types or rock formation that store and transmit water. It is of vital importance to study and understand aquifer system for proper groundwater management. Aquifers can either be of primary (characteristics developed during rock formation and linked to porosity) or secondary (developed due to subsequent processes like fracturing or intrusions) origin. Most of the Karoo basin aquifers are of the secondary type where their water-bearing properties were developed during secondary processes, such as faulting, fracturing and the intrusion of dolerites (Fourie, 2003). The hydrogeological role of the dense Jurassic dolerite intrusions has been demonstrated by Woodford and Chevallier (2002a and b) and Chevallier (2012). The combined use of seismic and high resolution magnetic data may be useful to better understand complex dolerite network of the Karoo (Scheiber-Enslin, *et al* 2014). The dolerites have proved to be good targets for groundwater in the shallowest 300 m of the Karoo formation; however, little or no information about the associated aquifer systems at greater depths is available. Using advanced technology and a holistic research approach, a better understanding of the geological structures and deeper aquifer systems can be obtained.

Existing geophysical techniques, including the magnetic, electromagnetic and resistivity techniques are still being used with varying success to locate groundwater targets in Karoo formations (Fourie, 2003). The magnetic method is used almost exclusively to locate intrusive magmatic bodies (e.g. dolerites), while electromagnetic and resistivity methods are used to map the conductivity and resistivity distributions associated with the subsurface lithologies and structures. These latter

methods offer the potential to detect resistivity/conductivity contrasts associated with possible water-bearing structures such as faults, fractured zones and weathered zones. However, the resolution capabilities of these techniques decrease with depth of investigation, and they are mostly used for investigating the shallow aquifer systems.

The geophysical techniques mostly used for deep (>300 m) investigations are the seismic reflection, time-domain electromagnetic (EM), very low frequency (VLF) and magnetotelluric (MT) techniques. Each of these techniques has its own strengths and weaknesses, as well as external constraints (e.g. costs, external sources of noise).

The current research study focuses on using the magnetotelluric method, in conjunction with airborne magnetic methods, to investigate the deeper aquifer systems in the vicinity of Beaufort West. Combined with drilling information and other geoscientific disciplines such as geology and geohydrology, the recorded geophysical data could assist in constraining the hydrostratigraphy within the study area.

The magnetotelluric method infers the electrical conductivity distribution in the subsurface by simultaneous measurements of the natural electric (**E**) and magnetic (**B**) fields. It depends on the time-varying nature of the Earth's magnetic field which induces electrical (eddy) currents that are detectable as electric field variations at the surface. MT has been used as a powerful tool for deep crustal electrical conductivity investigations, due to its ability to yield conductive information from much greater depths than artificial-source induction (Mohamed, 2002; Bera and Rao, 2012). The technique can be applied in exploration of different geological targets, including groundwater exploration. It is an essential technique for deep investigations in areas where seismic reflection performs poorly.

1.2 AIMS AND OBJECTIVES

The main aim of the current research project is to use geophysics to investigate the deep aquifer system near the town of Beaufort West. The need to understand the deeper aquifer systems arose from the possibility of gas exploration in the Main Karoo Basin at depths exceeding 1 500 m. Geophysics could play a major role in identifying stratigraphic makers (such as the carbonaceous Whitehill Formation, other major contacts), fractures, faults, dolerites dykes and sills and correlating them to possible deep and shallow aquifers. The results obtained from the study could assist in the development of a baseline monitoring programme to investigate the groundwater conditions prior to gas exploration activities. These baseline conditions could be used as the benchmark for future monitoring programmes to detect and evaluate the impacts of gas exploration and/or production.

The objectives of the study are:

- to record and interpret high resolution airborne (magnetic) and ground (magnetotelluric) geophysical data with a specific focus on the geological structures that could have a bearing on the geohydrological systems,
- to use the results of the geophysical investigations to delineate and characterise the aquifer systems,
- to use the gathered information to decide on the position of a deep borehole to intersect the deep aquifer systems,
- to gain further insight into the deep geology of the study area from information collected at the deep drilling site, and,
- to support a multidisciplinary geoscientific approach aimed at delineating the aquifer systems.

1.3 RESEARCH METHODOLOGY

To achieve the aims and objectives of this study, the following research methodology was followed:

- A literature review was done to understand the geology and geohydrology of the Karoo formations, both regionally and within the study area. The literature review also included an overview of the geophysical methods routinely used to investigate and delineate aquifer systems, as well as their advantages and limitations.
- An airborne magnetic survey was performed across the study area. The recorded data were subsequently processed and interpreted in terms of the local geological and geohydrological conditions.
- Based on the results of the airborne magnetic survey, positions for the ground geophysical (magnetotelluric) surveys were identified. However, due to the presence of electromagnetic noise in the form of power-lines and railroads, areas removed from such sources of noise had to be selected. The recorded MT data were processed and interpreted by incorporating all the available geological and geophysical data.
- Based on the results of the geophysical surveys, recommendations for the drilling of deep production and monitoring boreholes were made.
- As part of the investigations, two monitoring boreholes were drilled. However, the positions of these monitoring boreholes were removed by large distances from the positions of the MT surveys. This was due to the fact that the MT surveys had to be located at positions free from EM noise. Geological and geohydrological boreholes logs were compiled during drilling. The

information obtained from these logs was used in conjunction with the geophysical data to make inferences regarding the deep aquifer system in the vicinity of Beaufort West.

1.4 STRUCTURE OF DISSERTATION

The structure of the dissertation is as follows:

Chapter 1: Introduction

This chapter introduces the research framework, aim and objectives, and describes the structure of the dissertation.

Chapter 2: Literature review

This chapter provides a review of the literature relevant to the current investigations. First, an overview of the basic aquifer concepts is given. Next, the geology and the geohydrology of the Karoo formations are discussed. Then the various geophysical methods available for aquifer delineation are described. Brief explanations of the advantages and limitations of the geophysical methods are included. Finally, a few case studies of the application of geophysical techniques to aquifer delineation are discussed.

Chapter 3: Theoretical basis of the magnetotelluric method

Since, in this study, the magnetotelluric method is the geophysical technique used to investigate the deep aquifer systems near Beaufort West; this chapter discusses the theoretical basis of the magnetotelluric method in detail.

Chapter 4: Site description

This chapter describes the physical environment of the study area in terms of its location, geological setting, climatology, topography and drainage, and soil cover.

Chapter 5: Airborne and ground geophysical surveys

The airborne (magnetic) and ground (magnetotelluric) surveys conducted during the current investigations are described in this chapter. The description includes: the survey geometry, equipment used, data acquisition, data processing and the interpretation of the results in terms of the deep aquifer system.

Chapter 6: Drilling of monitoring boreholes

The results of the geological and geohydrological borehole logs compiled during the drilling of the two monitoring boreholes are discussed in the chapter. The drilling results are compared to the geophysical interpretations made from the available data. The lithological information obtained from the geological logs was compared with the lithology interpreted from the geophysical logs.

Chapter 7: Discussion

The results of the of the current investigations are discussed, with a specific reference to the conjunctive use of ground and airborne geophysical data, along with the geological data recorded at the two monitoring boreholes, to detect and delineate the deep aquifer system. Strengths and weaknesses of the methodology followed during this investigation are discussed.

Chapter 8: Conclusions and Recommendations

This chapter concludes the dissertation and gives recommendations for future investigations of the deep aquifer systems in Karoo formations.

Chapter 2:
LITERATURE REVIEW

2.1 INTRODUCTION

In this chapter, a review of the literature relevant to the current study is given. An overview of the basic aquifer concepts is given before the geology and the geohydrology of the Karoo formations are discussed. The various geophysical methods available for aquifer delineation are then described, including the advantages and limitations of these methods. Finally, a few case studies of the application of geophysical techniques to aquifer delineation are discussed.

2.2 BASIC CONCEPTS OF AQUIFERS

2.2.1 Introduction

The nature and distribution of aquifer are controlled by the lithology, stratigraphy and structure of the geologic deposits. The lithology of rocks is defined as the physical make-up of the geological systems (including mineral composition, grain size and packing). Stratigraphy describes the geometry and age relations between various formations in a geological system. Secondary structures such as cleavages, fractures, folds and faults are the geometrical properties of the geological systems produced by deformation after deposition or crystallization. Generally groundwater occurs in pore spaces of consolidated and unconsolidated of sedimentary rocks and weathered zones, in joints and fissures of hard rocks, in fault zones and in karst cavities.

Aquifers can be classified into confined, unconfined, leaky and perched (Figure 2-1). A confined aquifer is usually bounded above and below by an aquiclude, resulting in groundwater being subjected to pressure greater than the atmospheric pressure. An unconfined (water table) aquifer is bounded below by an aquiclude and no confining layer above it. A leaky (semi-confined) aquifer is bounded between confining layers of low permeability material through which recharge or discharge can occur. An aquifer consisting of a small body of groundwater that is separated from the underlying aquifer system by a confining layer is known as perched aquifer.

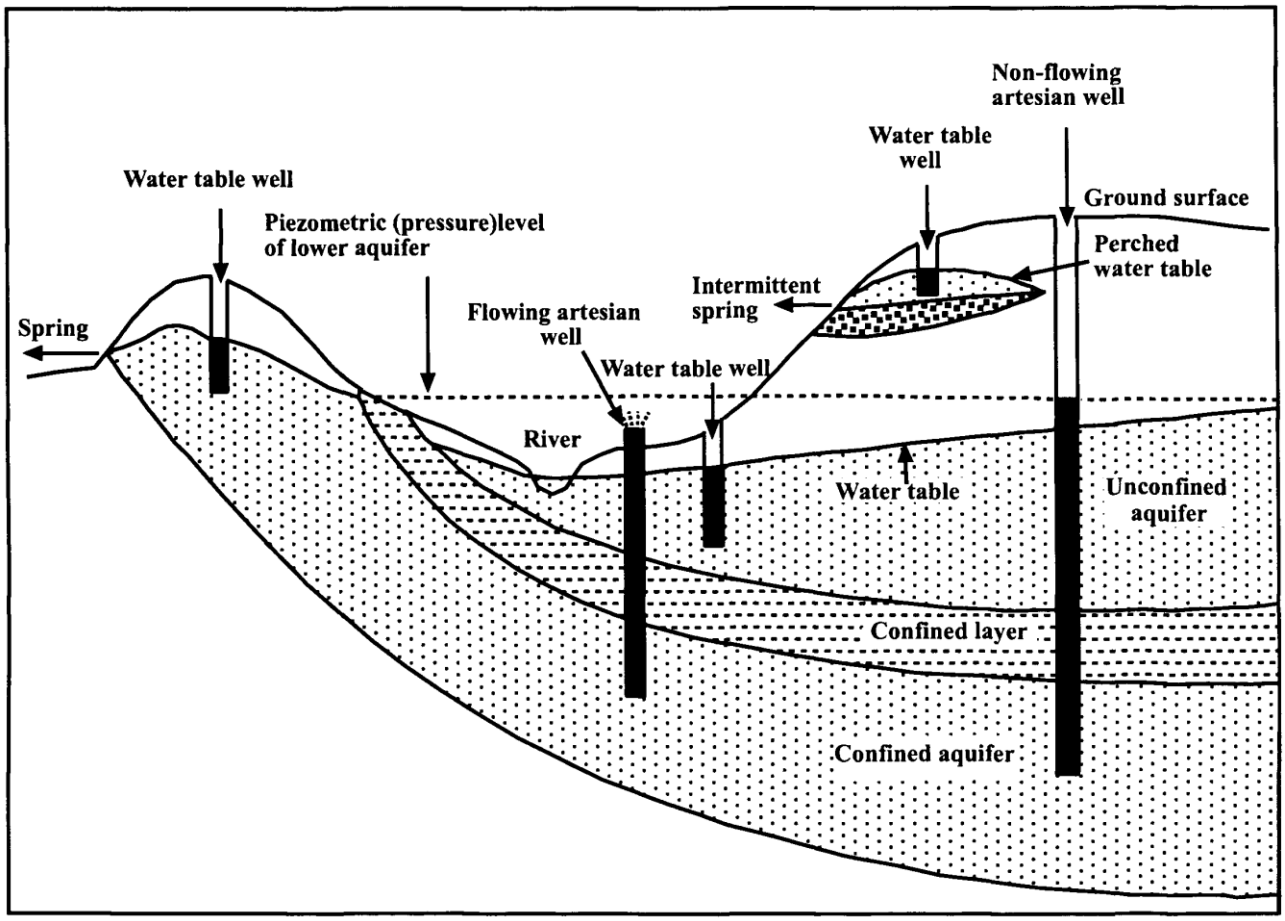

Figure 2-1: Schematic diagram showing different aquifers (Mohamed, 2002 as cited in Brassignton, 1998)

2.2.2 Aquifer properties

Storage and movement of groundwater in aquifer is controlled by some basic hydrological properties such as porosity, permeability, transmissivity, specific yield and storativity. These properties are briefly described below.

2.2.2.1 Porosity and permeability

Porosity is one of the determining factors for hydrogeologic parameter. It is defined as the volume of open space in rocks in relation to the total rock volume. Porosity usually expressed as a decimal fraction or as a percentage, can be defined as in Equation 2-1 (Kruseman and de Ridder, 1994):

$$n = \frac{V_v}{V_T} \qquad \text{Equation 2-1}$$

Porosity can be termed primary if the inherent characteristics developed during formation of rock or secondary if the characteristics are developed due to subsequent processes that occur after the formation of rock. Generally porosity is largely dependent on grain size sorting, such that it decreases with increasing grain size and well sorted material higher porosity than poorly sorted. In

groundwater hydrology porosity is important due to its ability to determine the maximum amount of water a rock can contain when it is saturated (Heath, 1983).

Another determining factor of aquifer properties is the permeability. It is defined as the ease with which water can flow through a geologic formation. Permeability depends on both porosity and pore connectivity, as well as the scale of grain or pore sizes. In some instances permeability is unrelated to porosity in that some rock formations may have high porosity but very low permeability (Mohamed, 2002; as cited in Price, 1985).

Clay rich soils usually have high porosity but very low permeability, due to clay particles been platy with large surface areas causing high molecular forces between the clay and water particles. Of which water is absorbed onto the clay minerals by these forces and therefore prevent free flow under natural conditions (Mohamed, 2002). Rock formations that contain large and small grains usually have low porosities because small grains tend to occupy larger grain voids which are generally interconnected to create higher permeability (Mohamed, 2002). The physical properties of rock change during consolidation because of compaction due to burial depth is shown in Table 2-1, listing porosity and permeability values for some rock formations.

Table 2-1: Variations of porosity permeability values of some rock formations (after Mohamed, 2002, as cited in Brassington, 1998)

Geological Material	Grain Size (mm)	Porosity (%)	Permeability (meters per day)
Clay	0.0005-0.002	45-60	$<10^{-2}$
Silt	0.002-0.06	40-50	10^{-2}-1
Alluvial Sand	0.06-2	30-40	1-500
Alluvial Gravel	3-64	25-35	500-10000
Shale	Small	5-15	$5x\ 10^{-8}$ -$5x10^{-6}$
Sandstone	Medium	5-30	10^{-4}-10
Limestone	Variable	0.1-30	10^{-5}-10
Basalt	Small	0.001-1 (up to 50 if vesicular)	0.0003-3 (secondary permeability)
Schist	Medium	0.001-1	10^{-7}-10^{-4}
Granite	Large	0.001-1(up to 50 if fractured)	0.003-0.03 (secondary permeability)

2.2.2.2 Transmissivity

Transmissivity is defined as the rate of flow of water through a vertical strip of aquifer of unit width and extend the full-saturated height under a hydraulic gradient equal to unity. It is denoted by *T* and expressed in m^2/day (Mohamed, 2002).

2.2.2.3 Storativity and specific yield

Storativity is the volume of water released from storage per unit surface area of the aquifer per unit decline in the component of hydraulic head normal to that surface. The dimensionless storativity ranges in value of confined aquifer from 5×10^{-5} to 5×10^{-3} (Kruseman and de Ridder, 1994). On the other hand, the specific yield is the volume of water that an unconfined aquifer releases from storage per surface area of aquifer per unit decline of water table. The values of specific yield are much higher than those of storativity of a confined aquifer. Both can be determined by means of pumping tests in which boreholes are pumped and the change in water levels measured in one or more nearby observation wells situated at known distances from the pumping well.

2.2.3 Recharge

Groundwater recharge can in very simple terms be defined as water that moves from the unsaturated zone into the saturated zone. The saturated flow between aquifers is excluded in the definition, from which it might be more precisely termed "aquifer system" recharge (Nimmo *et al*, 2005). Aquifer recharge studies are important in understanding the hydrologic cycle and effective water resource management (Nimmo *et al*, 2005). Recharge is an important natural mechanism which replenishes groundwater abstracted from an aquifer to keep regional static water levels (Leketa, 2011). In groundwater modelling recharge has proved to be an important parameter, however since it cannot be measured directly it yields uncertainties in modelling. To obtain information on recharge which provides the basis for groundwater resource management can be through recharge estimation. Aquifer recharge estimation is the most difficult of all measures in the evaluation of groundwater resources, in that estimates are normally and almost inevitably subject to large errors (van Tonder and Kirchner, 1990). Usually recharge estimation rely on a wide variety of models designed to represent the actual physical processes (van Tonder and Kirchner, 1990). There are about six methods currently used as suggested by van Tonder and Kirchner (1990):

- The soil water balance method (soil moisture budget)
- The zero flux plane method
- The one-dimensional soil water flow model
- The saturated volume fluctuation method (groundwater balance)

- Inverse modelling for estimation of recharge (two-dimensional groundwater flow model)
- Isotope techniques and solute profile technique

Generally, rainfall as the principal replenishment of moisture in the soil water system and recharge to groundwater, create large amount of water available for infiltration and runoff. Groundwater recharge mostly occurs during very high soil moisture through downward migration of water in the form of gravity flow. Aquifer recharge is affected by factors such as rainfall, geological environment, evapotranspiration, hydrology, unsaturated zone and flow mechanism. Recharge varies with time and location.

Recharge although usually travels through the unsaturated zone first by various means, may reach the aquifer directly from portions of rivers, canals or lakes (Nimmo *et al*, 2008). In some cases, surface water bodies are not always recharge sources, but may be associated with aquifer discharge. Thus a stream can either be gaining or losing if aquifer discharge or recharge dominates. The recharge within the unsaturated zone at great depth usually may be homogeneous over several years. In order to assess the aquifer vulnerability to contamination, prediction of zones of significant contamination and evaluation of remedial measures it is essential to study the recharging fluxes and their distribution.

As mentioned earlier that recharge is determined by estimation methods, in the Karoo as is the host to the current study the estimation technique is not different to other geological formation, except in case where application of methods relating to the unsaturated zone are limited due to the aquifer only covered by thin layer of soil (Woodford and Chevallier, 2002). Recharge in Karoo aquifers is highly variable due to varying thickness of the soil overburden, rock outcrops, collection of surface water in depressions and surface runoff (Makhokha, 2016). As the preferential recharge areas are generally rock and dolerite outcrops, the most reliable and practical method is the mass balance approach.

2.3 PREDICTING GEOHYDROLOGICAL PARAMETERS USING GEOPHYSICAL INFORMATION

Aquifer properties are strongly correlated to electrical properties and both relate to the pore space structure and heterogeneity. Electrical properties of soils and rocks are closely related to the underlying structure, although solid and aqueous phases of a porous soil/rock system act in a different way electrically. It is vital to note that electrical methods have gained interest for hydrogeological aquifer characterisation, since the in predominantly ion-conductive systems electrical and hydraulic conduction follow similar pathways through the interconnected saturated pores.

Usually aquifer properties are confidently obtained from pump test or laboratory experiments, alternatively in the event that such tests or experiments are unavailable non-invasive geophysical information can be applied. Porosity, for instance, can be determined using Archie's equation. For the case of no borehole data or laboratory measurements, these parameters cannot be determine reliably due to challenges associated with obtaining accurate values of m, ρ_f and also n when the pores are not fully saturated by fluid. The major determinants of rock conductivity/resistivity are the porosity and the conductivity of water (Vozoff, 1990). Thus porosity can be related to electrical resistivity of rocks by Archie's equation (Archie, 1942) as shown in Equation 2-2:

$$\rho_b = \mathrm{k}\rho_f \Phi^{-m} S^{-n} \qquad \text{Equation 2-2}$$

Where ρ_b is the rock resistivity, ρ_f is the resistivity of the pore fluid, Φ is the porosity, m is the cementation exponent, S is the pore saturation and n is the saturation exponent, k is constant (usually has the value of one). In a case if there is no borehole data or laboratory measurements through which accurate values of m, ρ_f and n when the pores are not fully saturated by fluid, it is challenging to derive porosity values from bulk resistivity obtained from inversion model.

2.4 KAROO AQUIFERS

The availability of water especially fresh or potable water has always been vital for basic human needs. Groundwater forms the largest source of available freshwater as most of the water is frozen in glacier and surface water contributes a small percentage (Botha et al, 1998). The surface water resources almost exploited their limits has been strained due to the growing population in South Africa, therefore groundwater resources will have to be greatly utilised as a supplement to the already existing resource as well as to meet the demands of population. Groundwater is found in geological formations that have the ability to store and permit movement of water; those formations are known as aquifers. Other than aquifers groundwater also occurs in aquitard impervious formations that store and permit little or no water movement. Aquicludes are impermeable geological unit that does not transmit water at all. Typical aquifers are mostly unconsolidated sands and gravels, permeable consolidated sedimentary rocks such as sandstones and limestones, and heavily fractured volcanic and crystalline rocks (Kruseman and de Ridder, 1994). The most common aquitards are clays and shales, while aquicludes are dense unfractured rocks (Kruseman and de Ridder, 1994). Many studies have been conducted previously in the Karoo Basin to characterize the aquifer systems to which the information was limited to shallow aquifers, which supply many local communities and farmers with water. To date the shallow aquifers up to depth of about 300 m is well understood due to detailed research and groundwater exploration (by

Department of Water and sanitation (DWS), the Water Research Commission (WRC), Institute for Groundwater Studies (IGS), Council for Geoscience (CGS) and various research organisations).

2.4.1 Hydrogeological stratigraphy of the Main Karoo

The Karoo Supergroup consisting mainly of sandstones, siltstones, shales and mudstone underlies approximately 50% of South Africa; suggestions are therefore made that most aquifers may originate from the Karoo rocks. It is vital to study and understand the aquifer system as it results in proper groundwater management processes. The following paragraphs summarize the hydrogeological stratigraphy of the Main Karoo basin in their chronological order.

Diamictite, shales and tillites of the Dwyka Group have very low hydraulic conductivities and virtually no primary voids and tend to form aquitards than aquifers. This low-yielding fractured aquifer Dwyka Group's water is confined within narrow discontinuities like jointing and fracturing. The late Carboniferous to early Permian Dwyka sediments were deposited during marine conditions therefore water in these aquifers is more saline. Generally the Dwyka Group may not be ideal for the large – scale development of groundwater, however in few localities where sand or gravel were deposited on beaches or where it has been significantly fractured, aquifers may be exploited (Botha *et al*, 1998). SOEKOR deep core boreholes have shown that folded Dwyka rocks in the southern Karoo Basin are well fractured (Woodford and Chevallier, 2002b).

The Ecca Group consisting mainly of shales with varying thicknesses ranging between 1500 m and 600 m south to north, was often overlooked as potential sources of groundwater due to dense shales. Ecca shales in the northern part of the Basin may constitute economically viable aquifers (Woodford and Chevallier, 2002b). Studies have reported sandstones of the Ecca sediments have very low permeabilities due to their poorly sorted and diagenesis lowering primary porosity considerably (Woodford and Chevallier, 2002b as cited in Rowsell and De Swardt, 1976). The Ecca aquifers were expected to be anisotropic due to the Ecca Group's depositional environment been fluvial.

The Beaufort Group deposited in a floodplain has the main sediment source area lying along the southern margin of the Basin and the sedimentary units within it are heterogeneous (Golder Associates, 2011). The Beaufort Group consist of coarser grained rocks near the Cape Fold Belt, whereas mudstone, shale and fine grained sandstone dominate the central and northern part of the Basin. The Beaufort sediments have low primary hydraulic conductivities and since deposited with similar environment as the Ecca Group, expectations were thus their aquifers may also be anisotropic. Due to the complication of the geometry of these aquifers by the migration of braided and meandering streams, it may be considered that these aquifers are multi-layered and – porous

with varying thicknesses. These multi-layered aquifers may cause piezometric pressure to drop faster than less permeable layer when pumped.

The Molteno Formation comprising of pebble conglomerates and coarse-grained sandstones at the base form an ideal aquifer due to their characteristics and depositional history. This applies as well to the sheet like sedimentary bodies that are more persistence than those of the Beaufort Group. The Elliot Formation comprising mostly of red mudstone represents more of an aquitard than an aquifer. However approach to exploiting for groundwater potential is to drill boreholes through the Elliot Formation into the Molteno Formation and pumping of water may be restricted to the more permeable Formation. The Clarens Formation consisting of well-sorted, medium- to fine grained sandstones, deposited as thick consistent layers; it is the most homogeneous Formation in the Karoo Supergroup. The Formation is poorly fractured and has very low permeability despite its relatively high and uniform porosity. Similar to the Elliot Formation, the Clarens Formation may as well be regarded as aquitard.

2.4.2 Basis of secondary type aquifer

The Karoo aquifer system has resulted in a complex and unpredictable behaviour, to which the primary permeability and porosity of the Karoo aquifers were found to be extremely low, leading to many exploration boreholes giving low yields of less than 1 L/s. Collective thoughts found that the Karoo aquifers do not contain large quantities of groundwater, hence the name Karoo a Hottentot word meaning dry (Botha *et al*, 1998). The permeability and porosity were enhanced during secondary processes (like fracturing, intrusion), resulting to many exploration boreholes been of secondary type aquifers and local communities rely on groundwater found in weathered and fractured-rock aquifers (Woodford and Chevallier, 2002a; Rosewarne *et al*, 2013). This has resulted in an assumption that most of South African aquifers are of secondary type where their water bearing properties such as fault, fractures, intrusive dolerites were developed during secondary processes (Fourie, 2003).

Fracture can geologically be defined as a plane along which lithostatic, tectonic and thermal stresses or high fluid pressure has caused a relative partial loss of cohesion in the rock (Pacome, 2010). Fractures form pathways through which groundwater flows. Much of South Africa's aquifer systems are fractured. As such groundwater in the Main Karoo Basin was found to occur in fractured hard rock (with low primary permeability and porosity), (Woodford and Chevallier, 2002a; Botha and Cloot, 2004). These fractured-rock aquifers of the Main Karoo Basin as can be defined as compartmented, sometime semi-confined, has been intruded by vertical and horizontal dolerites which dissect flat-lying sediment, enhancing permeability and porosity (Woodford and Chevallier, 2002b).

2.4.3 Knowledge about deep aquifer within the Main Karoo

Limited information about deeper aquifer formation and potential of groundwater occurrences, as well as possible interconnection to the shallow aquifer systems is known. The little that is known about the groundwater occurrences associated with deeper formations is through few thermal springs and sparse data from some deep exploration wells drilled by SOEKOR (Chevallier person communication). Deep groundwater was intercepted in borehole KL 1/65 with 3 artesian strikes in the Table Mountain Group below the Bokkeveld Group at around 3000 m (between 2999.232 m and 3319.272 m). Deep groundwater was also intercepted in borehole SA 1/66 in the Dwyka at 3150 m. artesian water was intercepted in borehole Vrede 1/66, next to Graaff Reinet at 600 m below dolerite sills (Hill and Chevallier, person communication).

2.5 GEOPHYSICAL METHODS FOR AQUIFER DELINEATION

Applications of geophysical methods include geological, geotechnical, hydrogeological and environmental investigations to characterize the subsurface. It is an indirect method used to identify and model geological strata. It also produces direct and indirect measurements of the physical properties of soil, rock, pore fluid and buried objects. Due to its non-invasive technique to measure subsurface strata it can be used as a tool for mapping groundwater resource as well as groundwater characterization. Geophysical techniques attempt to delineate geological structures in which groundwater can be found or with which groundwater can be associated. Previously geophysical methods on groundwater investigation was used to map geological structures, delineate aquifer boundaries, map fracture zones and chemical pollution plumes, delineate water saturated zones and seepage flow in landslide bodies (Vereecken *et al*, 2005). Advanced technology has focused application of geophysical methods to derive parameters and state variables characterizing aquifer systems. Multi-disciplinary approaches which include geophysics are often required to characterise the aquifer system. Common geophysical techniques used for groundwater investigations are the electromagnetic and electrical resistivity methods, since these methods directly measure variations in the physical properties of the subsurface that may relate to the aquifer properties. As many geophysical methods were applied previously to delineate and characterize the aquifer system, following are brief review their success and limitations.

2.5.1 The magnetic method

2.5.1.1 Introduction

The magnetic method is a potential field where attention is mostly focused on exploiting magnetic minerals (magnetite, pyrrhotite, hematite, ilmanite/titanohematite and maghematite) that occurs in

rocks. Two types of magnetization including induced and remnant that perturb the Earth's primary field. Magnetic rocks contain various combinations of these magnetizations. The magnitudes of these magnetizations depend on the quantity, composition, and size of magnetic-mineral grains. Magnetic method has the ability to directly detect some iron ore deposits and useful in deducing subsurface lithology and structure. The versatile easy to operate magnetic method is a geophysical tool applied to various subsurface exploration problems. The magnetic method maps variations in the magnetic field of the earth which is attributable to changes of structure or magnetic susceptibility in near surface rocks

2.5.1.2 The Earth's magnetic field

The Earth possesses a magnetic field caused primarily by sources in the core (ASCE, 1998). Thus this earth's magnetic field is a resemblance of the field of a large bar magnet situated near the centre of the earth. Most magnetic measurement on the surface of the earth is dominated by the earth's magnetic field. Small-scale magnetic anomalies related with magnetized rocks covers the earth's large-scale magnetic field (Ernstson, 2006) as shown in Figure 2-2.

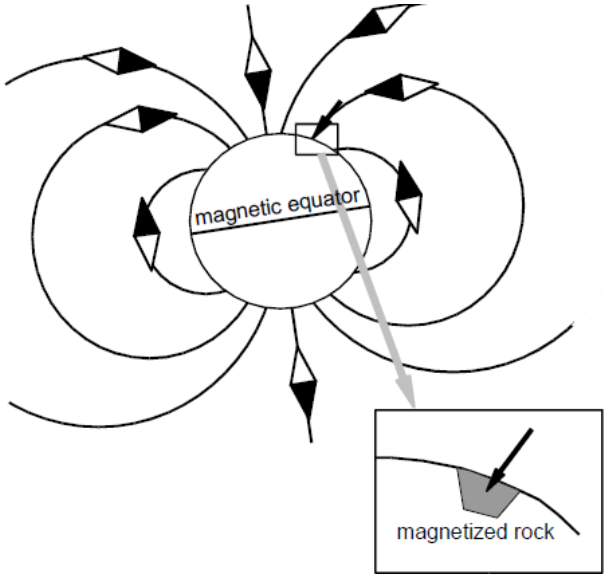

Figure 2-2: The earth magnetic field and the magnetization of rocks (Ernstson, 2006)

2.5.1.3 Induced magnetism and remanent magnetism

The heterogeneity in rocks and their impregnation by ferromagnetic minerals yield random magnetic anomalies. These anomalies are produced by the variation in the intensity of magnetization of rock formations. The magnetization of rocks of the Earth's magnetic field is partly due to induced and remanent magnetization. The induced magnetism of a body is usually in the same direction with the present day earth's field, while remanent magnetism is not in the same

direction and could even oppose the earth's field. The induced magnetism may disappear if the earth's field could be removed, but remanent magnetism will remain.

2.5.1.3.1 Induced magnetism

The magnetic field usually attracts the lines of force towards and into it and takes on the aspects of a magnet with a North and South Pole, when a magnetic material such as soft iron is placed into it. The magnetic field intensify closer to the Poles and intensity is reduced as movement from the poles increases. The induced magnetization can be referred to as a material placed in a magnetic field may acquire a magnetization in the direction of the field and is lost when the material is removed from the field. The degree of induced magnetism is dependent on the earth's field intensity at a particular location and the magnetic susceptibility. The induced magnetization is equal to the product of the volume magnetic susceptibility and the induced field of the earth (ASCE, 1998), as defined by Equation 2-3:

$$I = kF \qquad \text{Equation 2-3}$$

where:

k = volume magnetic susceptibility (unitless)

I = induced magnetization per unit volume

F = field intensity in tesla (T)

.

2.5.1.3.2 Remanent magnetism

The intensity of remanent magnetization depends upon the geological history of the rock. Remanent magnetisation can also be referred to as permanent magnetisation of a material in the absence of an external magnetic field, occurring only in the materials which exhibit hysteresis (Mahanyele, 2010 as cited in Hunt *et al.,* 1994). The remanent magnetism of some rocks and minerals may completely dominate the induced magnetism and can be in a different direction to that of the earth's magnetic field.

Rocks can acquire remanent magnetism by either primary or secondary magnetisations. The process of acquiring primary remanent magnetisations is through cooling and solidification of an igneous rock from the above Curie temperature to normal surface temperature (Reynolds, 2011). For secondary remanent magnetisation (chemical, viscous or post-depositional remanent magnetisation) may be acquired later on in the rock's history (Reynolds, 2011). Typical example of the secondary

remanent magnetisation is the igneous rocks that may have later undergone one or more periods of metamorphism.

2.5.1.4 Magnetic susceptibility

Magnetic susceptibility, as the measure of the degree to which a material can be magnetised, is an important property of rock and minerals. High susceptibility mostly occurs in rocks with significant concentration of ferro –and/or ferromagnetic minerals. Usually ultrabasic and basic igneous rocks have high susceptibility, while acidic igneous and metamorphic rocks have intermediate to low. Sedimentary rocks have generally very low susceptibility. Table 2-2 shows magnetic susceptibility of common rocks.

Primarily the intensity of the induced magnetization is therefore dependent on the magnetic susceptibility and the magnetizing field. Although rock forming minerals reveal a very low magnetic susceptibility, the magnetism of rocks is related to the magnetism of rock-forming minerals

Table 2-2: Magnetic susceptibility of various rock types (after Molaba, 2017, as cited in Telford *et al*, 1990)

Rock Type	Susceptibility x 10^3	
	Range	**Average**
Sedimentary		
Dolomite	0 - 0.9	0.1
Limestone	0 - 3	0.3
Sandstone	0 - 20	0.4
Shale	0.01 - 15	0.6
Average for various	0 - 18	0.9
Metamorphic		
Amphibolite		0.7
Schist	0.3 - 3	1.4
Phyllite		1.5
Slate	0 - 35	6
Gneiss	0.1 - 25	
Quartzite		4
Serpentenite	3.0 - 17	
Average for various	0 - 70	4.2
Igneous		
Granite	0 - 50	2.5
Rhyolite	0.2 - 35	
Dlorite	1 - 35	17
Augite-Syenite	30 - 40	
Olive-diabase		25
Diabase	1 - 160	55
Porphyry	0.3 - 200	60
Gabbro	1 - 90	70
Basalt	0.2 - 175	70
Diorite	0.6 - 120	85
Pyroxenite		125
Peridotite	90 - 200	150
Andesite		160
Average acidic igneous	0 - 80	8
Average basic igneous	0.5 - 97	25

2.5.1.5 Application of the magnetic method in groundwater exploration

Magnetic survey was mainly focused on mineral exploration with little attention for groundwater exploration. However combination of gravity and magnetic methods was used to map regional aquifers and large scale basin features. It was then that magnetic method gained recognition due to its ability to locate and delineate intrusive magmatic bodies. These bodies including contact zones between host rocks and intrusive bodies are considered targets for groundwater exploration.

Tessema *et al* (2010) conducted a magnetic survey in order to map structures and lineaments in Mafikeng, North West Province, South Africa. Using G-856 proton precession magnetometer the spacing between the measurements was 20 m. The positive magnetic intensity identified the presence of dyke, while the negative magnetic intensity detected the presence of reverse magnetization dyke.

Araffa *et al* (2015) used magnetic method to investigate the upper surface of the basement and indirectly thickness of the sedimentary cover in the eastern bank of the Suez canal of northwestern part of Sinai around Al Qantara East. Using Envi-mag proton magnetometer (Scintrex) of sensitivity 1nT, about fifty seven ground magnetic stations have been measured covering the study area. The high magnetic intensity was associated with thin sedimentary cover and shallow basement relief. The low magnetic intensity which is a high frequency may be related to thick sedimentary cover and deep basement relief. In order to estimate the depth of the magnetic bodies the 2D magnetic modelling was carried out. The result estimated the depth to the basement to be very deep.

For the recent developments of shale gas exploration information obtained from magnetic method may become useful to detect shallow dykes that can extend to reservoir depth and was difficult to interpret using seismic data (Scheiber-Enslin, *et al* 2014).Thus the magnetic method has always been useful in locating and delineating these intrusive dolerite bodies which plays a major role in groundwater exploration, however in the absent of such bodies magnetic data is of little use. The magnetic method estimates the depth to the subsurface information; as such the depth cannot be confidently trusted as the true representation of the subsurface if no apriori information is available.

2.5.2 The gravity method

2.5.2.1 Introduction

The gravity method depends on the density contrast of earth's material; i.e. gravity surveying is only useful if the structure investigated involves bodies of different densities with the host rock. Assuming the Earth's materials were layered horizontally with uniform density, there would be no

density contrasts. They are however a number of different factors that control density contrast; these are grain density of particles forming the material, porosity of the material and the interstitial fluids within the material.

2.5.2.2 Basic principle of the gravity method

Gravity method is based on Newton's law of gravitation which states that "force of attraction between two particles of mass is directly proportional to the product of the masses and inversely proportional to the square distance between them" (Gordon-Welsh, 1981), this law can be expressed by Equation 2-4:

$$F = G\frac{m_1 m_2}{r^2}, \qquad G = 6.67 \times 10^{-11} \qquad \text{Equation 2-4}$$

Where:

F = the force of attraction between the two particles of mass

M_1 = the mass of the first particle of mass

M_2 = the mass of the second particles of mass

R = the distance separating the centre of mass of the two particles of mass

G = gravity constant

The gravity method is a non-destructive potential field method that measures variations in the Earth's gravitational field. The gravity method is based on the principle that the lateral density changes in the subsurface cause a change in the force of gravity at the surface. Generally, gravity surveys may detect natural or man-made voids, variation in the depth to bedrock and geological structures of engineering interest. Measurements can be taken from the surface of the Earth or from aircraft or ships. The success of the gravity readings depends on the density contrast of the Earth's material. Gravity surveys are only useful if the structure investigated involves bodies of different densities within the host rock. Assuming the Earth's materials were layered horizontally with uniform density, there would be no density contrasts.

Gravity surveying is sensitive to variations in rock density and density contrast is affected by factors including the grain density of the particles forming the material, porosity of the material and the interstitial fluids within the material. Figure 2-3 shows bulk density ranges for selected rock types.

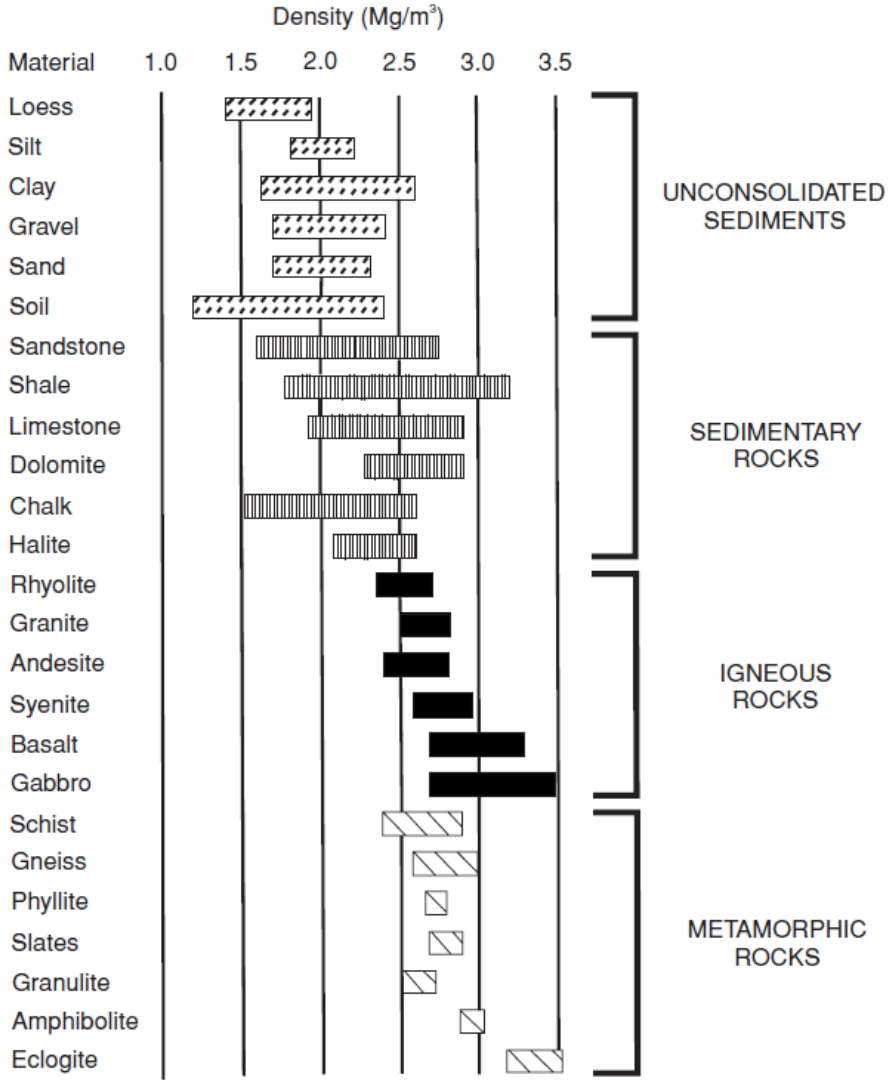

Figure 2-3: Variations in rock density of different rock types (Reynolds, 2011, as cited in Telford *et al.*, 1990)

Sedimentary rocks are generally the least dense. Density in sedimentary rocks is affected by factors such as composition, cementation, age and depth of burial, tectonic processes, porosity and pore-fluid type (Reynolds, 2011). In igneous rocks, density increases with decreasing silica content. As such, basic rocks are denser than silicic rocks and plutonic rocks tend to be denser than their volcanic equivalents (Reynolds, 2011). Metamorphic rocks show increasing density with decreasing in silicate minerals and with an increasing grade of metamorphism.

2.5.2.3 Gravity reduction

The raw gravity data have to be corrected before interpretation in geological terms can commence. The correction process known as gravity reduction removes the effects of features that are not of geological interest. Reduction includes instrument drift, latitude, free-air and Bouguer slab corrections. The data reduction for a small to medium sized gravity survey, meaning a survey where it is possible to read the base every hour, is not as complicated as for a large survey stretching over several square kilometres and several days.

2.5.2.3.1 Instrument drift

Gravimeter readings change with time due to elastic creep in the spring which produces an apparent change in gravity at a given station (Reynolds, 2011). To overcome these changes, measurements should be repeated at the same stations at different times to determine the instrument drift. The net result of drift is that, over a period (days or hours), repeated readings at the same station will give a series of different gravity values. In order to compensate for the drift, the survey line must always be closed at the starting station, referred to as the base station. The drift per minute can be calculated using the following formula in Equation 2-5:

$$D = K \times \left(\frac{B_2 - B_1}{T_2 - T_1}\right) \qquad \text{Equation 2-5}$$

Where:

D = Drift in milligal/min, where 1 gal = 1 cm/s2

K = Gravimeter constant

B_2 and B_1 = Beginning (B_1) and end (B_2) of gravimeter readings at the base station

T_2 and T_1= Beginning (T_1) and end (T_2) time readings at the base station.

The drift correction is then applied to all the readings of the survey line to correct them for the drift, using Equation 2-6:

$$DS = D \times (T_s - T_B) \qquad \text{Equation 2-6}$$

Where:

DS = Drift at station

D = Drift per minute

T_S = Time at station

T_B = Time at base station

2.5.2.3.2 Latitude correction

The Earth's shape has an influence on the variety of the values of acceleration due to gravity over the surface of the Earth (Reynolds, 2011). Centrifugal acceleration exists due to the rotation of the Earth, maximum at the equator and zero at the poles that opposes the gravitational acceleration. Polar flattening, however, increases the gravity at the poles. The latter effect is partly counteracted

by the increased attracting mass at the equator. It is thus necessary to apply a latitude correction in cases of any appreciable north–south excursions of the grid stations.

The latitude must be known to calculate the theoretical absolute gravity value. Thus, the latitude correction is calculated by subtracting the theoretical gravity using the International Gravity Formula from the observed value, as follows (Equation 2-7):

$$g_{teo}^{ABS} = 978.0318 \times 1000 \times (1 + 0.005304 \times \sin^2(\phi)) - (0.0000058 \times \sin^2(2\phi)) \quad \text{Equation 2-7}$$

Where:

g_{teo}^{ABS} = Theoretical absolute gravity value in milligal

ϕ = Latitude of the station in radians.

The latitude correction can be made simpler for small scale surveys which extend over a total latitude range of less than one degree and that are not tied to the absolute gravity network.

2.5.2.3.3 Free-air and Bougeur correction

Free-air correction makes allowance for the reduction in magnitude of gravity with height above the geoid, regardless of the nature of the rock below (Reynolds, 2011). This correction can be defined as the difference between gravity measured at sea-level and at an elevation with no rocks between. Free-air correction accounts for the elevation of the gravimeter station above sea-level using the expression in Equation 2-8:

$$g_{boug} = 0.3086 \times h \quad \text{Equation 2-8}$$

Where:

h = height above sea-level in meters.

The gravitational attraction of the material between the observation point and the datum must now be taken into account. An observation point located at an elevation above the datum will have more mass underneath it than an observation point at the datum. Although the topography in reality does not have a uniform thickness, the Bouguer slab correction approximates the excess mass between the datum and the observation point by a slab of constant density and thickness. This approximation works well as a first step to correct for topographic effects, since the gravitational attraction is inversely related to the square of the distance to the source. The Bouguer slab correction can be calculated using the following Equation 2-9:

$$g_b = 0.04193 \times \rho \times h(mGal) \quad \text{Equation 2-9}$$

Where

ρ is the average density of the slab in g/cm^3

h is the thickness of the slab (elevation difference between the datum and the observation point) in metres.

An average density of 2.67 g/cm^3 was used for the Bouguer slab correction calculation.

2.5.2.4 Application of the gravity method in groundwater studies

Gravity surveys are useful in determining the regional structures associated with groundwater aquifers or petroleum traps. This method has also been used to obtain information about the bedrock depths and top of rock. Gravity and magnetic methods can be used to complement one another in that a denser material may be high magnetic, i.e. intrusive dolerite bodies.

The gravity method was used by Chandler (1994) to investigate the thickness and potential ground-water resources of the Quaternary and Cretaceous fill in Rock County, Minnesota. The survey was conducted on eleven profiles of about 190 gravity stations. The results deduce that gravity method was found to be an effective reconnaissance-scale tool for groundwater exploration

Generally gravity method in groundwater exploration detects structural trends controlling the regional geometry of the groundwater aquifers (Araffa *et al*, 2015 as cited in Murty and Raghavan, 2002). For the same reason Araffa *et al* (2015) used gravity method to determine the structural elements affecting the subsurface layers on their study area. They carried out about sixty three gravity stations using Auto-grav (CG3) gravimeter of sensitivity of 0.01 mGal. The results show the inference of faults from the residual anomaly map.

Gravity and magnetic methods detect only lateral contrasts in density or magnetization, respectively. In contrast, electrical and seismic methods can detect both vertical and lateral subsurface information. Similar to the magnetic method, the gravity method estimates the depth to the subsurface information through modelling; as such the depth remains uncertain as the true representation of the subsurface if no apriori information is available.

2.5.3 The resistivity method

2.5.3.1 Introduction

Electrical resistivity method as one of the oldest and most commonly used geophysical exploration technique provide cost-effective answers to geological, geohydrological and engineering questions. Furthermore besides surveys on the land surface it can also be used across boreholes and in aquatic

areas. The direct current resistivity is an active geophysical method which is based on the behavioural subsurface flow of electrical current, and it is possible to control depth of investigation since it uses artificial energy source.

2.5.3.2 Basic principles of the resistivity method

To understand the concept of electrical resistivity in geophysics may be through the context of current flow through a subsurface medium consisting of layers with different resistivity contrast (Herman, 2001). Ohm's law which governs the flow of current in the ground is fundamental physical law used in resistivity surveys. Ohm's law which states that the potential difference across an ideal conductor is proportional to the current flowing through it, is given by Equation 2-10

$$V = IR \qquad \text{Equation 2-10}$$

Where V = the potential difference,

I = electrical current and

R = electrical resistance.

If an electrical uniform cube of length L through which a current I is passing is considered, the material within the cube resists the conduction of electricity through it which results in potential a drop V between opposite faces. Therefore the resistance is proportional to the length L of the resistive material and inversely proportional to the cross-sectional area, is given by Equation 2-11:

$$R = \rho \frac{L}{A} \qquad \text{Equation 2-11}$$

The resistivity of the material, an intrinsic property of the material, is then related to experimentally measure extrinsic parameters by Equation 2-12:

$$\rho = \frac{V}{I}\frac{A}{L} \qquad \text{Equation 2-12}$$

For this Equation 2-12 the product of the apparent resistance and geometry factor carrying information about the geometry of the cylinder provides the resistivity. To succeed at an expression for the resistivity that is not as geometrically simple as the uniform cylinder has proved to be challenging. The simplest case is the homogeneous subsurface (Figure 2-4), in which current flows radially away from a single electrode and the potential varies inversely with the distance from the current source (Herman, 2001).

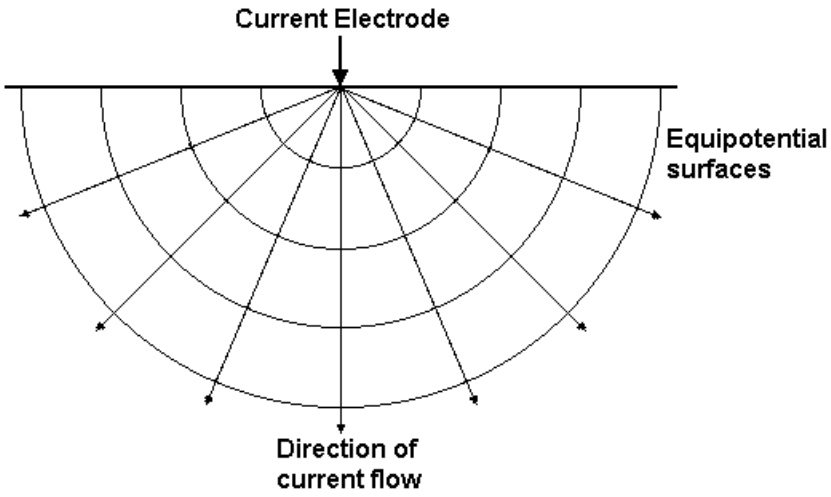

Figure 2-4: Current flow and equipotential surfaces in a level field with homogeneous subsurface structure (Herman, 2001)

Electrical surveys deduce the subsurface resistivity distribution by making measurements on the ground surface. From these measurements, the true resistivity of the subsurface can be estimated. The ground resistivity is related to various geological parameters such as the mineral and fluid content, porosity and degree of water saturation in the rock. When conducting resistivity surveys, assumptions are that the medium being measured is not a homogeneous, isotropic earth. Therefore measurements are normally made by injecting known current through one pair of electrodes (current electrodes) into the ground and the potential established in the earth by this current is measured with the second pair of electrodes (potential electrodes) as shown in Figure 2-5.

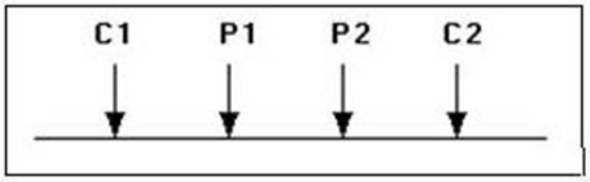

Figure 2-5: Illustration of electrode configuration as used in resistivity survey to measure subsurface resistivity

The ratio of the measured potential compared with the potential (theoretical potential) that would have been observed in a homogeneous, isotropic earth is called apparent resistivity (Botha *et al*, 2001). The formula that converts current and potential measurements into an apparent resistivity is given by Equation 2-13:

$$\rho_a = k\frac{\Delta V}{I} \qquad \text{Equation 2-13}$$

where:

ρ_a = apparent resistivity

k = geometric factor

V = potential

I = current

2.5.3.3 Electrode geometry

Arrangements of the current and potential electrodes (arrays) may be used in several ways, with the spacing chosen to match the needs of particular survey site. Each of these electrode configurations have their own advantages and disadvantages depending upon the type of survey to be performed. The suitability of an array depends on many factors such as sensitivity to the target of interest, signal -to -noise ratio, depth of investigation; lateral data coverage and efficiency affect the array. Most commonly used arrays in practice for 2-D imaging surveys are Wenner, dipole-dipole, and Schlumberger (Figure 2-6). When choosing best array to be used for the field survey the following characteristics should be considered:

- The array sensitivity to vertical and horizontal changes in the subsurface resistivity,
- Depth of investigation,
- Horizontal data coverage, and,
- Signal strength.

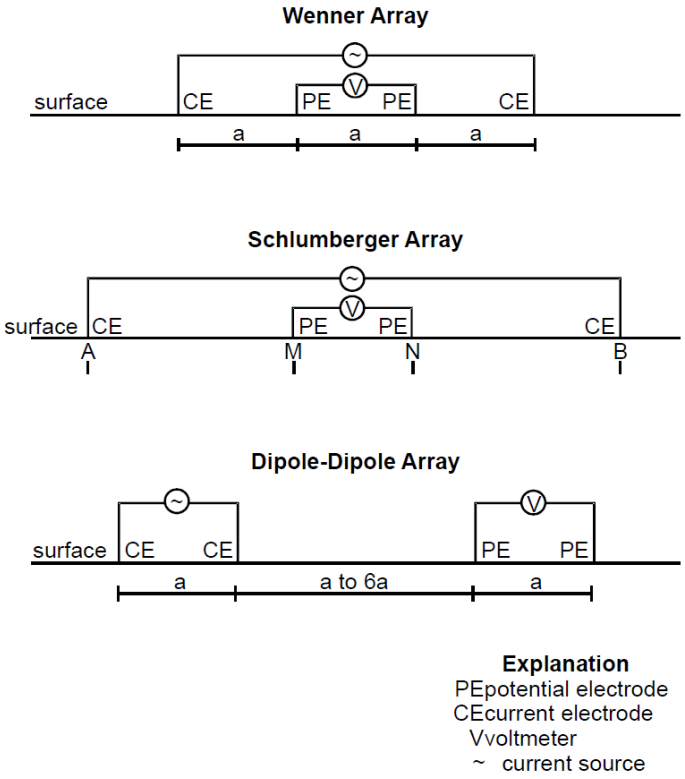

Figure 2-6: Common arrays used in resistivity surveys

The robust Wenner array consist of four electrodes of equal interval and its geometric factor is smaller than other arrays. This array with the strongest signal strength is mostly preferred in mapping horizontal structures. Its limitation is in poor resolving of vertical structures and poor horizontal coverage. Dipole – dipole array uses dipoles to measure the curvature of the potential field. The array is good mapping vertical structures and has better horizontal data coverage. Its disadvantage is the very small signal strength and the insensitivity to vertical changes in resistivity. Schlumberger array is mostly used for resistivity sounding surveys. The array is moderately sensitive to both horizontal and vertical structures. It has smaller signal strength than Wenner, but higher than the dipole-dipole array.

2.5.3.4 Depth of investigation

The depth of investigation in practice using the standard four electrodes depends on the distance between the electrodes and a particular electrode array used. The most robust estimate is the median depth of investigation, which is the depth above which the area under the curve is equal to half the total area under the curve (Loke, 2014). This tells us the depth into which a particular array can obtain. The actual depth of investigation could differ if large resistivity contrast exists near the surface.

2.5.3.5 Electrical resistivity survey

Resistivity surveys can either be conducted by vertical electrical sounding (VES) which is the distribution of electrical resistivity with depth is studied by progressively increasing the depth of investigation, or horizontal profiling which is the lateral distribution of electrical resistivity is studied by an electrode array where the depth of investigation remains constant.

For sounding either Schlumberger or less effectively Wenner may be used, since all commonly available interpretation methods are based on the two arrays. During the VES survey on either array the center point is kept at a fixed location, while the electrode locations are varied around it. Thus the center point serves as the reference for the interpreted apparent resistivity and layer depths. As the distance between the current electrodes is increased, the depth to which current penetrates also increases.

Horizontal profiling can be useful for the investigation of any geological feature that can be expected to offer resistivity contrast from the surrounding. The profiling mode means moving the array along a line of traverse, although horizontal variations may also be investigated by individual measurement made at the points of a particular grid.

2.5.3.6 Application of the resistivity method in groundwater studies

In groundwater exploration, resistivity method has been widely used based on the success that electrical properties are often correlated to properties that are critical to aquifer systems. The electrical resistivity which largely depends on its porosity and salinity of water in the pore space is often useful for determining shallow and deep geological and hydrogeological conditions.

Vertical electrical sounding (VES) was acquired to detect the Nubian sandstone aquifer in the eastern part of Sinai (Araffa and Pek, 2014). About seven deep vertical electrical soundings were measured using Schlumberger configuration with spacing between current electrodes ranging from 5 m to 3000 m. One of the VES was acquired near the borehole to calibrate the model of resistivity data with borehole results. The following were the findings of the VES data calibrated by the borehole results:

- According to borehole data the first layer up to the depth of 30 m was interpreted as wadi deposits
- The fourth geoelectrical unit represent by the second layer up to depth of 80 m was related to cherty limestone
- The third layer of less resistivity value was associated with shale layer
- Chalky limestone and shale at depth ranging from 80 m to 110 m represent the fourth layer
- Dolomitic limestone at depth of 380 m represent the fifth layer
- At depth ranging from 380 m to 845 m is the Nubian sandstone aquifer representing the sixth layer

There was a good correlation between the results of the resistivity data with those of the borehole data, in that the interface depths between different geological units coincided. Other six VESes were represented by geoelectrical cross section.

Sakala and Sekiba (2017) used geophysical methods to identify various geological structures (dykes, geological contacts, and fractures) and lithologies that could control groundwater occurrences in different geological environments. The electrical resistivity of any material as largely dependent on its porosity and salinity of water in pore spaces was one of the geophysical methods used. The authors employed vertical electrical sounding to acquire resistivity data using an iris syscal pro resistivity meter. A Schlumberger configuration with current electrode spacing

ranging from 2 m to 800 m was used to acquire a total of 38 soundings of varying geological conditions. The following was deduced:

- Eight characteristic resistivity-depth curves types were identified; four for the sites surveyed in basement and volcanic terrain and the other four for consolidated sediment terrain
- Generally the VES sites located in basement terrain fit well a six layered earth model with increasing resistivity with depth
- The VES data acquired in areas hosted by consolidated sediments fitted with five layered earth models with decreasing resistivity values with depth.
- Some sites surveyed in the Shire River Basin Plains had a very low resistivity zones (less than 10 Ohm*m) at depth probably depleting salinity conditions within the subsurface.

Due to its ability to map subsurface resistivity distribution, van Zijl (2006) used resistivity method as a way to complement the seismic reflection study by SOEKOR especially in areas intruded by dolerites. A good physical contact between current electrodes and the earth is necessary in order to force large enough current into the earth. The resistivity method is also challenged to locate Karoo aquifers due to lack of contrast between the surrounding rock and fractured zone (Fourie, 2003). Another challenge with the resistivity method is that it requires longer cables and the capability of resistivity meter for deeper probing.

2.5.4 Seismic methods

2.5.4.1 Introduction

Seismic methods are based on the propagation of elastic wave in the earth generated through the seismic source at the land surface to return to the surface after reflecting or refraction off of geologic layers and features at depth. The returned signal is measured in units of elapsed travel-time, typically microseconds to seconds. Seismic reflection profiles models changes in acoustic impedance and is used to construct profile of the reflected images in the subsurface as well as it provide fine structural detail. Seismic energy is refracted and diffracted at boundaries in the subsurface where a significant velocity contrast exists. A Seismic refraction model is created using travel-time of the first arrival and provide precise estimates of depth to lithologies of differing acoustic impedance. The method is challenged to shallow application where low-velocity layers may be encountered. To overcome the challenge, seismic reflections occur owing to changes in the elastic impedance of the medium, product of velocity and density in a layer. Therefore detecting low-velocity layers and density changes can be possible provided the wavelength of seismic signal

is small compared to the layered structure. This method have received limited utilization due to the challenge in acquiring, processing and interpreting the seismic data, particularly in strongly faulted and mafic igneous intrusions, as well as its high cost constraint.

2.5.4.2 Basic principle of seismic methods

The seismic refraction survey measures the travel time of direct and refracted acoustic waves travelling from the surface through one layer to another and back to the surface where the first arrivals are recorded. The seismic refraction survey is mostly used as it is easy to determine the P-wave. This method is also used to study the water table, for engineering purposes, to identify poorly consolidated layer near the ground surface and determining near-surface corrections for deep reflection traces. This kind of survey is primarily applied for determining depth and thickness of geologic layers. The depths of measurements can be shallow or deeper depending on the source of energy. The seismic refraction survey uses the change of direction to derive subsurface information, which can be obtained when seismic energy travelling in a straight line strikes two media of different seismic properties at an angle. Therefore the arrival time of the first impulses from a shot at a set of detectors (geophones) is then recorded. Refraction measurements require that the geophones and the energy source be in contact with the ground. These measurements are sensitive to acoustic noise and vibrations. The method is limited to detecting thin layers.

2.5.4.3 Application of seismic methods in groundwater studies

In groundwater exploration seismic velocities are dependent on aquifer properties and state variables. Temporal groundwater variations can be monitored by detecting associated changes in seismic velocity. The success of the seismic methods was generally on mapping water table depth in aquifers. Detecting near-surface water has since be a challenge due to elastic properties of sediments exceeding any perturbations caused by the presence of water (Vereecken *et al*, 2005). Mafic intrusion such as dolerite dykes and sills are characterized by high velocity P-wave ranging from 5 to 7 km/s (Planke *et al*, 2014). These intrusion being very hard and brittle results in poor signal to noise ratio for deep reflectors due to seismic energy reflected back from shallow dolerite sill boundaries, while sills on the other hand has led into interpretation difficult due to producing stronger reflections than sediments (Fatti, 1970 and Fatti, 1987). However conventional seismic reflection data may detect a 10 m thin sill, while sills with thickness of about 40 m can be resolvable (Planke *et al*, 2014). The geometry of the sill a factor that influence seismic imaging can be mapped with seismic method, but shallow dykes and sills remains difficult to identify (Scheiber-Enslin *et al*, 2014). In contrast with seismic data unable to image dykes, high resolution magnetic data may be the answer.

2.5.5 The electromagnetic method

2.5.5.1 Introduction

Electromagnetic (EM) methods are the most useful geophysical techniques that maps variation in electrical properties, in which the main physical property is the inductive electrical conductivity. The inductive electrical conductivity is the measure of the ease with which current pass through a material. The EM method operates in a manner that the transmitter coil radiates an electromagnetic field which generates eddy currents in the subsurface; the eddy current further generates secondary electromagnetic field, which is then intercepted by a receiver coil (EPA, 1997). The receiver coil measures the voltage which is related to the subsurface conductivity. The conductivity is complex function which is depended on the conductivity of solid material, conductivity of pore fluids, porosity, arrangement of pores and the degree of saturation

2.5.5.2 Basic principle of electromagnetic method

The electromagnetic method uses the ground response to move through the electromagnetic fields made up of two vector components (electric intensity and magnetising force), in a plane perpendicular to the direction of travel (Keary *et al*, 2002; Reynolds, 2011). To generate electromagnetic field can be possible by permitting alternating current through either a small coil containing many turns of wire, or a large loop of wire. Generally the primary electromagnetic field travels from a transmitter coil to a receiver moving through above and below the surface. In homogeneous media no difference between the fields propagated above surface and through the ground can be revealed other than a slight reduction in amplitude of the latter with respect to the former. If the ground contains a conductive media, this results in the magnetic component of the incident electromagnetic wave inducing eddy current within the conductor. It is then that eddy currents generate their own secondary fields detected by the receiver (Figure 2-7). Similarly the primary field travelling through the air is also detected by the receiver which will then have the response of the receiver as the combined effect of both primary field and secondary field. However the measured response differs in both phase and amplitude relative to the unmodulated primary field. Vital information about the geometry, size and electrical properties of any subsurface conductor is revealed by the degree to which these components differ.

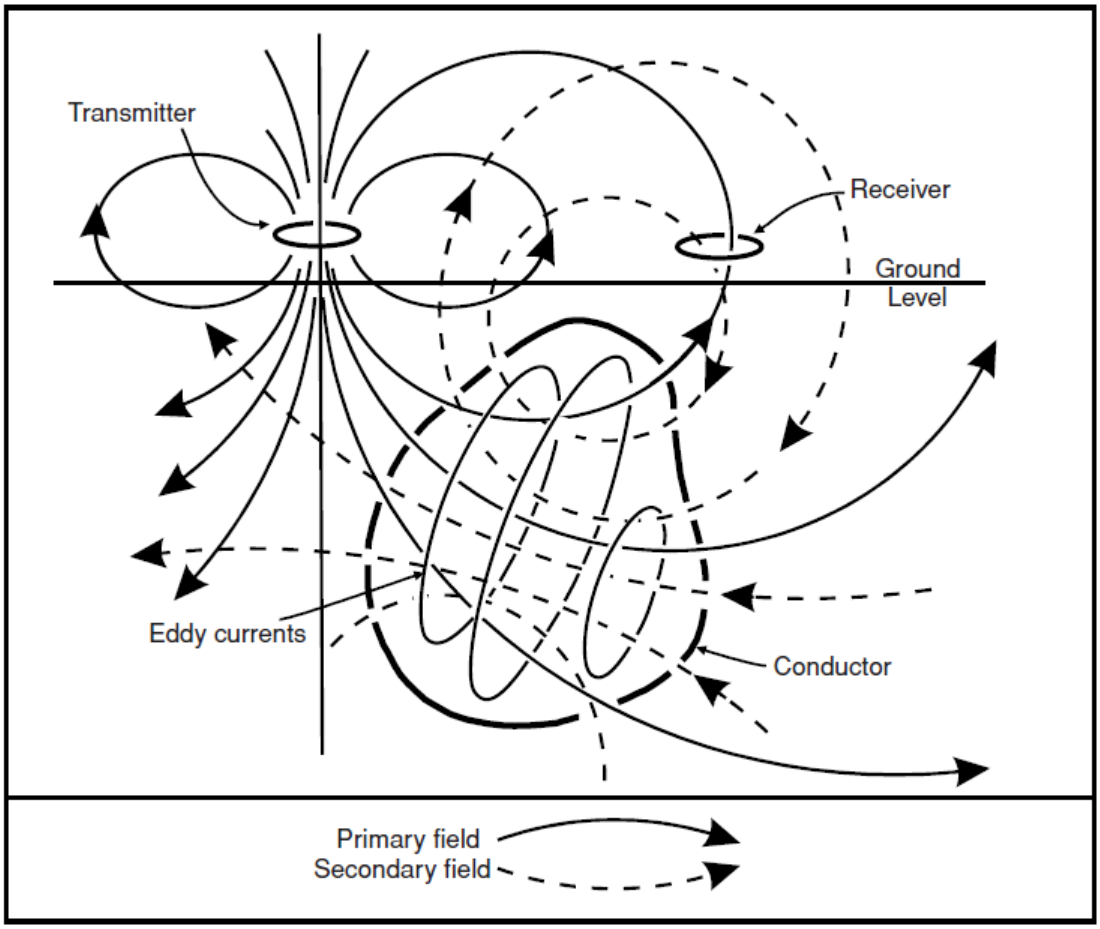

Figure 2-7: Generalised schematic of the EM surveying method (Reynolds, 2011; as cited in Grant and West 1965)

The penetration depth of the electromagnetic radiation is dependent on the frequency and the conductivity of the media present through which it travels. If both frequency and ground conductivity decreases, the depth of penetration increases. The major advantage of the EM methods is that no direct contact with the ground is required, as compared to electrical resistivity. One disadvantage is the lack of suitable inversion routing and restricted in depth penetration. The electromagnetic methods has the ability to be used either as passive or active source.

2.5.5.3 Frequency Domain and Time domain electromagnetic method

Two basic types of EM methods are Frequency domain electromagnetic (FDEM) and time domain electromagnetic (TDEM). FDEM make use of one or more frequencies, whereas TDEM makes measurements as a function of time. Both FDEM and TDEM can be referred to as active source as they use artificial generated energy to make measurement. Electrical conductivity is a function of soil and rock as well as the composition of fluids that fill the pore spaces (Technos, 2004). Technos (2004) suggested that conductivity values may be related to groundwater properties like specific conductance or total dissolved solids.

Time domain electromagnetic

The TDEM exciting the subsurface through a series of electromagnetic pulses is based on the principle of using electromagnetic induction to generate measurable responses from sub-surface features. The principle of TDEM is based on reducing transmitter current to zero inducing a short duration voltage pulse in the ground, which causes a loop to flow in the vicinity of the transmitter wire (Figure 2-8). After transmitter current is turned off, the current starts to decay inducing voltage pulse which causes more current to flow at a lager distance and greater depth from the transmitter loop. Thus the amplitude of the current flow as a function of time is measured by measuring its decaying magnetic field using a small multi-turn receiver coil (ASCE, 1998).

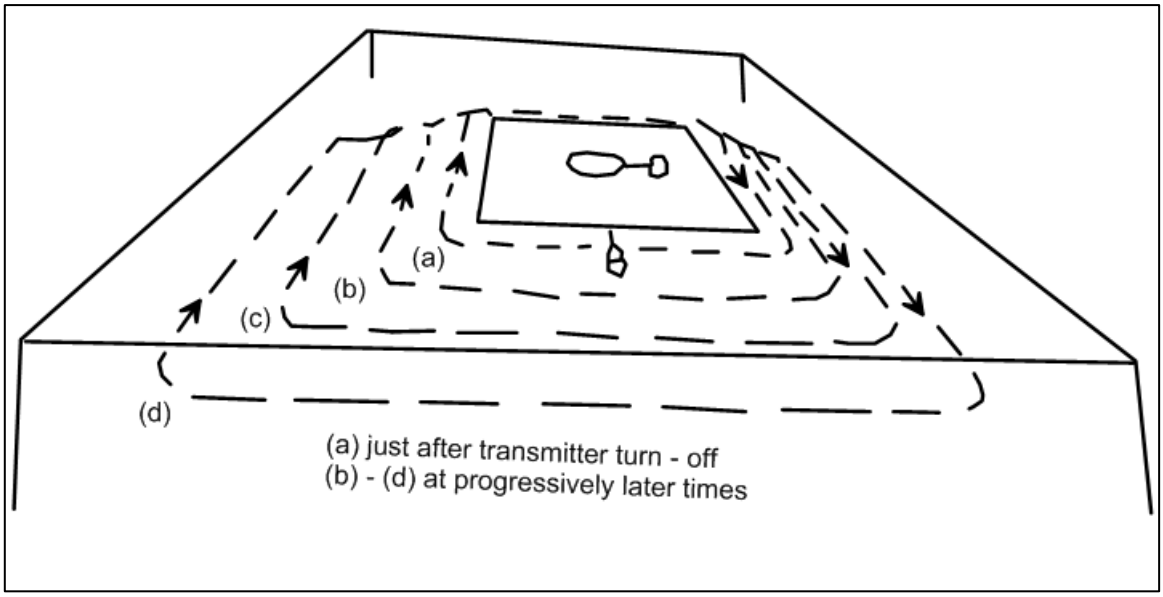

Figure 2-8: Transient current flow in the ground (after ASCE, 1998)

Frequency domain electromagnetic

The FDEM measures the electrical conductivity of the subsurface using the magnitude and phase of the secondary field which results from induced electromagnetic currents (ASTM, 2003). The system operates with two coils separated by a reference cable, where one coil serves as a transmitter to generate the primary field and the other as a receiver (Figure 2-9). The inter-coil spacing which determines the penetration together with the coil orientation is maintained at fixed distance, while moving the dual coil pair along the survey transects in a discrete intervals. The FDEM make use of sinusoidal (AC) excitation of the subsurface and measure the phase shift between the primary and secondary magnetic fields to calculate the subsurface apparent conductivity.

The application of the FDEM is in profiles for detecting and mapping lateral changes in geologic and hydrogeological conditions. There are many FDEM operating systems which includes Geonics EM31, EM34-3 and EM38, VLF, CSAMT, Phoenix MT, etc. The magnetotelluric (MT) was the

method used on this study due to its ability to obtain information about the electrical properties at great depth. The Phoenix MT system was the system used to investigate subsurface conductivity distribution. The magnetotelluric is one of the passive electromagnetic methods that use naturally generated energy.

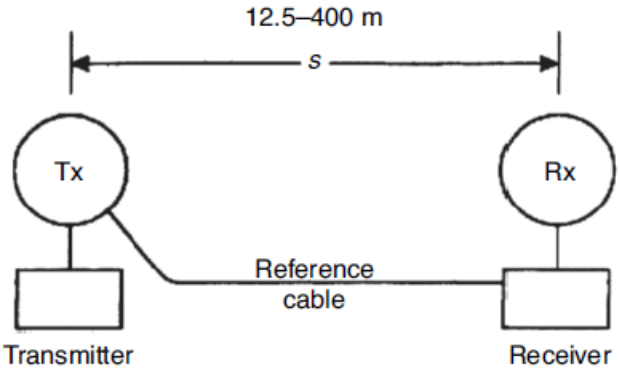

Figure 2-9: Moving dual-coil EM systems (Reynolds, 2011)

2.5.5.4 Application of electromagnetic method in groundwater studies

The electromagnetic methods have previously and still been used for groundwater investigation due to its ability to map the conductivity contrast of the subsurface. Most commonly the frequency domain is used for shallow investigation, whereas time domain for deeper investigations. Two approaches that may be considered are firstly general investigation of the groundwater regime, where groundwater is dominant within the aquifer. Secondly is studying the local bedrock for fractures that may contain small but usable reservoirs of potable water.

Electromagnetic survey was conducted to map areas with increased electrical conductivity which shows an increase in moisture contents in rocks in Malawi (Sakala and Sekiba. 2017). Terrain conductivity method highlighted areas with increased conductivity value typical response of thicker and wet weathered zones

The electromagnetic methods are mostly useful to determine the subsurface conductivity distribution, of which inference of the subsurface geology can be made and geological structures can be mapped from the conductivity information obtained (Fourie, 2003; Makhokha, 2016). The success of the methods depends on the conductivity contrast between the geological formations, if the very conductive superficial layers are present often challenges the penetration. In case of lack of contrast between the country rock and fracture zone in the Karoo Basin electrical conductivities are frequently challenged.

2.5.6 The magnetotelluric method

The magnetotelluric (MT) method is an electromagnetic geophysical technique that maps the subsurface conductivity distribution using natural sources of external origin. The uniqueness of the method is its capability to penetrate to very great depths without artificial power sources. The external energy, also known as the primary electromagnetic field, is mostly reflected back from the Earth's surface, but small amounts propagate vertically downward into the subsurface. With the Earth acting as an electrical conductor, electric currents are induced, producing a secondary magnetic field. MT measures the time variation of both the magnetic field (**B**) and the induced electric field (**E**) simultaneously. The subsurface electrical conductivity distribution influences the relationship between components of the measured electric and magnetic fields, with the amplitude, phase and direction.

The penetration of electromagnetic fields is according to the property of electromagnetic waves in the conductors dependent on the frequency. Thus depth of penetration is determined by the frequency of electromagnetic fields. The frequencies of the natural source magneto-telluric method range between 10^{-3} to 10 Hz, whereas audio magnetotelluric (AMT) operates at higher frequencies ranging between 10 to 10^4 Hz (Reynolds, 2011). The natural source MT method is challenged by erratic signal strength. Sferics which is generated by lightning strike causing fluctuations of the earth's electromagnetic field in the frequency range from 1 to 10^5 Hz, is used by AMT as the main energy source (Reynolds, 2011). The short of this method is that the distant lightning activity has a signal minimum between 1 and 5 kHz, which can be termed AMT 'dead' band (Reynolds, 2011). MT soundings are usually time consuming and expensive due to variability in source strength and direction requiring substantial amount of stacking time of about 5 to 10 hours per site (Reynolds, 2011). Recording for long hours is necessary especially for low frequencies to obtain many samples for meaningful statistical average of the data. The high frequency AMT measurements are more rapid than MT, but data quality can deteriorate in the presents of local thunderstorm and signal attenuation of around 1 Hz and 2 kHz (Reynolds, 2011).

The higher frequency AMT has been used in exploration for groundwater/geothermal resources, as well as major base metals deposits at depths from 50 – 100 m to several kilometres (Vozoff, 1991). Although the main application of the MT method has been in hydrocarbon exploration particularly in areas where seismic reflection is either expensive or ineffective, i.e. areas where dense mafic intrusion occurs may have difficulty in the interpretation of seismic reflection data. This low frequency MT sounding may also be applied to determine stratigraphy at depth and to delineate the deep aquifers down to about 1000 m (Krivochieva and Chouteau, 2002). Generally MT surveys are challenged by acquiring data in electrically noise areas or where the surface is unstable. To

overcome the shortcoming experienced by the MT surveys the controlled-source magnetotelluric (CSMT) was introduced during the year 1970 (Reynolds, 2011). The CSMT which operate within the frequency band of 0.1 Hz and 10 kHz has the ability to speed data acquisition and improve the reliability of results (Reynolds, 2011).

MT requires placement of electrodes in the ground and measuring the contrast of electric currents through different rocks induced by natural electric charges in the atmosphere. Acquiring high-quality data over a broad period range is vital in MT surveys. The MT field layout comprising of two orthogonal electric dipoles which measures two horizontal electric components and the corresponding magnetic component is measured by two magnetic sensors parallel to the electric dipoles, with the vertical dipole measured by the third sensor is shown in Figure 2-10. The MT surveys measures five parameters at each sounding location as a function of frequency. An apparent resistivity curve is produced when the change in magnetic and electric fields are measured over a range of frequency. Greater depth of penetration can be obtained at low frequency.

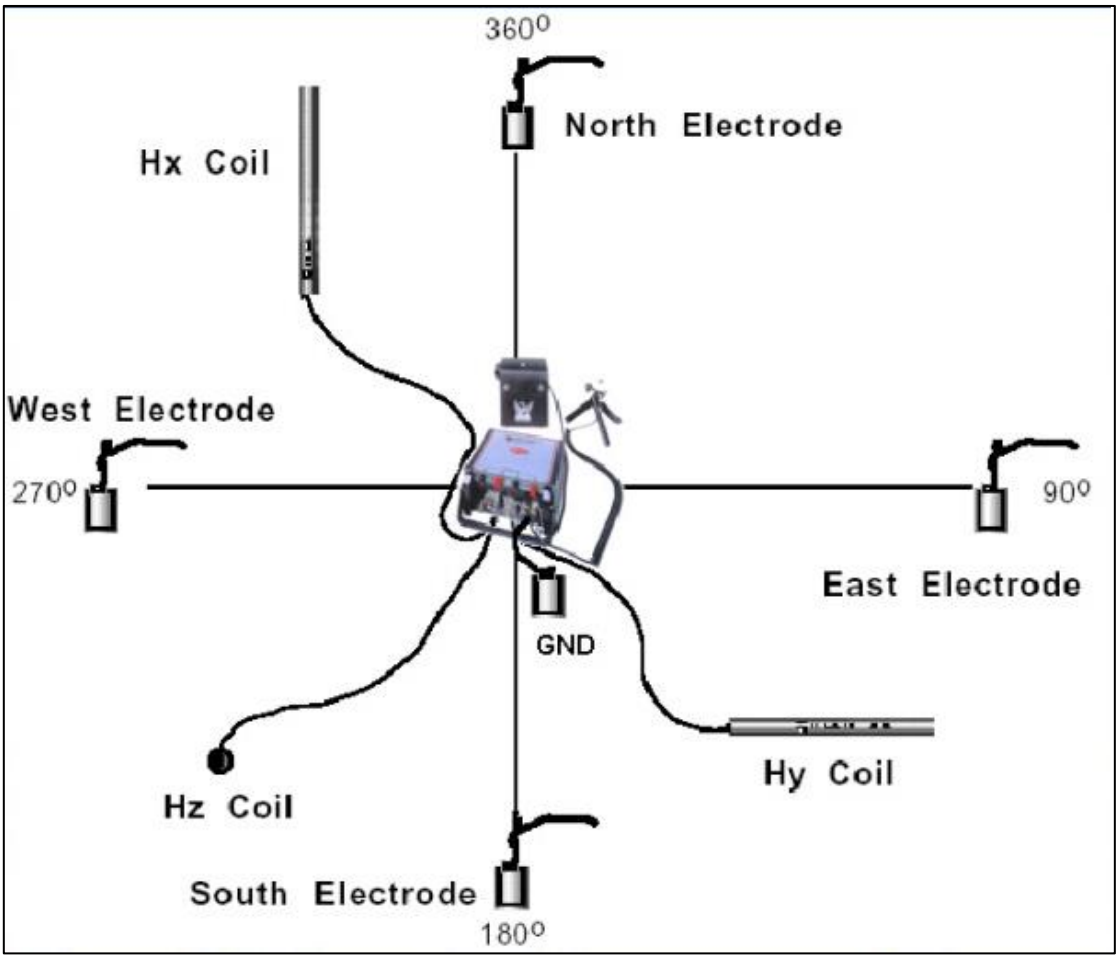

Figure 2-10: Generalised field layout of the magneto-telluric survey (MTU/MTUA user guide, 2010)

2.5.7 Electrical conduction in rocks

Electromagnetic method measures the distribution of electrical conductivity in the subsurface. In most purposes conductivity depends on the knowledge of the geological composition and conditions. It is vital to consider two distinct transformation (measurement to the distribution of the subsurface conductivity and conductivity structure to a quantitative petrographic description of the earth material being probed) in order to fully use MT and other EM methods. These transformations can be used for drilling targets as well as in areas where direct measurement and observation may not be possible, i.e. upper mantle. Conductivity of most common rocks depends almost entirely to the ions dissolved in water filling the pores of the rock. The Earth is made up of different types of rocks and fluids with varying bulk composition, thus one would intuitively expect its conductivity structure to vary vastly (Khoza, 2016).Electrical resistivity ranges of most common rocks types are shown in Figure 2-11. The importance of establishing regional resistivity-lithology relationship is revealed in Table 2-3.

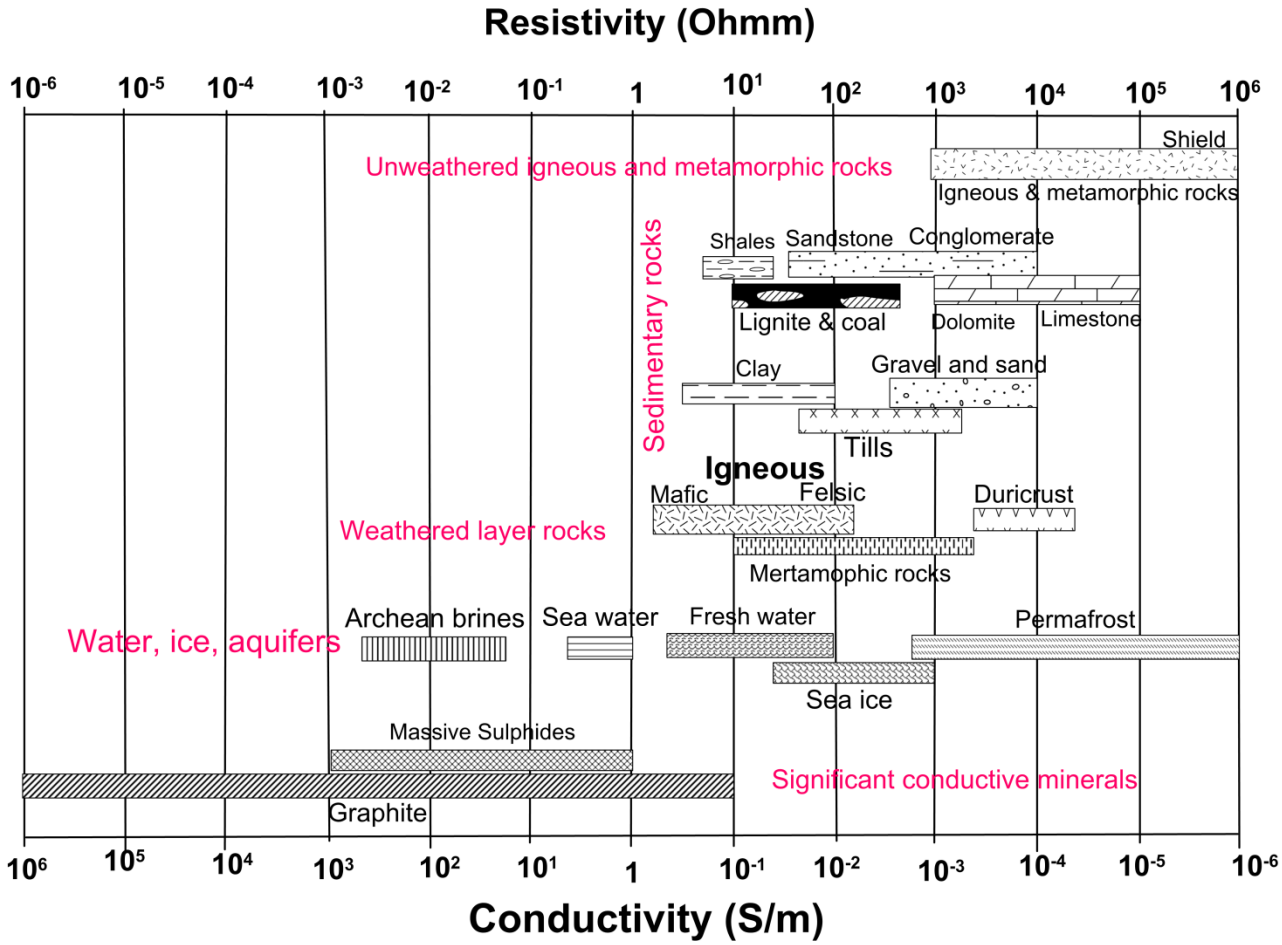

Figure 2-11: Resistivity ranges of common rock types (modified from Khoza, 2016 as cited in Palacky, 1987; Marti, 2006 and Miensopust, 2011)

Table 2-3: Rock resistvities (after Vozoff, 1990)

Rock	Minimum Resistivity (Ωm)	Maximum Resistivity (Ωm)
Granite	3×10^2	1×10^6
Gabbro	1×10^3	1×10^6
Limestone	50	1×10^7
Sandstones	1	6.4×10^8
Shale	0.3	2×10^3
Marls	3	70

The relationship between rock conductivity, water conductivity and fractional porosity is based on Archie's law. This law assumes the saturation of water within the rock pores. Porosity and the conductivity of water are the major factors affecting distribution of the subsurface conductivity within the rocks. Thus the major determinants are dependent on salinity and temperature for regional and depth variations. Figure 2-12 shows the relationship between salinity, conductivity and temperature. Archie's law does not seem to recognize permeability although it is another important factor for aquifer characterization. It has appeared that permeability depends on the distribution of grain size and porosity (Vozoff, 1990, cited in Bear, 1972). Newer information on Archie's law was reported when only using measured quantities and not considering empirical constant relates permeability and conductivity in porous rocks (Vozoff, 1990; cited in Katz and Thompson, 1987). Both permeability and porosity decrease at greater depth due to increase pressure, as such water may be assumed to be no longer the major medium of conduction because temperature and pressure may direct water into hydration in the rock-forming minerals and others enters the vapour phase.

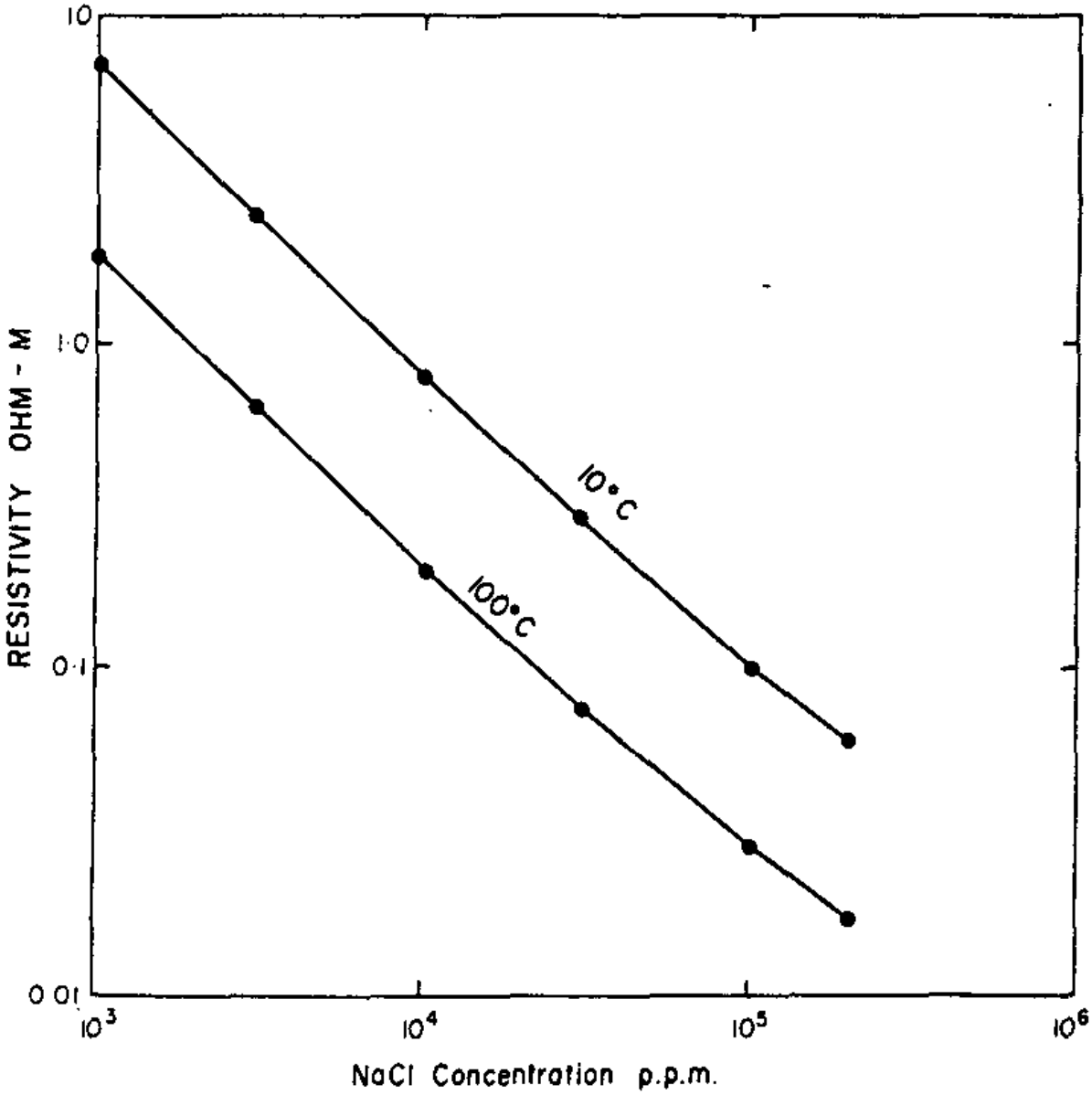

Figure 2-12: Dependence on temperature and NaCl concentration of brine resistivity (Vozoff, 1990)

2.6 CASE STUDIES ON THE APPLICATION OF GEOPHYSICAL METHODS TO AQUIFER DELINEATION

2.6.1 Case Study 1: Geophysical and Hydrogeological Investigation of Groundwater

Geophysical and hydrogeological investigation was carried out in Sawmills, Zimbabwe (Danielsen *et al*, 2007). The study was aimed on the assessment of the groundwater potential within the Karoo sedimentary basin to supply water to the city of Bulawayo. Data was collected using two geophysical methods which include continuous vertical electrical sounding (CVES) and transient electromagnetics (TEM). The choice of the survey area was based on approri information from the borehole logs indicating favourable stratigraphy for groundwater availability and high yields result

from the aquifer test. CVES was used to delineate near surface geological structures, whereas TEM for deeper structures.

Danielsen *et al* (2007) presented TEM results for line 2 as a model section shown in Figure 2-13a. The model section depicts a low resistive bottom layer which may be associated with Karoo Sediments. Top layer has slightly high resistivity values corresponding to an area where surface observation identified soils derived weathered basalts and sandstone. Higher resistivity values may be related to outcrops of fresh basalts. These results may geological be interpreted as fresh basalts at the surface, followed by weathered basalts and/or sandstone, then Upper Karoo Group sediments at the base. The Upper Karoo Group sediments represented by low resistivity values consists interbedded layers of mudstone.

The CVES inversion results (Figure 2-13b) presented as depth section shows a three layer structure at line section from 0 to 4600 m. Interpretation have shown less resistive layer overlain by a resistive layer, then lower resistivity at the base. This interpretation provides a great correlation to the TEM results. Inference of the geology was that less resistive may be associated with fresh basalt interbedded by sandstone, underlain by resistive fresh basalt, followed by lower resistivity Upper Karoo Group sediments.

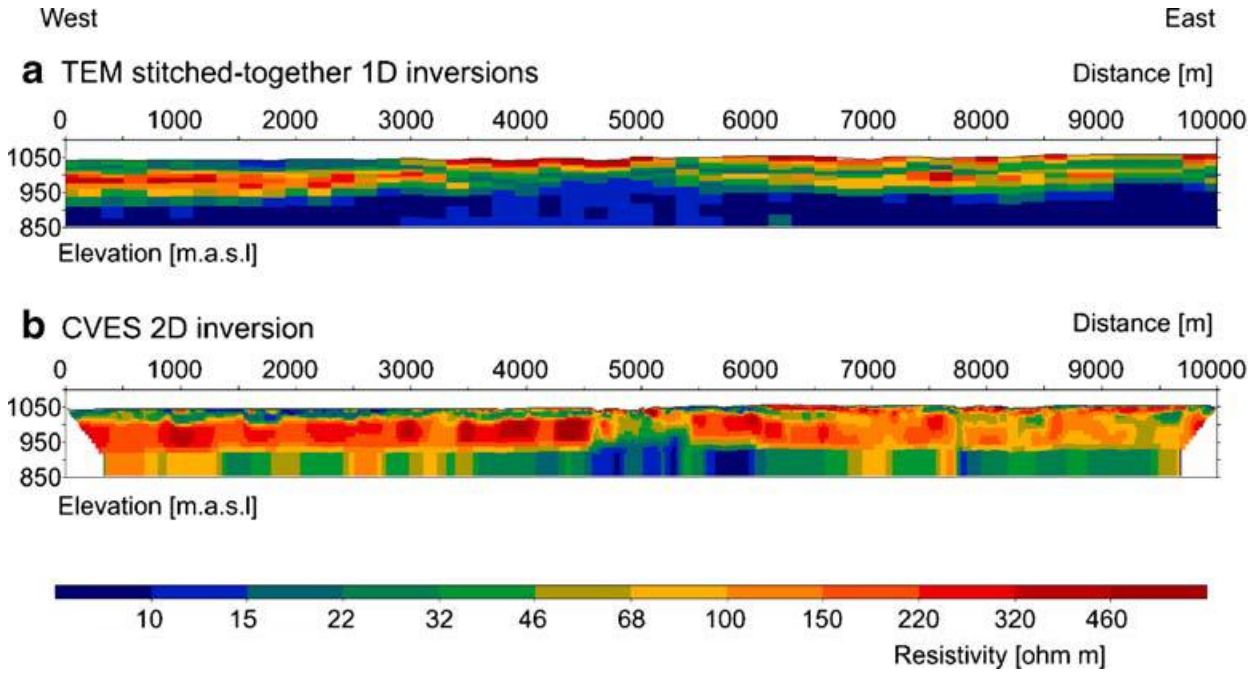

Figure 2-13: Inverted model section of line 2: (a) is the one dimensional TEM results and (b) is the two dimensional CVES inversion results (Danielsen *et al*, 2007)

Line 5 was surveyed perpendicular to line 2 within the faults zone. The TEM results (Figure 2-14a) shows a multi-layer model section able to differentiate between Lower and Upper Karoo Groups. High resistivity values was interpreted as fresh basalts, whereas low resistivity values of around 15 – 20 Ωm. The CVES result (Figure 2-14b) was unable to support the TEM interpretation. However

the CVES was able to delineate the Kalahari sand represented by top high resistive layer. The fault zone was clearly imaged by CVES profile of line 5 in the N-S direction.

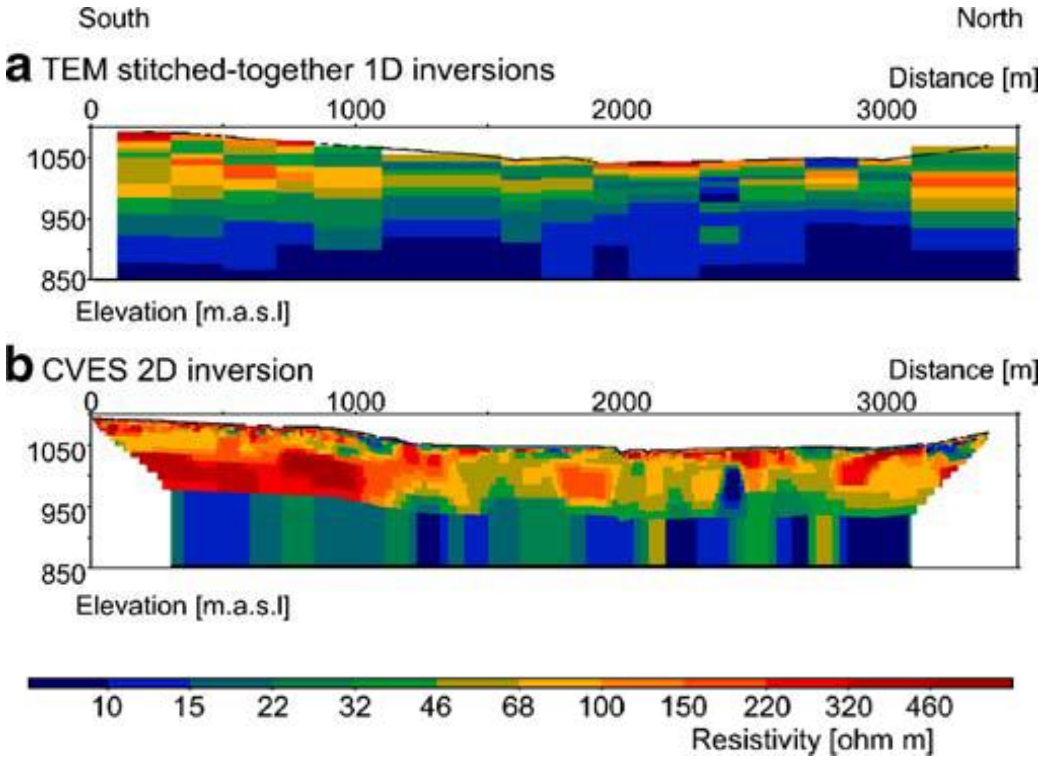

Figure 2-14: Inverted model sections from line 5 at Sawmills (a) is the one-dimensional multi-layer inversion TEM data, (b) is the is two-dimensional robust inversion of CVES data (Danielsen *et al*, 2007)

Concluding remarks

Application of the TEM and CVES geophysical methods in the investigation of aquifers and the hydrogeology at Sawmills can be concluded as follows:

- The Karoo basalt consists of less compact and more weathered basalt horizons or interbedded sandstone layers in between which have lower resistivity and layering results in electric anisotropy.
- The Upper Karoo Group has sandstones with some clay bands that can result in anisotropy, this may results to lower resistivity than the overlying basalts within the Upper Karoo Group due to clay content and the alkaline groundwater.
- The Lower Karoo Group characterized by shales, coal and mudstone and the abundance of alkaline groundwater probably has even lower resistivity.
- TEM plan maps in the form of depth slices outlined the major tectonic features such as faulting; however the resolution of the maps becomes worse as depth increases.

- The CVES provided better images and more detail on the tectonic structure in the fault zone due to the dense data cover, 2D inversion method used and shallow depth due to uplifted Karoo sediments.
- Interpreting TEM and CVES data combined using LCI accounts for anisotropy and provides a better estimation of the true resistivity and depth of the layers.

2.6.2 Case Study 2: Aquifer Characterisation using Resistivity Methods

Bratus and Santarato (2007) used geophysical methods for the characterization of the aquifer system in Friuli-Venezia Giulia, northeastern Italy. Geophysical methods used include Electrical Resistivity Tomography (ERT), Magnetotelluric (MT) and Time-Domain electromagnetic (TDEM). ERT was able to obtain shallow subsurface information, whereas MT and TDEM were used to obtain surface information at greater depth.

The ERT survey was conducted on 2D and 3D. Two profiles located within the NW portion of the study area were conducted for 2D ERT survey. The field layout of the two profiles was 128 electrodes at 5 m spacing. Electrodes were arranged in a linear array known as Wenner to collect good quality data and favour the interface of the horizontal discontinuities. 3D survey was carried on two zones located in the NW and SE portion of the study area. Dipole – dipole linear arrangement array was used to collect data of the 16 profiles consisting of 64 electrodes at 5 m spacing. The choice of array was due to its ability to obtain maximum lateral resolution. The 3D survey was aimed on obtaining detailed information of the overburdened sediments to assess vulnerability against contamination of the first confined aquifer.

MT data was acquired using the stratagem equipment in the frequency band between 10 Hz and 90 kHz. The frequency band is useful to reach sufficient desired depth of investigation. The TDEM data was acquired on a total of sixteen central and out-of-loop soundings, were their positions resulted in an almost regular grid of 200 m spacing.

Authors used available litho-stratigraphic data of boreholes within the area to derive a realistic 2D subsurface model in order to optimise data acquisition phase. They calculated the resistivity response of subsurface by forward modelling the geological sections using a free 2D modelling code. The parameters employed in the forward modelling were then used to collect the apparent resistivity data. These resulted in good quality apparent resistivity data showing RMS error of 2.1% and 1.29 % respectively for both profiles. Less resistive values of around 14.5 Ωm was interpreted as clay layer (Figure 2-15). High resistivity values around 90 Ωm was associated with sandy level (also known as A1 aquifer). Clay – silt level was associated with slightly high resistivity values of around 40 Ωm.

The 3D data was inverted using the same 2D inversion software and the volume distribution of the resistivity data was achieved by geostatistical interpolation as the subsurface geometry was known to be simple. Figure 2-16 shows two 2D inversion profiles that concern the electrical stratigraphy of the two 3D areas, where the first profile relating to the NW 3D survey shows lateral heterogeneous overburden sediments and the second profile relating to the SW 3D survey indicates high resistivity values which may be associated with coarse grained sediments. The authors reported the ability of ERT to obtain shallow subsurface information to a depth of about 100 m.

The TDEM survey (Figure 2-17) was able to probe to depth of not less than 500 m, where at greater depth S/N ratio is too low to accurately map the bottom of high resistivity layer at depth around 450 m. At depth around 50 m a resistive horizon which wedges southwards was identified. The resistive horizon gives a very good correlation to the ERT results and may be associated with A1 aquifer. The authors reported that MT soundings results were influenced by signal to noise ratio which was strong for periods greater than 3.10 - 3s. Therefore MT results did not form part of the case study.

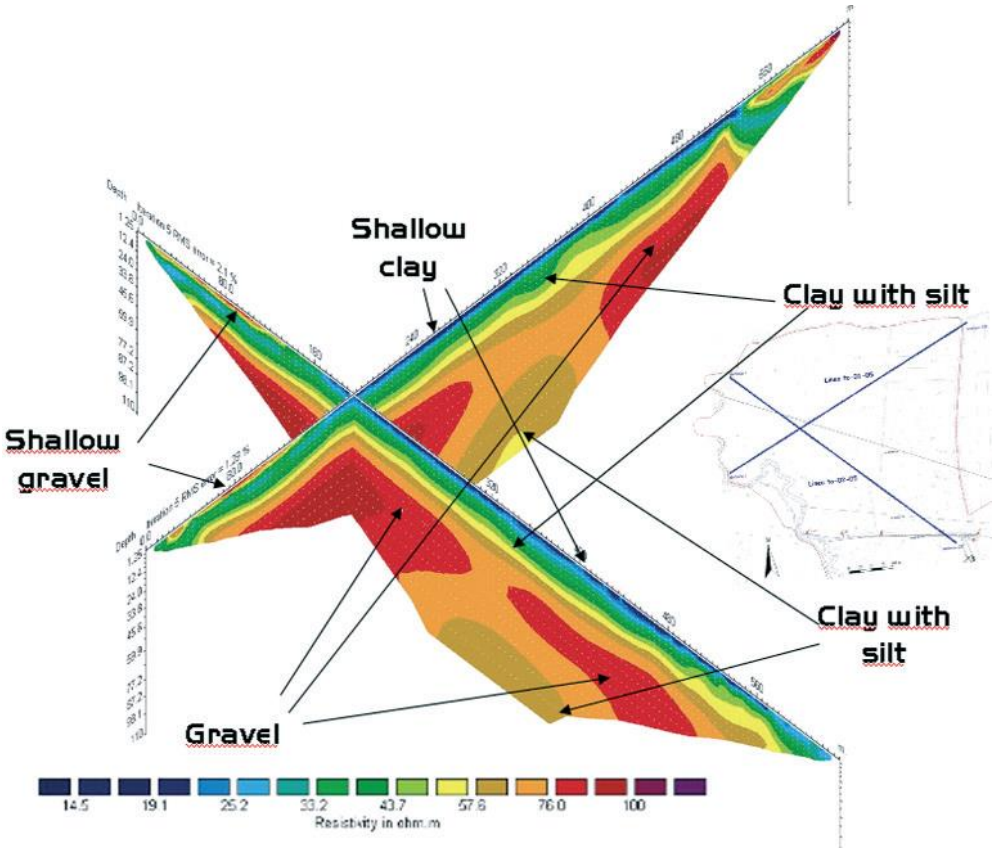

Figure 2-15: Fence resistivity diagram of the two 2D ERT models (Bratus and Santarato, 2009)

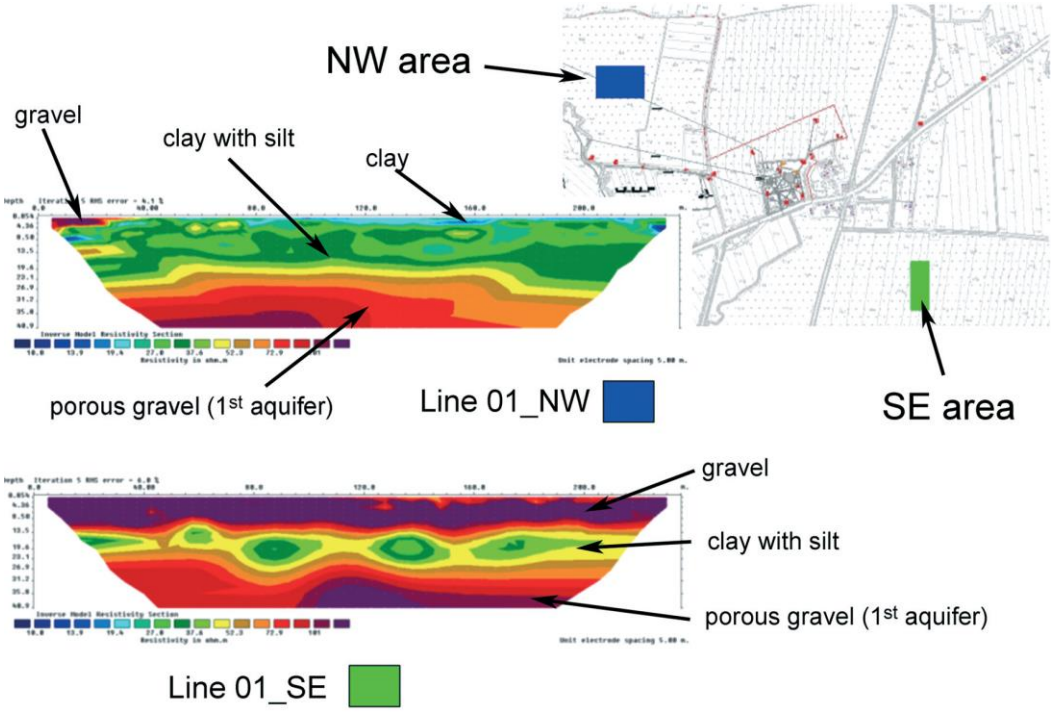

Figure 2-16: 2D resistivity models obtained from the two 3D acquisition areas (Bratus and Santarato, 2009)

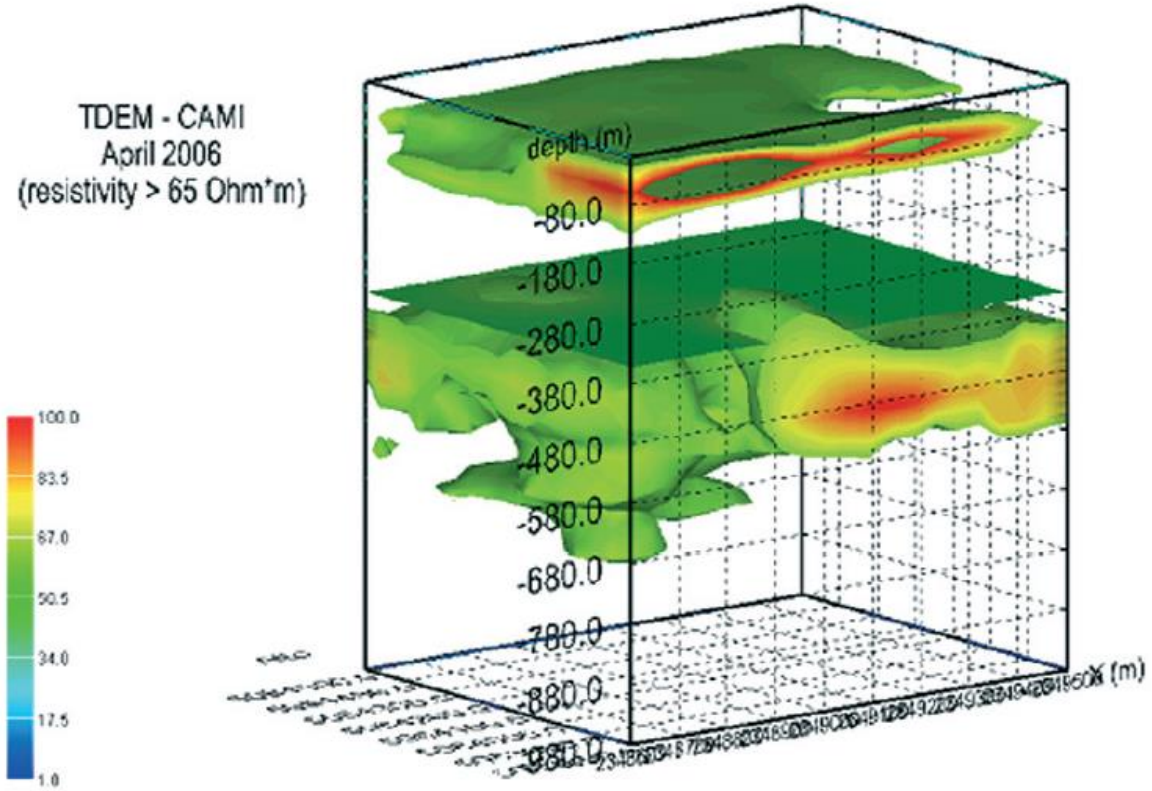

Figure 2-17: 3D modelled of estimated resistivity (Bratus and Santarato, 2009)

2.6.3 Case Study 3: Characterisation and Delineation of Aquifer using the Electromagnetic Method

Integration of Electromagnetic methods was used to characterise and delineate deep aquifer in the region of Santa Catarina, located in the Chalco Sub Basin of the Mexico Basin. The study was aimed on determining the geometry of the fresh water aquifer and confirms the continuity of the basaltic flows between the volcano and the sedimentary basin. The choice of the methods was based on the excellent resolution of the conductive targets, greater penetration depth and rapid deployment on the sounding sites. Magnetotelluric (MT) and time-domain electromagnetic (TDEM) was the two methods adopted for the study. MT soundings acquired at low frequency was able to define the stratification at depth and delineate deep aquifer. TDEM sounding was used to verify the presents of pathways for migration of contaminated groundwater.

The survey was conducted over a sedimentary basin with MT station totalling to about eleven and about five deep TDEM soundings. The north – south MT profiles were conducted parallel to the line of water wells. Seven fields were recorded at each station with a frequency of 300 to 0.002 Hz using a V5 system from the Phoenix Geophysics, Canada. Base and reference station ranged to a typical distance of about 100 and 150 m.

Shallow TDEM survey was conducted in the areas of highly resistive layers along the volcano range using Geonics TEM47 transmitter and Digital Protem receiver. Three profiles consisting of about 37 TDEM station were recorded, orientated perpendicular to the expected regional groundwater flow to enable to map lateral extend of the groundwater flow. Five deep TDEM soundings data were collected close to the MT stations over the sedimentary Basin using EM37 and EM47 transmitters. The EM 47 was used as vertical component high frequency receiver coil. The vertical magnetic field time derivative was recorded for time windows from 6.8 μs to 7 ms, using frequencies of around 285, 75 and 30 Hz. For shallow exploration on the volcano flanks a 40 x 40 m transmitter loop with currents of 0.5 – 3A were appropriate. The EM37 system was used with a three component low frequency receiver coil. Frequencies of around 30, 7.5 and 3 Hz were used to record voltage for time range from 88 μs to 70 ms. For deep investigations within the basin 100 x 100 m transmitter loop with current of around 8 – 13 A was used.

The hydrogeological perspective of the Catarina aquifer system consist of very low permeability unit (Zone 1), granular aquifer (Zone 2) and deep permeable fractured volcanic rocks (Zone 3) as shown in Figure 2-18. The water in Zone 3 is recharged through infiltration of rain water in the Santa Catarina and Chichinautzin ranges. The hydrogeological zones interpreted as follows:

- Zone 1: Unsaturated layer of sand, volcanic ash and clay, underlain by a layer of 220 m thick sands and ashes saturated with mineralized water and less conductivity ranging 1.5 Ωm.
- Zone 2: Intermediate 60 m thick layer of fine sand, coarse sand and gravel with resistivity values ranging 4 to 6 Ωm, saturated with mixed water.
- Zone 3: A unit of fractured basalts and pyroclastic material forms the fresh water aquifer. The resistivity values ranges between 6 to 60 Ωm.

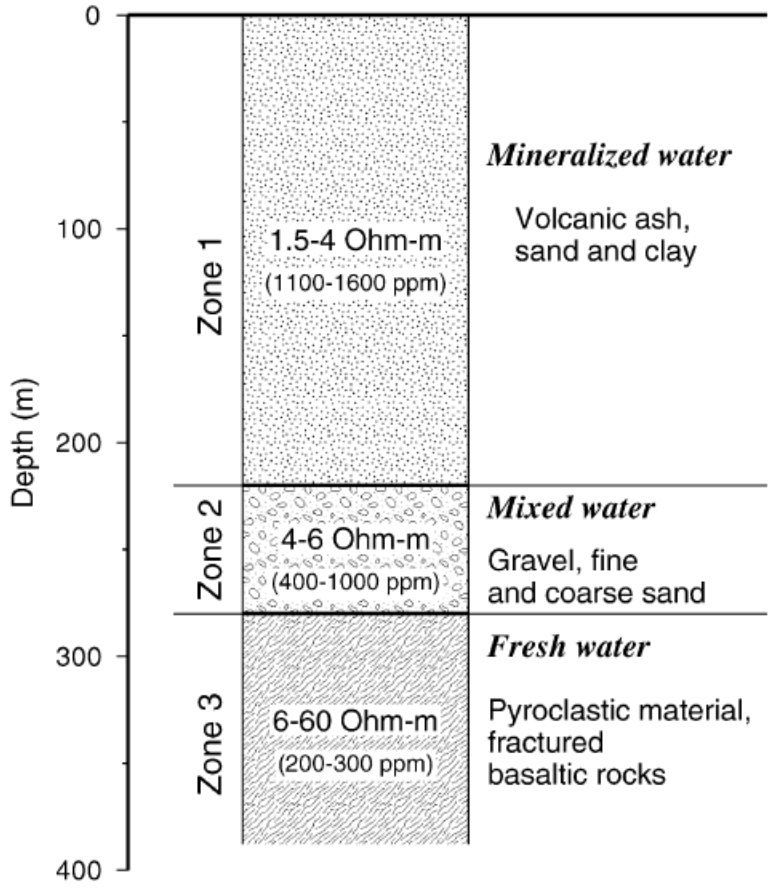

Figure 2-18: hydrogeological zoning obtained from resistivity logging in Santa Catarina wells (Krivochieva and Chouteau, 2003)

1D results

Five TDEM stations (Figure 2-19) presents an excellent fit of data with error varying between 2% and 4%. A very conductive subsurface down to about 100 – 115 m is shown in stations 40 to 43. The resistivity values of around 1.5 and 2.2 Ωm very well resolved by the inversion was interpreted as sands and gravels saturated by mineralised water, this can be related to zone 1 aquifer system. With resistivity values increasing with depth last layer appears to be more resistive. The 1D inversion is illustrated by Figure 2-20 and Figure 2-21. The results of the inversion indicates resistivity values around 1.7 - 2.6 Ωm may be associated with shallow zone of ash, sand and clay.

Resistive layer at depth of 38 m corresponds to fractured basaltic flow. Less resistive layer of around 1.4 – 2 Ωm extending to depth of around 150 – 200 m may be associated with ash, sand and clay sequence saturated with strong mineralised water. Slightly high resistive layer of values around 6 – 30 Ωm at depth ranging 400 – 600 m may be related to upper part of aquifer consisting of sand, coarse sand, gravel , pyroclastic material and fractured basalts. Zone of high resistive values of around 60 – 120 Ωm may be associated with fresh water in the fractured basalts.

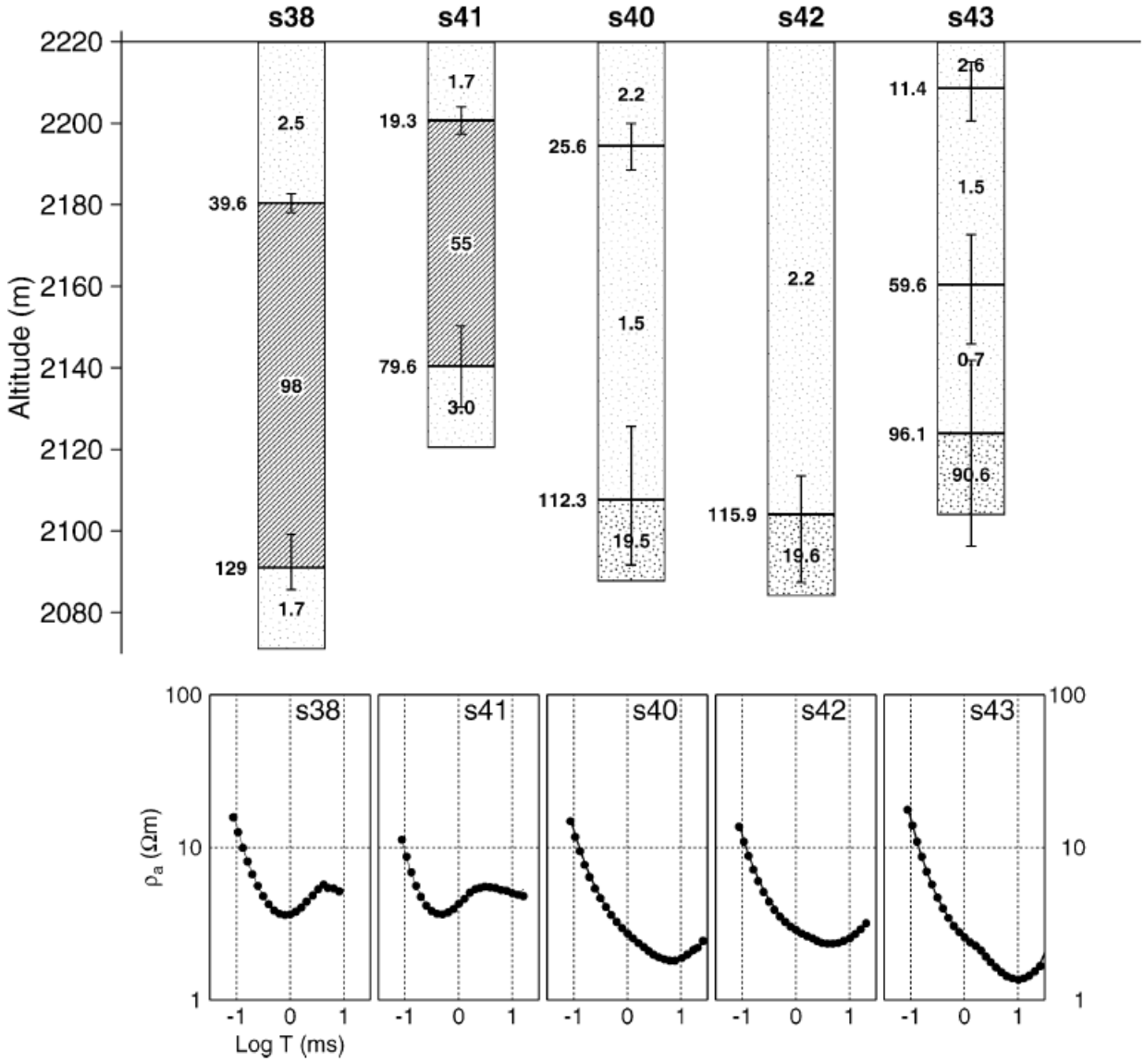

Figure 2-19: TDEM curves and 1D interpretation of central loop soundings (Krivochieva amd Chouteau, 2003)

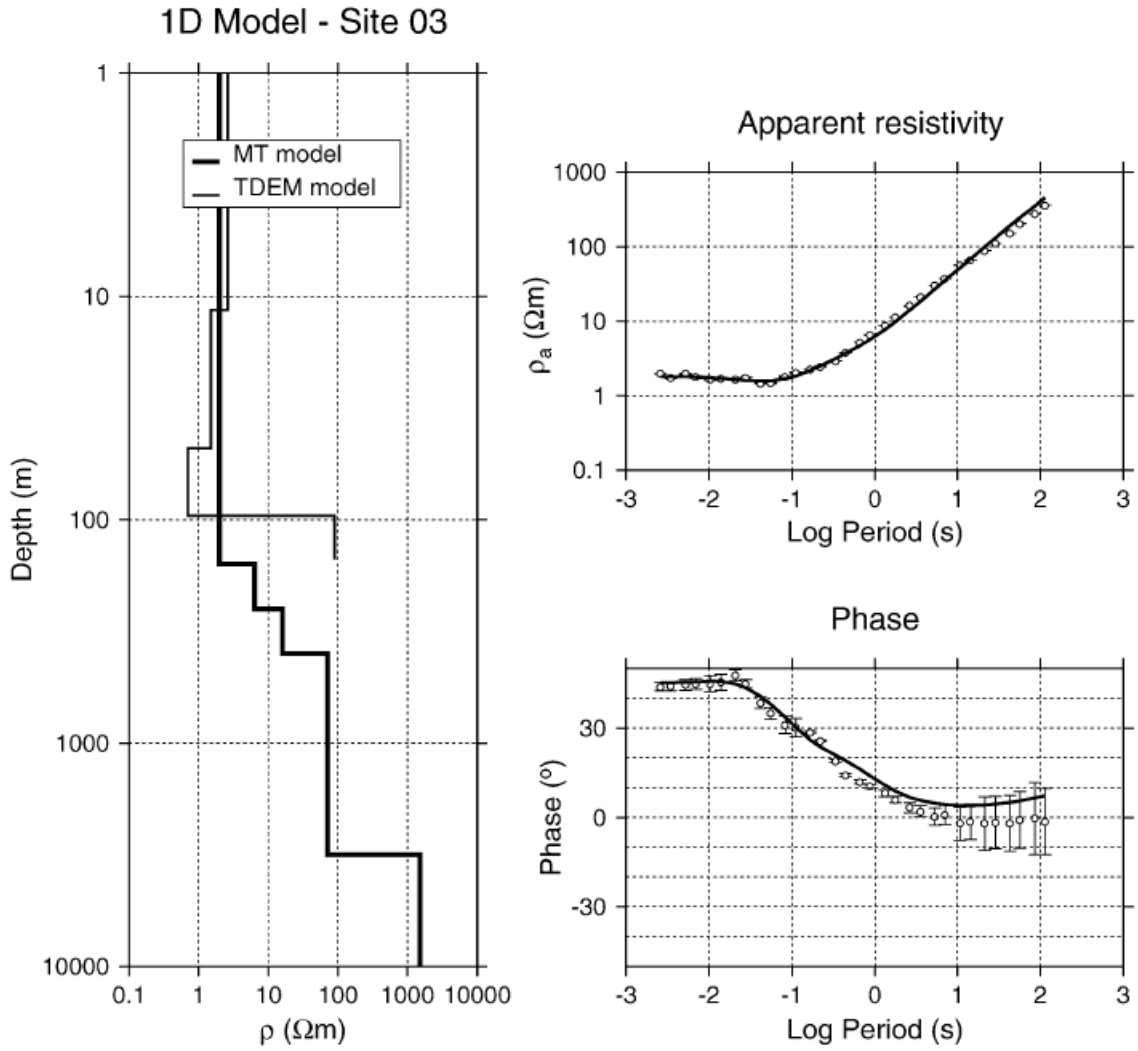

Figure 2-20: 1D inversion of sounding curves from MT station 3 (Krivochieva and Chouteau, 2003)

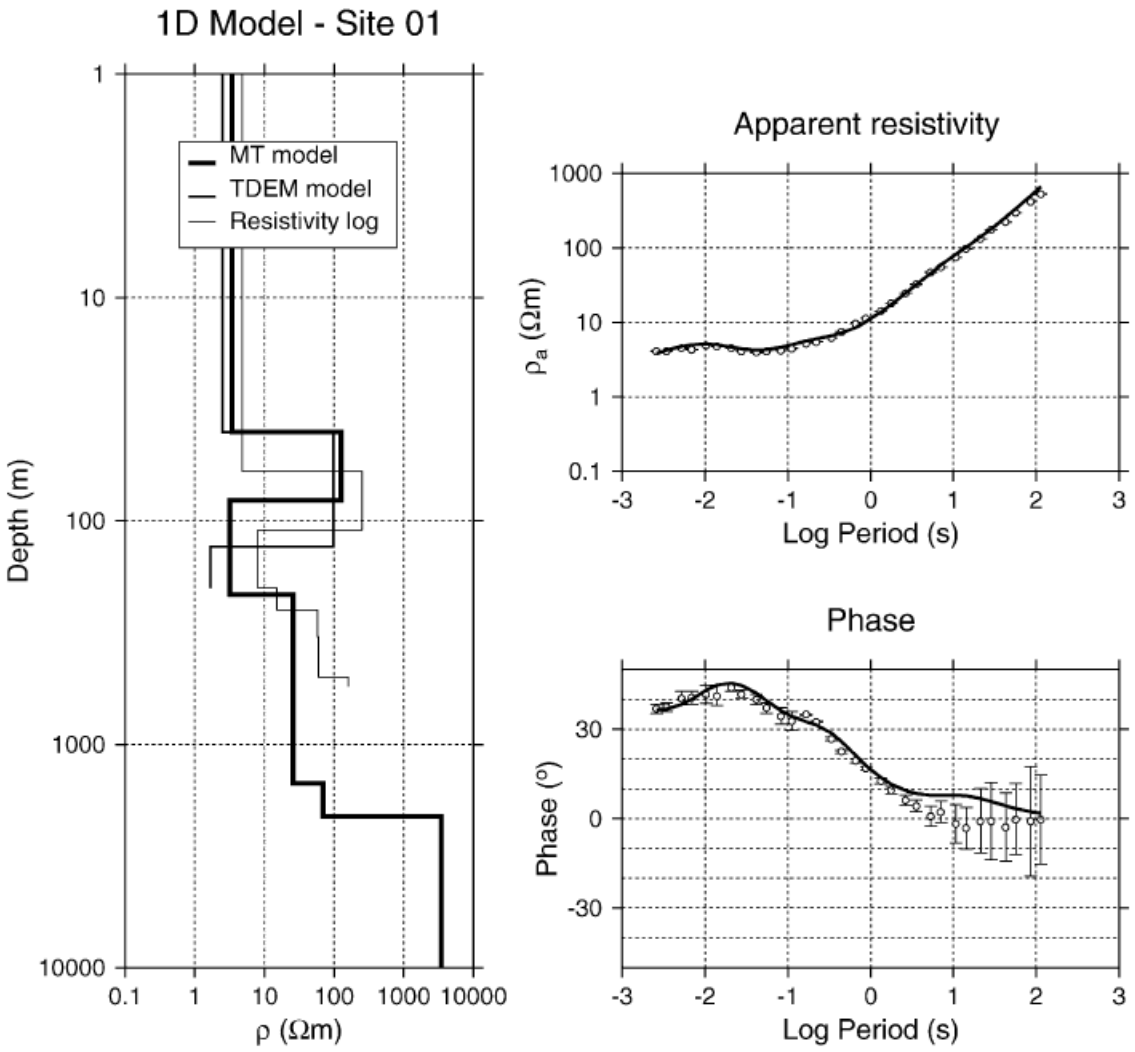

Figure 2-21: 1D inversion of sounding curve from MT station 01 (Krivochieva and Chouteau, 2003)

2D results

Results of all features interpreted in 1D layered models are verified by 2D model (Figure 2-22), showing a very conductive zone down to 250 m. This zone might be associated with sand, ash and clay saturated with mineralised water. Resistivity values of around 60 Ωm were interpreted as fractured basalt with high permeability. At depth of 800 m to south and depth larger than 1000 m to the north a resistive substratum was reached. The variation could be inferred as thick pyroclastic sequence with the northern part of basin.

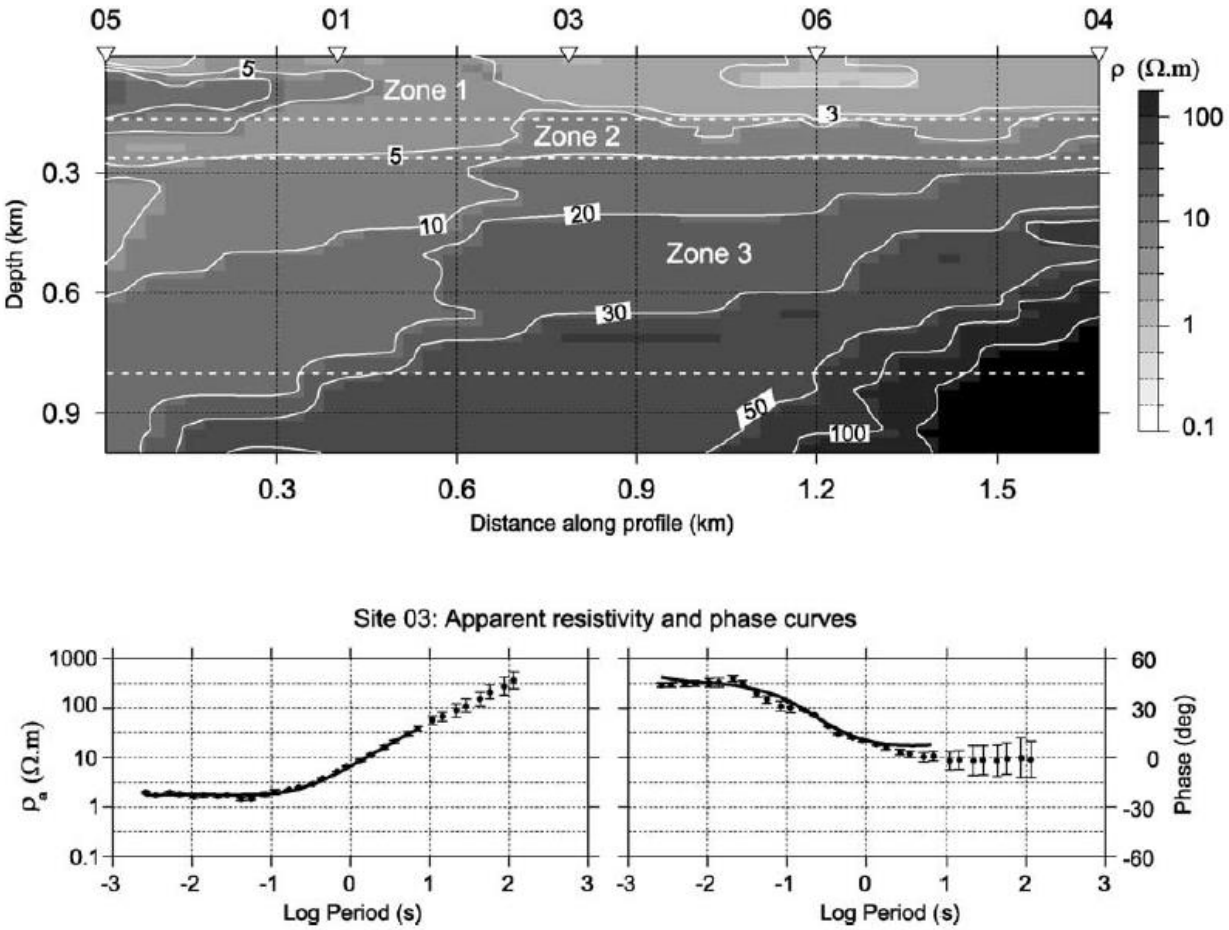

Figure 2-22: Resistivity model obtained from TM 2D inversion for depth 0 – 1 km (Krivochieva and Chouteau, 2003)

2.7 SUMMARY

The potential of geophysical methods to derive properties and state variables that are critical to aquifer has played a major role in many studies to characterise and delineate the aquifer system. The use of geophysics has been and still is the best practise for groundwater studies to avoid the risk of drilling dry borehole and cost implication associated with poor groundwater production. Near-surface geophysical methods have proved to be successful for groundwater applications including mapping the depth and thickness of aquifers, mapping aquitards or confining units, locating preferential fluid migration paths such as fractures and fault zones and mapping contamination to the groundwater.

The geophysical methods discussed above in this section have limitations in acquiring information on deeper formation, but may still be useful for shallow formations. Seismic reflections are able to probe deeper but the data quality deteriorates in areas where dense mafic intrusion occurs. The reason is that signal to noise ratio for deep reflectors is poor due to seismic energy reflected from shallow dolerite sill boundaries. Seismic reflection was further found to be expensive and difficult to interpret small faults or fracture zones within bedrock or distinguish subtle changes in

stratigraphy. For effective and efficient exploration at great depths the Magnetotelluric was the method that gained recognition in recent years as it is able to produce economic, structural and stratigraphic details at those depths. This method (MT) determines subsurface electrical resistivity distribution by measuring time-dependent variations of the earth's natural electric and magnetic fields. Thus this method can be used as a tool to delineate the aquifer systems that cannot be reached by shallow drilling.

Chapter 3:
THEORETICAL BASIS OF THE MAGNETOTELLURIC METHOD

3.1 INTRODUCTION

This chapter provides a theoretical background of the magnetotelluric method. This method derived its name from a combination of telluric inferring electric fields (tellus is Latin meaning "earth") and magneto inferring magnetic fields in the ground. Basically magnetotelluric compares the horizontal components of the magnetic and electric fields with the flow of the telluric currents.

3.2 MAXWELL'S EQUATIONS

The relationship between the electric and magnetic field in any medium is described by the four Maxwell's equation (Chave and Weidelt, 2012). Maxwell's equation can be expressed in differential form with the international system of units (SI) as shown in Equation 3-1 to Equation 3-4

$$\nabla \cdot \mathbf{D} = \rho_e \qquad \text{Equation 3-1}$$

$$\nabla \cdot \mathbf{B} = 0 \qquad \text{Equation 3-2}$$

$$\nabla \times \mathbf{E} = -\partial_t \mathbf{B} \qquad \text{Equation 3-3}$$

$$\nabla \times \mathbf{H} = \mathbf{J} + \partial_t \mathbf{D} \qquad \text{Equation 3-4}$$

where:

B = Magnetic induction

H = Magnetic field

D = electric displacement

E = Electric field

J = Electric current density

ρ_e = Electric charge density

Equation 3-1 to Equation 3-4 state that: (1) the electrical field diverges from electric charges (Gauss's law for electricity); (2) there are no monopoles (Gauss's law for magnetism); (3) Faraday's law, states that the time variations in the magnetic field corresponding fluctuations in the electric field flowing in a closed loop with its axis oriented in the direction of the inducing field; (4)

Ampére's law, states that any closed loop of electrical current will have an associated magnetic field of magnitude proportional to the total current flow. For the case (Simpson and Bahr, 2005) of time-varying displacement currents are assumable neglected Ampére's law can reduce to Equation 3-5:

$$\nabla \times \mathbf{H} = \mathbf{J_f} \qquad \text{Equation 3-5}$$

For linear, isotropic medium, two relationships have been expressed:

$$\mathbf{B} = \mu\mathbf{H} \qquad \text{Equation 3-6}$$

$$\mathbf{D} = \varepsilon\mathbf{E} \qquad \text{Equation 3-7}$$

Variations in electrical permittivities (ε) and magnetic permeabilities (μ) of rocks can be neglected in MT studies, compared to variations in bulk rock conductivities.

Considering the constitutive relations that connect the field components with material properties of the medium in which they occur, Maxwell's equation can be expressed in the form of Equation 3-8 to Equation 3-10:

$$\mathbf{J} = \sigma\mathbf{E} \qquad \text{Equation 3-8}$$

$$\mathbf{D} = \varepsilon\mathbf{E} \qquad \text{Equation 3-9}$$

$$\mathbf{B} = \mu\mathbf{H} \qquad \text{Equation 3-10}$$

where:

σ = Electrical conductivity (S/m)

ε = dielectric permittivity (F/m)

μ = magnetic permeability (H/m)

σ, ε and μ are description of intrinsic properties of the materials through which the electromagnetic fields propagate. These magnitudes are scalar quantities in isotropic media, whereas in anisotropic material are expressed in a tensorial. Earth material electrical conductivity varies, with wide spectrum of several orders of magnitude and sensitive to small changes in minor constituents of the rock. Most rock materials have very low conductivity; as such the conductivity of rock depends generally on the interconnectivity of minor constituents or presence of highly conductive material.

According to Simpson and Bahr (2005) Equation 3-11 assumes that no current sources exist within the earth:

$$\nabla \cdot \mathbf{J} = \nabla \cdot (\sigma\mathbf{E}) = 0 \qquad \text{Equation 3-11}$$

Homogeneous half-space is expressed in Equation 3-12 (Simpson and Bahr, 2005):

$$\nabla \cdot (\sigma \mathbf{E}) = \sigma \nabla \cdot \mathbf{E} + \mathbf{E} \nabla \sigma = \sigma \nabla \cdot \mathbf{E} \qquad \text{Equation 3-12}$$

When the curl of Faraday's law Equation 3-3 or Ampére's law Equation 3-4 is taken, diffusion equation can be derived in terms of the time-varying electric field and information concerning conductivity structure of the Earth can be extracted. This is illustrated by the proven vector identity in Equation 3-13:

$$\nabla \cdot (\nabla \times \mathbf{F}) = (\nabla \cdot \nabla \cdot \mathbf{F}) - \nabla^2 \mathbf{F} \qquad \text{Equation 3-13}$$

Where **F** is any vector

The skin depth is a measure to which exponentially decaying amplitude becomes 1/e (37%) of its surface value is given by Equation 3-14:

$$\delta(\omega) = \sqrt{\frac{2}{\omega \mu \sigma}} \qquad m \qquad \text{Equation 3-14}$$

Which is

$$\delta(\omega) \approx 0.5\sqrt{\rho T} \qquad km$$

where: δ = skin depth

The skin depth can be defined as estimation used for the penetration depth which increases according to the square root of the product of medium resistivity and period. It has been defined mostly considering homogeneous media; it can also be used for heterogeneous media (Naidu, 2012).

3.3 ASSUMPTIONS OF THE MAGNETOTELLURIC METHOD

A number of simplifying assumptions applicable in electromagnetic induction in the earth are considered (Simpson and Bahr, 2005):

- Maxwell's electromagnetic equations are obeyed.
- The Earth does not generate electromagnetic energy, but only dissipates or absorb it.
- All electromagnetic fields are treated as conservative and analytic away from their source.
- Natural electromagnetic source fields utilised, being generated by large – scale ionospheric current systems that are relatively far away from the Earth's surface, may be treated as uniform, plane – polarised electromagnetic waves impinging on the Earth at near-vertical incidence.

- No accumulation of free charge is expected to be sustained within a layered Earth. However, in multi-dimensional earth, charges can accumulate along discontinuities. This generates a non – inductive phenomenon called static shift.
- Earth behaves as an ohmic conductor obeying Ohm's law ($\mathbf{J} = \sigma\mathbf{E}$), where **J** is the total electric current density (A/m^2), σ is the conductivity of the sounding medium (S/m) and **E** is the electric field (V/m).
- The time varying displacement currents (arising from polarization effects) are negligible compared with time varying conduction currents and promotes the treatment of electromagnetic induction in the Earth purely as diffusion process.
- Variation in the magnetic permeability and electrical permittivity of rocks are assumed negligible compared with variations in bulk rock conductivities.

3.4 THE MAGNETOTELLURIC IMPENDANCE TENSOR

The MT method is a passive method that measures the fluctuations in the natural electric (**E**) and magnetic (**B**) fields in the orthogonal directions at the surface of the Earth. The relation of the orthogonal components of the horizontal electric and magnetic field at a specific period is described by the second-rank, frequency-dependent matrix impedance tensor **Z** as shown by Equation 3-15.

$$\begin{pmatrix} E_x \\ E_y \end{pmatrix} = \begin{pmatrix} Z_{xx} & Z_{xy} \\ Z_{yx} & Z_{yy} \end{pmatrix} \begin{pmatrix} B_x/\mu_0 \\ B_y/\mu_0 \end{pmatrix} \qquad \text{Equation 3-15}$$

or

$$\mathbf{E} = \mathbf{Z}\,\mathbf{B}/\mu_0$$

According to Khoza (2016) and Miensopust (2010) (as cited in Weaver *et al*, 2000) the MT tensor **M** an identical description of the transfer function was introduced and derived using the **B** instead of **H** field. Both **Z** and **M** are complex, where each matrix element is a complex number containing real and imaginary parts.

$$\begin{pmatrix} E_x \\ E_y \end{pmatrix} = \begin{pmatrix} M_{xx} & M_{xy} \\ M_{yx} & M_{yy} \end{pmatrix} \begin{pmatrix} B_x \\ B_y \end{pmatrix} \qquad \text{Equation 3-16}$$

or

$$\mathbf{E} = \mathbf{M}\mathbf{B}$$

3.5 CHALLENGES OF MT SURVEYS

MT soundings are influenced by industrial electromagnetic inductive and galvanic noises (Bubnov *et al*, 2007). The inductive noise is due to electric power lines, whereas galvanic noise is caused by more intense current leakages from electrified railroads. At high frequencies weaker MT signals are dominated by galvanic noise caused by the electric circuit between the locomotive and the nearest power substation as shown in Figure 3-1. Galvanic noise disappears and MT curve returns to normal when acquisition was done at greater distance from the railroad. For very strong industrial noise the use of controlled source measurements are necessary.

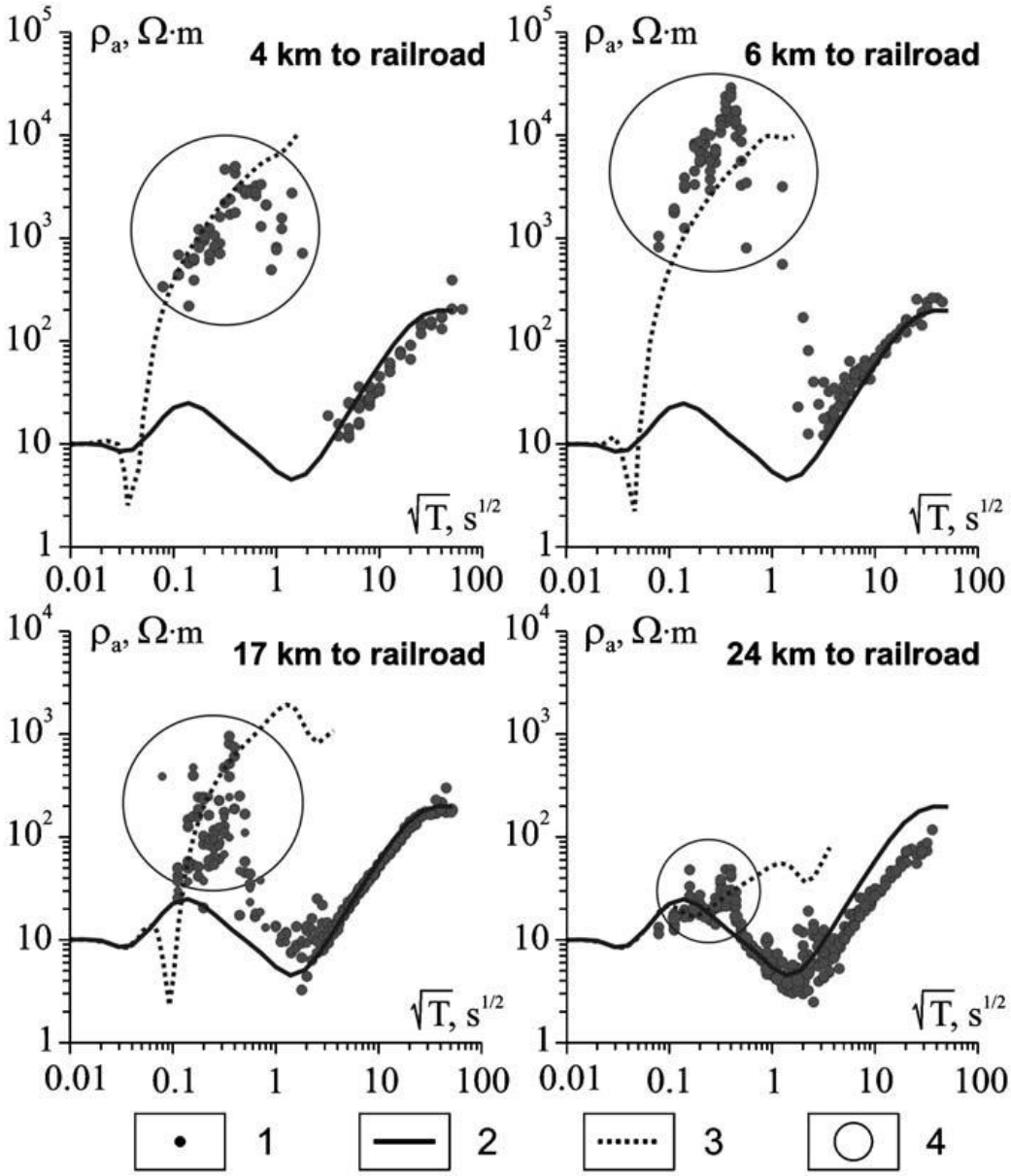

Figure 3-1: Observed and modelled apparent resistivity curves near electrified railroad). 1 – Observed curve, 2 – result of forward modelling using plane wave source, 3 – the same using horizontal electric dipole as a source, 4 – zones where apparent resistivity is influenced by the electrified railroad (Bubnov *et al*, 2007)

Chapter 4:
SITE DESCRIPTION

4.1 REGIONAL SETTING

The town of Beaufort West in the Central Karoo is geographically situated $32^0$21'S; $22^0$35'E, about 450 km north east of Cape Town along N1 route to Johannesburg. The town was originally established as a service centre for rail and road transport and to a lesser degree of rural agriculture during the historic years. Today both rail transport and agriculture have decline as economic opportunity, with only road transport been maintained for growth with minimal level managed. The town Beaufort West has been chosen as a suitable location of the study area, which the survey begun within the vicinity of the dry Beaufort West Dam (Figure 4-1). North of Beaufort west about 1450 m above mean sea level Nuweveld Mountains rises up to a plateau (van Wyk, 2010). The Nuweveld Mountains are flat topped and capped by more resistant thick dolerite sheets. The base of the escarpment acting as a watershed between the north and south flowing river accommodated Beaufort West (van Wyk, 2010).

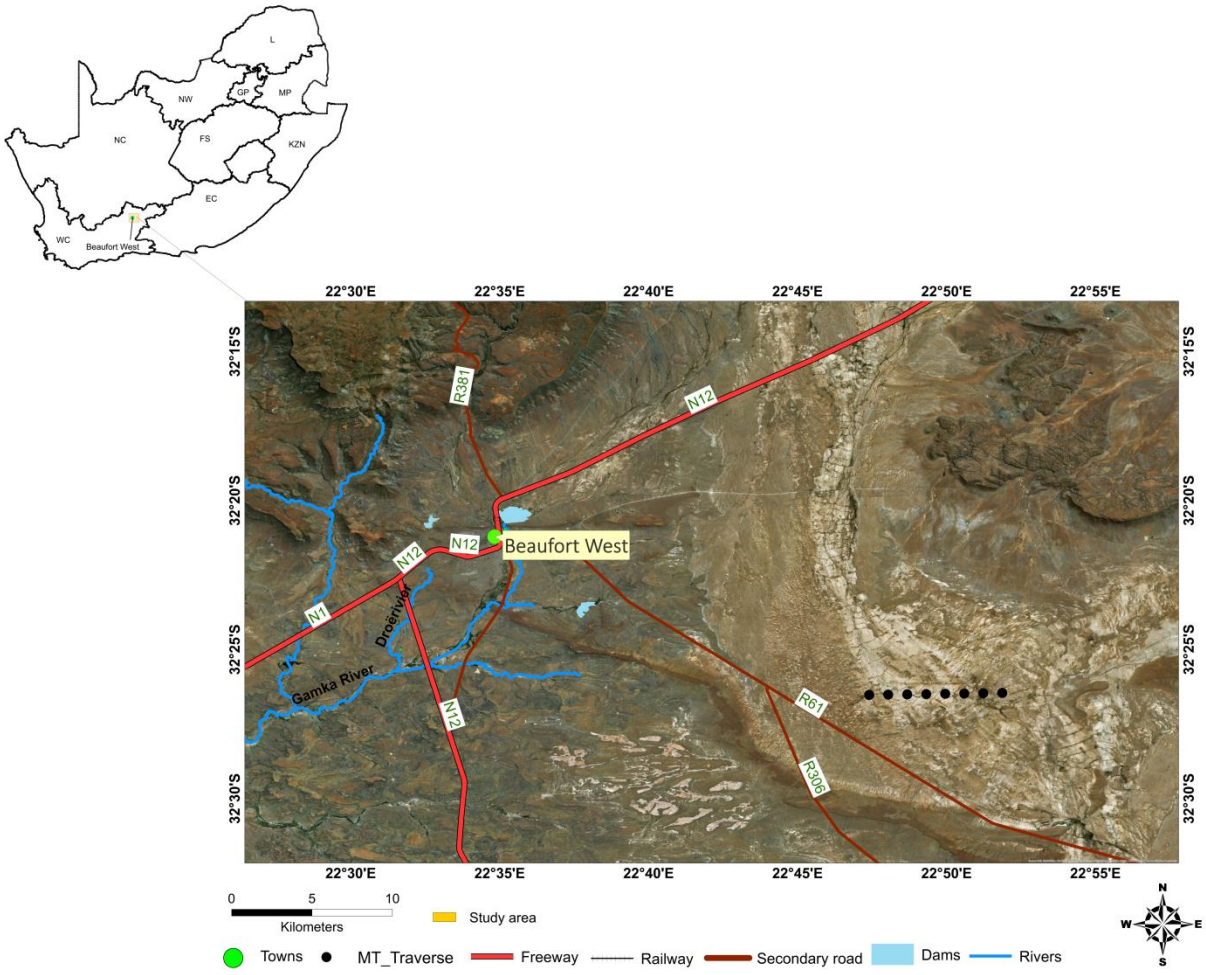

Figure 4-1: Location of the study area in Beaufort West

4.2 THE GEOLOGY OF THE KAROO SUPERGROUP

4.2.1 Regional geology

The economically important Karoo Supergroup covering more than half of South Africa is the host to all coal and uranium deposits in the Republic. It covers an area of about 700 000 km^2 in the southern- central portion of South Africa (Figure 4-2). The Karoo Supergroup comprises the Karoo sedimentary basin intruded by the Karoo dolerite dykes and sills and capped by a Drakensberg lava pile. The term "*Karoo*" has been used to describe the sedimentary fill of other similar-aged basins across Gondwana. The Karoo Supergroup sediments were deposited during the late Carboniferous (300 Ma) to early Jurassic 183 Ma periods (Catueanu *et al.*, 2005*;* Nhleko, 2008) and has a maximum cumulative thickness of about 12 km^2 in the southeastern part of the basin (Johnson *et al*, 2006).

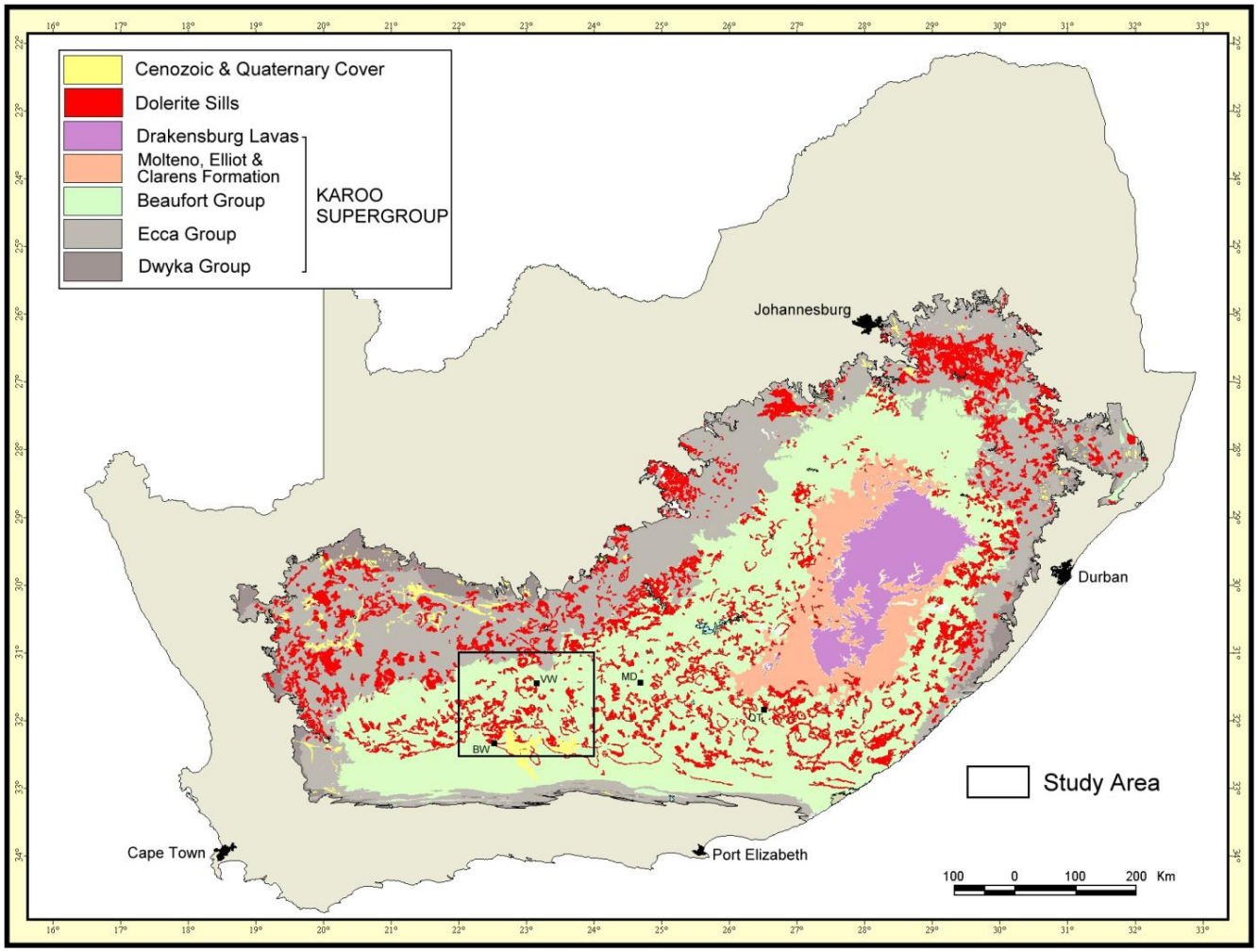

Figure 4-2: Location of the Karoo Supergroup including schematic areal distribution of lithostratigraphic units in the Main Karoo Basin of South Africa in relation to the study area (Cole *et al*. 2016)

The Main Karoo Basin situated inbound of a palaeo-magmatic arc can be classified as a retro-arc foreland basin which is underlain by a stable floor consisting of the Kaapvaal Craton in the north

and the Namaqua – Natal Metamorphic Belt in the south, and bounded along the southern margin by a fold thrust belt (Johnson *et al*, 2006). The major lithostratigraphic units of the Karoo Supergroup outcropping in the Main Karoo Basin are shown in Figure 4-2. These comprised of the basal Dwyka Group (tillites), overlaid by the Ecca Group (marine shales), Beaufort Group (terrestrial mudstone, siltstone and sandstone), Stormberg Group (terrestrial and aeolian sandstone, mudstone and siltstone) and Drakensberg Group (volcanic basalts), Johnson *et al*, (2006).

The Dwyka Group consists of a variety of glacial to periglacial sediments deposited during the late Carboniferous to early Permian forms the basal unit of the Karoo Supegroup. At sites in the northern part of the basin well-developed, striated glacial pavements on pre-Karoo basement rocks are present. The Dwyka Group is dominated by diamictite or "tillite", but subordinate mudstone, sandstone and conglomerate and other glacial related rocks occur. The Dwyka Group unconformably overlies the Cape Supergroup in the south, but progressively older Precambrian rocks northward. In the east it unconformably overlies the Natal Group and Msikaba Formation (Johnson *et al*, 2006).

The Permian Ecca Group which contains significant coal deposits underlies much of the Karoo Basin (Figure 4-2). Rocks of the Ecca Group outcrops all round consist of a clastic sequence of mudstone, siltstone, minor conglomerate, sandstone and coal in the northeastern part of the basin (Catuneanu *et al*, 2005). The Ecca Group has a maximum thickness of about 3000 m in the southern part of the Main Karoo Basin and is characterized by formations which reflect lateral facies changes.

The Permo-Triassic Beaufort Group reaches maximum thickness of about 5000 m, is made up of mudstone and subordinate interbedded sandstone and conformably overlies the Ecca Group. The group has been lithostratigraphcally subdivided into a lower Adelaide Subgroup and an upper Tarkastad Subgroup. The Adelaide Subgroup, which dominates the study area, was deposited during Late Permian times (~ 260 - 252 ma) and is composed of fine- to medium- grained, bluish-grey mudstone with alternating grey sandstone. The Early Triassic (~ 252 - 240 ma) Tarkastad Subgroup is dominated by sandstone and red mudstone. The Beaufort Group absolute age was reported by Catuneanu *et al*. (2005) as not perfectly constrained but due to abundance of fossil tetrapods and vast exposure in the Main Karoo Basin biostratigraphic subdivision was considered as shown in Figure 4-3. However, more recently, Rubidge *et al* (2013) used U-Pb dating of zircons in volcanic tuffs to date the interval between the zones pristerognathus and cistecephulus (Figure 4-3) at between 261 and 255 ma.

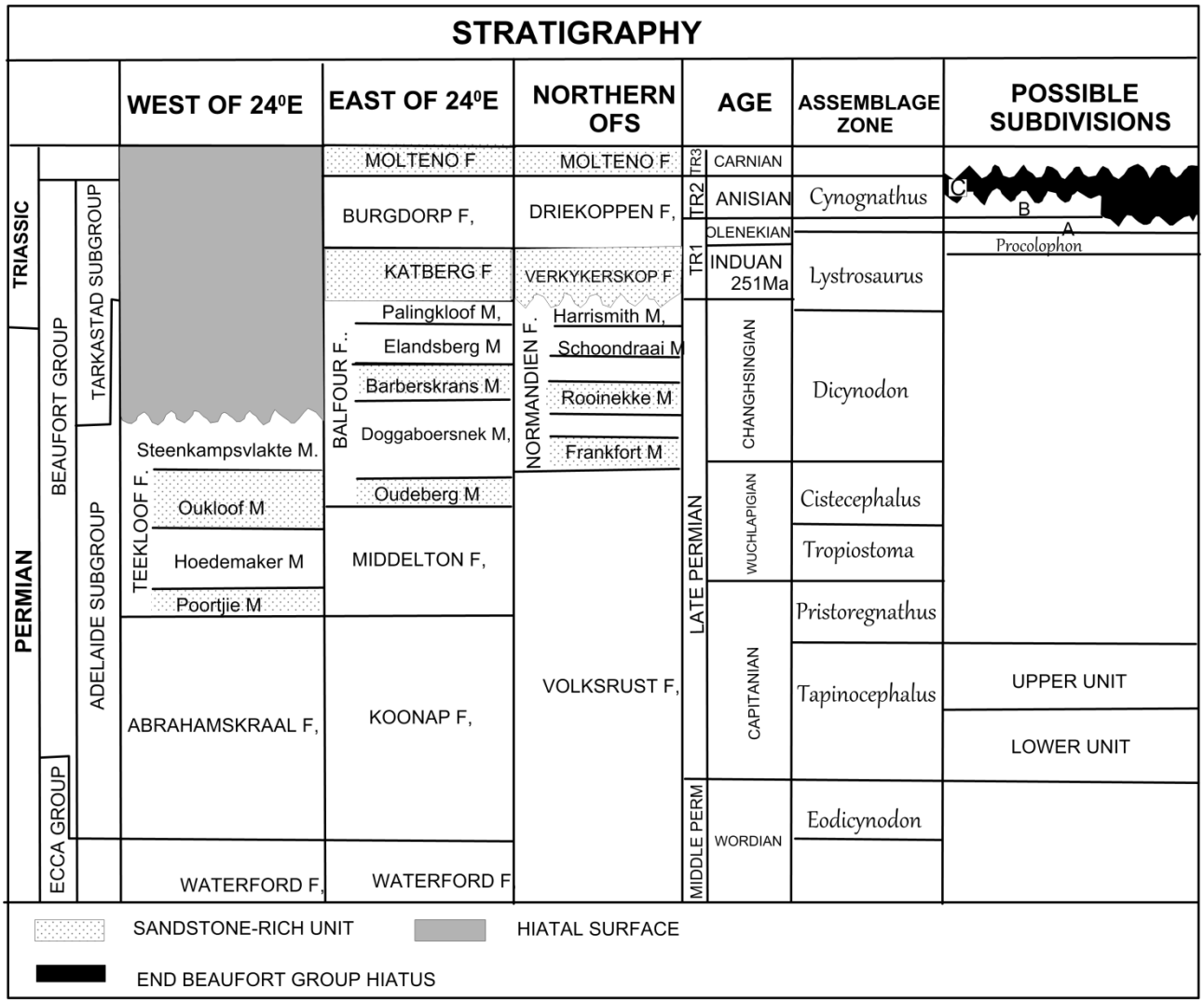

Figure 4-3: Relationship between the biostratigraphy and lithostratigraphy of the Beaufort Group in Main Karoo Basin of South Africa (Catuneanu *et al,* 2005)

The Stormberg Group which predominantly consists of limnic continental sediments is made up of the Molteno, Elliot and Clarens Formations (Figure 4-3) and has been separated from the underlying Tarkastad Subgroup by a major stratigraphic gap of the late Anisian- Ladinian (Tamssar, 2013; Nyathi, 2014). The Molteno Formation of Late Triassic age (~237 – 220 ma) is characterized by medium-to fine-grained, pale sandstones and pale olive mudstones. The late Triassic to early Jurassic (~220 – 190 ma) Elliot Formation is made up of fine-to medium-grained sandstones and predominant greyish-red mudstones (Johnson *et al*, 2006). The Clarens Formation was deposited during early Jurassic (~190 – 183 ma) comprises of well-sorted wind-blown, fine grained sandstone and siltstone (Nhleko, (2008), cited in Johnson *et al*., (1997)). The Drakensberg Group marks the end of sedimentation in the Main Karoo basin during the early Jurassic at around 183 ma. It is composed of mafic volcanic basalt with minor felsic rhyolite in upper part. In the upper most part of the underlying Clarens Formation, basaltic lava flows are present, indicating a conformable succession (Johnson *et al*, 2006).

4.2.2 Dolerite intrusions and volcanic activity

The following description by Chevallier (in Cole *et al*., 2016a) refers:

The Jurassic dolerite dykes and sills were intruded into the Karoo sediments during a period of extensive magmatic activity that took place over almost the entire Southern African subcontinent during one of the phases in the Gondwanaland break-up.

The dolerite intrusions represent the roots and the feeders of the extrusive Drakensberg basalts that have been dated circa 180 My (Duncan *et al*., 1997; Fitch and Miller, 1984; Richardson, 1984) and are one of the largest outpouring of flood basalt in the World. The total volume of magma extruded on the Southern African Continent has been estimated at 10 million km^3 (White, 1997).

The Jurassic Karoo sills and dykes comprise up to 30% of the Basin's thickness and are present within the entire basin area representing at least 340,000 km^3 of dolerite (Chevallier and Woodford, 1999). The dolerite intrusions consist of an interconnected network of dykes, sills and ring-like (saucer –shape) intrusions, and it is nearly impossible to single out any particular intrusive or tectonic event (Figure 4-4). Recent U–Pb zircon (and baddeleyite) ages have been obtained for fourteen samples of Karoo sills, rings and dykes spaced across the Karoo Basin (Svensen *et al*. 2012). The samples yield coherent ages in a narrow range from 183.0±0.5 to 182.3±0.6 myr. Probability modelling indicates that basin scale emplacement took place within an interval of about 0.47 myrs (less than 0.90 myrs with 95% confidence), and confirm that it could have represented a single magma emplacement event. Combining the new ages with the estimated volume of sills in the Karoo Basin gives an emplacement rate of 0.78 km^3/yr (Svensen *et al*.2012). It would therefore appear that a very large number of fractures were intruded simultaneously by magma and that the dolerite intrusive network acted as a shallow stockwork-like reservoir.

The term Karoo dolerite includes a wide range of petrographical facies which extends from leuco-gabbro to granophyric dolerite, with the mostly abundant dolerite sensu stricto (Chevallier and Woodford, 1999).

This massive sill and dyke emplacement led to widespread phreatic and phreatomagmatic activity and the release of thousands of gigatons of carbon gas from the contact metamorphosed organic-rich sediments (Svensen *et al*., 2007).

Large-scale erosion of the main Karoo Basin has revealed large portions of the intrusive system and a degree of tectonic complexity not encountered in the other major continental intrusive systems in

the world. Many near vertical dykes are branching onto the sill and rings or cutting through them. Du Toit (1905, 1920) was the first researcher to describe these dolerite sills and rings complexes in the vicinity of Queenstown. For the past twenty years the Water Research Commission and the Department of Water and Sanitation have coordinated and funded numerous research projects on Karoo fractured aquifers related to dolerite dykes and sills (Burger *et al*. 1991, Woodford and Chevallier, 2001, 2002; Chevallier *et al*. 2001, 2004, Dondo *et al*. 2004). They involved both intensive localized and extensive regional studies and were aimed at understanding the structure, the dynamics and the exploitability of these aquifers. The research was completed by collaboration conducted by various research institutions, universities, governmental organizations, private consultants and international collaboration. The saucer-shape model showing the relation between the dykes, the sills and the ring-like inclined sheets and the groundwater occurrences was published by Chevallier and Woodford (1999).

Because of this structural complexity dolerite intrusion has always been and still good prospective targets for groundwater.

Dykes: Dolerite dykes that are vertically to sub vertical discontinuity generally range from 3 to 15 m in thickness. Long dykes (500 km to 800 km) can be very thick. The E-W dyke north of Victoria West attains a thickness of 65 m in places. Dykes thinner than 3 m, are usually limited in length. Dykes, representing thin, linear zones of relatively higher permeability, have always been the preferred drilling targets for groundwater (Woordford and Chevallier, 2002a). These structures are easily identified by a line of green bushes, mostly during dry seasons. However geophysical techniques can also be used in areas where green bushes are limited. Woodford and Chevallier (2002a) reported dykes as the preferred drilling targets by many groundwater practioners, with strikes down to 200 m and blow yield up to 15 l/s.

Sills and rings: Dolerite sills intruded Karoo sediments as sheet like forms that tend to follow bedding planes (Botha *et al*, 1998). Thin extensive flat sills are found at the base of the Karoo succession whereas ring-like dolerite inclined sheets, forming part of the rims of the sills are found towards the top. The dolerite sills and inclined sills are responsible so-called saucer shape dolerite intrusion the emplacement of which have been studied by Chevallier and Woodford (1999) and Poltaeu (2004). Inclined sheet/rings have been found to be good targets for groundwater with strikes down to 300m and blow yield up to 30 l/s (Chevallier *et al*., 2001). Generally due to their complex structure, size, thickness they have been subject overlooked by geohydrologist and drillers.

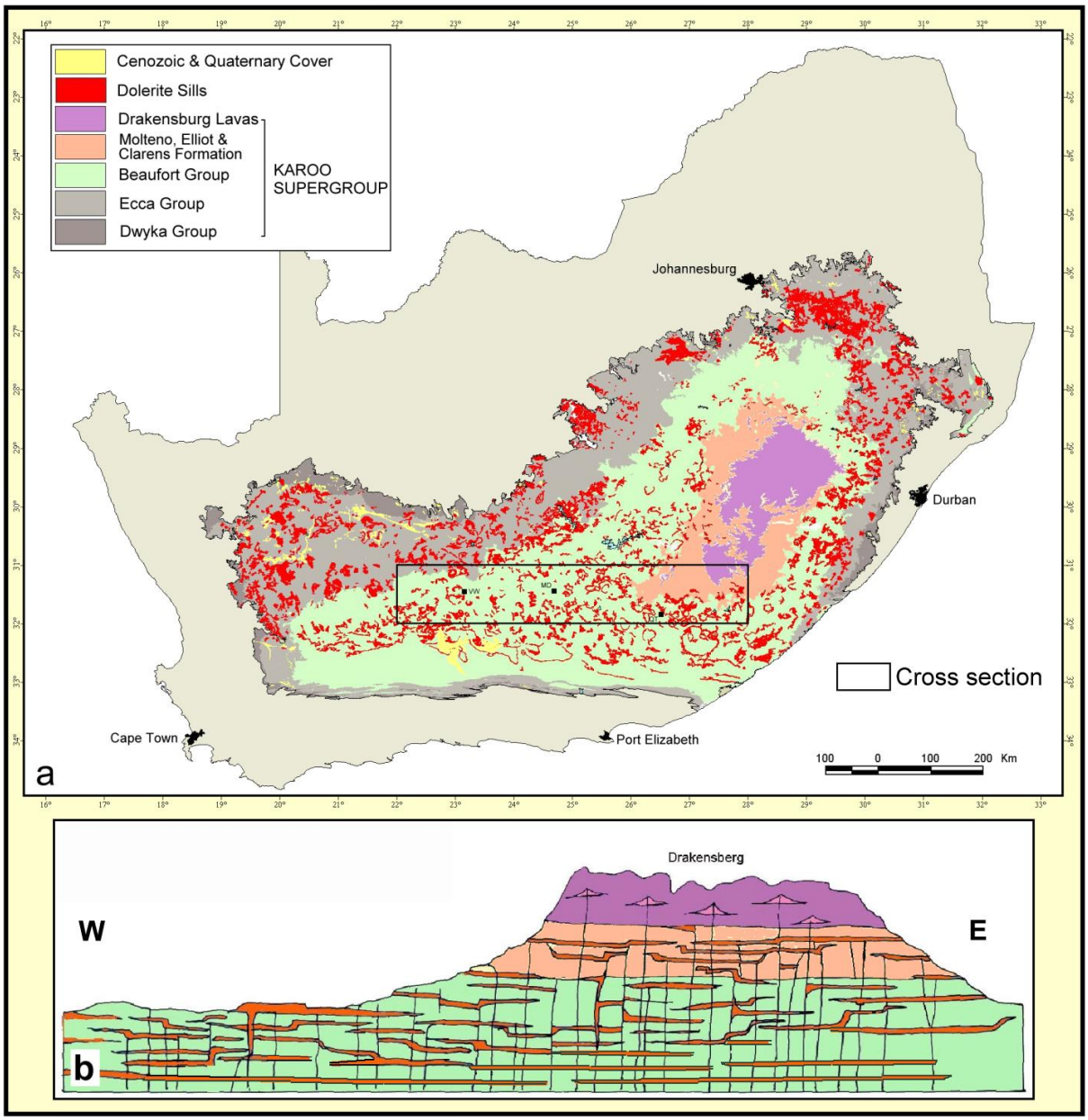

Figure 4-4: General extends and habit of the Karoo dolerite intrusions (after Chevallier *et al.* 2001). (a) Geological map showing the extent of the Jurassic magmatic rocks (Drakensberg lavas and dolerite intrusions) (b) Schematic W-E cross-section of the Karoo Basin showing the complexity of the dolerite dykes, sills and saucer-shape intrusion network forming a shallow crustal stockwork-like reservoir below the erupted Drakensberg

4.2.3 Local Geological Setting

The Beaufort Group lying conformably on the Ecca Group was deposited in a terrestrial environment during the late Permian to middle Triassic times. The transitional and diachronous Ecca – Beaufort boundary records a gradual change from deltaic to fluvial depositional systems taking into consideration the tilling of the basin and northward progradation of Beaufort Group sediments (Turner, 1981; Catuneanu *et al*, 2005). The Permo-Triassic rocks cover a surface area of about 200 000 km^2 or about 20% of the total surface area of South Africa and thicken to about

7000 m in the fore deep in the south of the basin and thin rapidly northwards (Catuneanu *et al.*, 2005; cited in Johnson *et al*., 1997).

The Beaufort Group comprising predominantly of mudstone and siltstone with subordinate, lenticular and tabular sandstone is subdivided into the Lower Adelaide and Upper Tarkastad Subgroups, of which the former, completely occupies the study area (Figure 4-5). The late Permian Adelaide Subgroup attains a maximum thickness of about 2000 m and was formerly divided into the Koonap, Middleton and Balfour Formations in the south-eastern part of the basin, and the Abrahamskraal and Teekloof Formations in the southwestern part of the basin (Johnson *et al*, 2006; van Wyk and Witthueser, 2011). However, the Karoo working Group of the SACS has amalgamated the two sets of formations into Abrahamskraal, Middleton and Balfour Formations, in ascending order (Cole *et al*, 2016a).

The Abrahamskraal Formation in the study area represents sediments that were deposited with the more abundant murdocks representing flood-basin deposits and the sandstones of sinous fluvial channel and less abundant ephemeral. The Abrahamskraal Formation confined to the south-western portion of the map area, is gently folded towards the south and has an estimated maximum thickness of 300 m (Cole *et al*, 2016a). The Middleton Formation in the study area contains a lower sandstone-rich unit named Poortjie Member and an upper mudstone-dominated unit named the Hoedemaker Member (Cole *et al*, 2016a). It is mostly present in the lower portion of the Great Escarpment and on the peneplain south of the escarpment. The beds are gently dipping and intruded by dolerite sills and dykes (Figure 4-5).

The Poortjie Member consists of a series of thick sandstone bodies between 5 and 15 m thick interbedded with mudstone and subordinate siltstone (Cole *et al*, 2016a). The sandstones represent fluvial channel deposits and the mudstone and siltstone (mudrock) represent overbank and floodplain deposits. The Poortjie Member has an estimated thickness of 204 m in the map area (Cole *et al*, 2016a). In the study area, the Hoedemaker Member has a maximum thickness of 285 m in the Karoo National Park and is characterised by a predominance of reddish-coloured mudstone (Cole *et al*., 2016a). Subordinate dark greenish grey mudstone and isolated sandstone bodies up to 19 m thick occur in places (Cole *et al*., 2016a). The presence of thick reddish-coloured mudstone suggests deposition on a vast arid floodplain with rare influxes of meandering rivers giving rise to the sandstone bodies (Smith, 1990).

The Hoedemaker Member of the Middleton Formation is overlaid by a sandstone-rich unit, which is named the Oukloof Member and forms an extensive marker horizon at the base of the Balfour Formation (Cole *et al*., 2016a). It has a maximum thickness of 180 m in Molteno Pass and is

overlaid by a mudstone-dominated unit, named the Steenkamps Vlakte Member, with both members constituting the Balfour Formation (Cole *et al*., 2016a). This formation is present in the Great Escarpment and on the plateau north of the escarpment (Figure 4-5). The beds are flat or gently-dipping and intruded by dolerite sills and dykes (Figure 4-5).

The Oukloof Member consists of a series of thick sandstone bodies between 5 and 15 m thick interbedded with reddish-coloured mudstone and subordinate siltstone. The sandstone bodies represent fluvial channel deposits, whereas the interbedded mudstone and siltstone represent overbank and floodplain deposits (Cole *et al*., 2016a). In the study area, the Steenkamps Vlakte Member has a maximum thickness of 150 m in the Karoo National Park, but much of the unit has been significantly removed by erosion as shown by a thickness of 500 m outside the study area at its type locality, 90 km northwest of Beaufort West. The member consists predominantly of reddish-coloured mudstone, with isolated sandstone bodies up to 5 m thick. The presence of thick reddish-coloured mudstones suggests deposition on a vast arid floodplain with very rare influxes of meandering rivers giving rise to the sandstone bodies (Smith, 1990).

Several dolerite sill-rings intruded the Middleton and Balfour Formations, mostly in the Great Escarpment and on the plateau north of the escarpment (Figure 4-5). The sills vary between 50 and 150 metres in thickness. Two of these sill/rings outcrop in the lower near Beaufort West. Dolerite dykes are also present and are between 3 and 15 m in thickness. The major trends are E-W, like Tweeling-Brandwag dyke North of Beaufort West and NNE-SSE. No dyke is found near Beaufort West (Cole *et al*., 2016a).

A Quaternary cover of unconsolidated alluvial, colluvial, eluvial and scree sediments, as well as calcrete, cover large parts of the ground service within the study area, particularly south of the Great Escarpment (Figure 4-5; Cole *et al*., 2016a). Two sediment filled valleys are crossing the study area (Mosavel *et al*., 2016): the Gamka Valley going through Beaufort West (with thick alluvial deposit 2 to 10 m thick) and the Platedooring in the East (filled with alluvials 10 to 30 m thick).

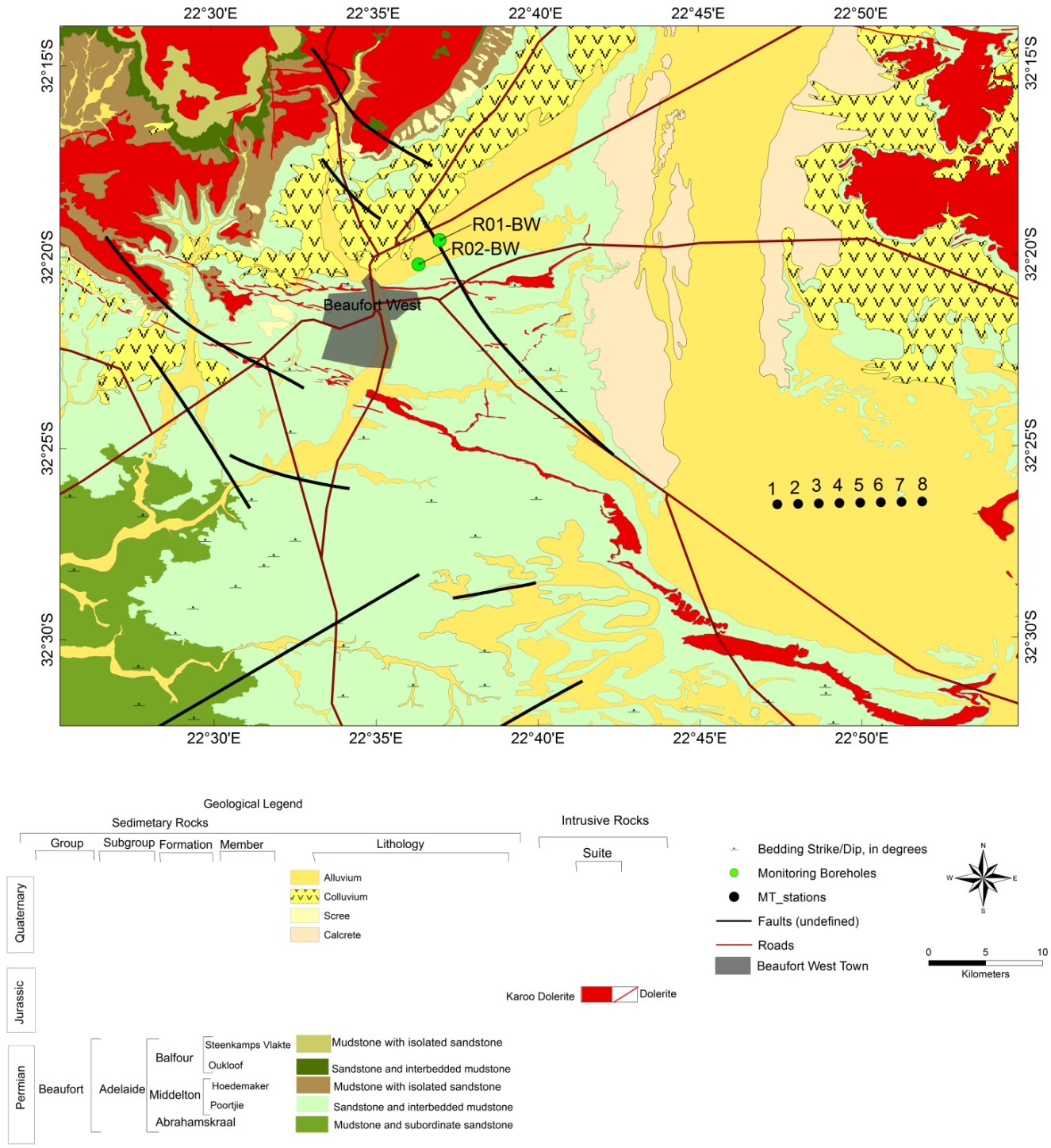

Figure 4-5: The geology map of the study compiled by Cole *et al.* (2016a). Note that the Poortjie and Hoedemaker Members form the Middleton Formation and the Oukloof and Steenkamps Vlakte Members form the Balfour Formation

4.3 TOPOGRAPHY AND DRAINAGE

The study area falls within the Gamka sub-area covering an area of 19 051 km² with surface elevations ranging between 750 mamsl to 1000 mamsl, as compared to other low lying. The topography is characterised by hills in the north- North West (Figure 4-6). The resistant dolerite

sheets which controls the morphology and forms topographical highs, may receive more rainfall than flat lying regions.

The study area is found in the north eastern portion taking up 4% of the Gamka sub-area. The two main perennial rivers which make up surface water bodies are Gamka and Kwagga. The Gamka River (Figure 4 6) rising from the mountains of the Great Karoo north of Beaufort West forms the major part of catchment J21A. Leeuw and Koekemoers Rivers of quaternary catchment J22A joins Gamka River at Leeuw Gamka and flows southwards into the Gamkapoort Dam. Gamka River forms part of the main Gouritz River tributaries. The Gouritz River which drains an area of about 45 702 km^2 enters the Indian Ocean in quaternary catchment J40E (Nxokwana et al, 2018a).

The two main dams found in catchment J21A are Gamka and Springfontein dams. The Gamka Dam is located north of Beaufort West and is managed by the South African Department of Water and Sanitation and operated by the Beaufort West Municipality. The Gamka Dam has a total capacity of 1.8-1.9 million m^3, with 0.6 Mm^3used mainly for municipal domestic water supply to the local town (Nxokwana et al, 2018a). The Springfontein Dam lies immediately outside Beaufort West, towards south west. It is currently owned by the municipally. The Springfontein Dam which lies immediately outside Beaufort West towards south west is currently owned by the Municipality and has an unknown capacity, although the dam is used for local water supply.

4.4 CLIMATE

The Beaufort West similarly to the Karoo Region receives summer rainfall (Dec-Feb) which was measured as highest rainfall ranging between 200 to 300 mm, however the value may increase to 400 mm in high mountainous terrain and decrease to about 100 mm in flat lying plains (Nhleko and Dondo, 2008; Nhleko, 2008; van Wyk, 2010; Beaufort West Municipality annual report 2012/2013). Van Wyk, (2010) have obtained from the Beaufort West Municipality a continuous long term rainfall data over the past thirty eight years which indicate a high pick in the 1970's and 80's (Figure 4-7).

The mean annual precipitation is averaged to more than 400 mm, while mean annual evaporation is averaged to more than 2400 mm. As mentioned earlier in this sub-section higher elevation areas receive more rain than lower, was confirmed by the statement "there is a direct correlation between elevation above sea-level and rainfall" (Nhleko, 2008 as cited in Smart, 1998).

The site has extremely high temperatures during summer seasons of about 40^0C and may drop to below zero (± -5^0C) during winter season.

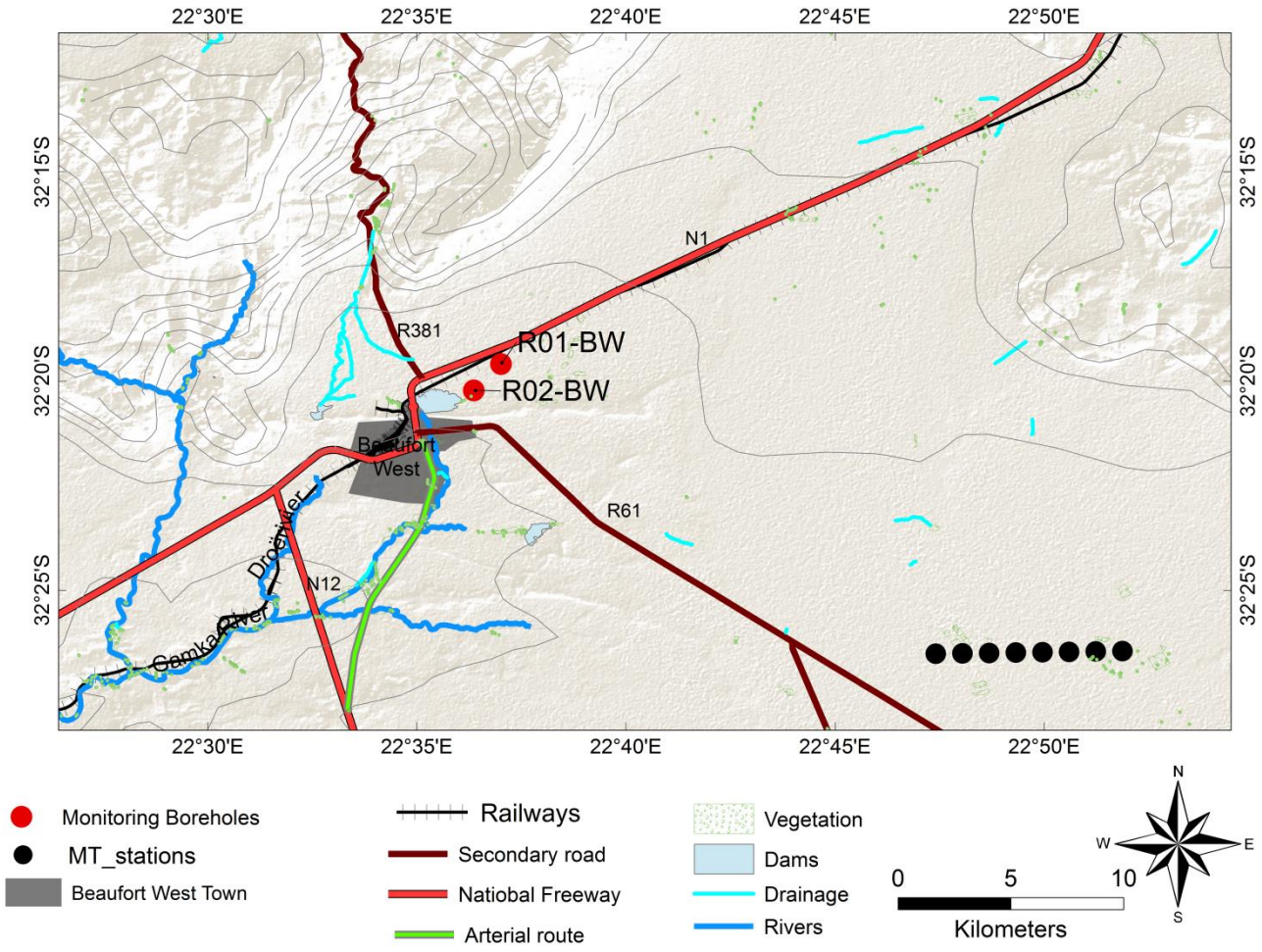

Figure 4-6: Topographical map showing drainage and major river

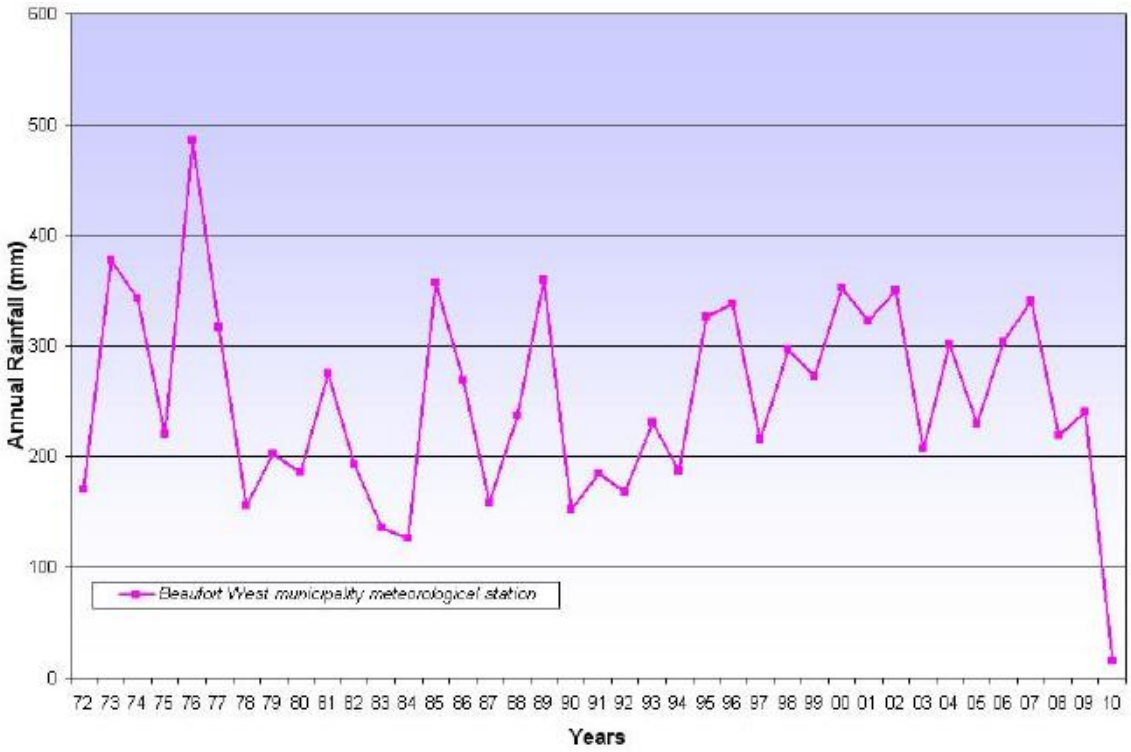

Figure 4-7: Long-term annual rainfall for Beaufort West (van Wyk, 2010)

4.5 SOIL COVER

The area is covered with loam sand, and mixture of loam sand and sand loam type of soil. It is only in the north western part of the quaternary where loamy sand-sandy loam type of soil is found (Nxokwana *et al*, 2018a).

4.6 HYDROGEOLOGY

Sandstone and mudstone of the Beaufort Group are generally characterized by low primary porosity and permeability due to diagenesis. The movement and storage of groundwater is therefore controlled by secondary hydrogeological properties like sedimentary discontinuity or structural complexity (degree, density, continuity and interconnection of fracturing, dolerite dykes and sills) processes. Thus the lateral migration of meandering streams over a floodplain complicates the geometry of the Beaufort aquifers. This has assumed the aquifers in the Beaufort Group to be multi-layered and porous with variable thicknesses. The fracture Karoo rocks (mainly caused by dolerite intrusions) are multi-layered, highly heterogeneous and isotropic comprises of low and variable permeability. Most of the study area is characterised by fractured-rock aquifers as highlighted by the 1:500 000 hydrogeological map series 3122 of Beaufort West. Intergranular were also found to exist due to occurrence of alluvium. High yielding boreholes value averaged to about 5 l/s, but reaching as high as 30 l/s are found within the fractured rock aquifers, while dual porosities produce yields ranging between 0.1-0.5l/s (van Wyk, 2010 as cited in Rose, 2008).

More locally the hydrogeology study of the Beaufort West commonage by Nhleko and Dondo (2008) divided the aquifer systems into three aquifer horizons. Shallow aquifer (top aquifer) which extends to a depth of about 10 m where paleo-channels are not intercepted is characterized by weathered intergranular material comprising of sandstones, mudstones, siltstone and possible dolerites. It is probable that this top aquifer is directly recharged by precipitation and surface water sources. Based on secondary processes associated with dolerites intrusions, secondary fractured rock aquifer (aquifer II) found at depth 50 m or more is characterized by mainly sandstones and mudstones (Nhleko and Dondo, 2008). Furthermore aquifer at depth between 80 – 90 m was identified by Nhleko and Dondo (2008) through correlation of borehole log data. The aquifer comprises of sandstone and other sediments that have been fractured during dolerite intrusions (Nhleko and Dondo, 2008).

Chapter 5:
AIRBORNE AND GROUND GEOPHYSICAL SURVEYS

5.1 INTRODUCTION

Geophysical investigation often plays an important role in exploration projects. For the success of the project it is crucial to invest time and money for geophysical investigations on initial phase of the exploration program. For the current study the company Aerophysix was contracted to conduct airborne survey across the study area. The results will be essential in updating the geology map and delineate intrusive magmatic bodies that are not outcropping to the surface.

Geophysics a geoscientific discipline that studies the Earth using principle of physics is increasingly being used to characterize the subsurface. Despite its advantage to minimize the risk of wasteful expenditure by drilled uninformed holes, geophysical data suffers from non-uniqueness and ambiguity in the interpretation of results. An effective approach to overcome this challenge is to integrate geophysical methods in conjunction with other geophysical techniques and geoscientific disciplines.

5.2 SURVEY GEOMETRY

For the current study, a combination of high resolution aeromagnetic and deeper probing ground geophysical data were used to better understand the aquifer system within the study area. High resolution magnetic data is necessary in mapping sills and dykes that are not exposed at surface. Deeper probing surface geophysical data is useful in obtaining information at depth that shallow drilling could not reach.

5.2.1 Airborne magnetic survey

High resolution aeromagnetic data was flown by Council for Geoscience (CGS) as part of the Karoo deep drilling programme (Figure 5-1). The aim of the survey was to assist in updating geological information as well as mapping sills and dykes that are not outcropping. The aeromagnetic data covering a total of about 72 300 line kilometres was acquired at a ground clearance of ±80 meters (subject to safety) and a line spacing of 200 m. The orientation of the flight lines were west-east assuming that the general strike direction of most lithological units was nearly south-north. The data was flown between May and September 2017 by Aerophysix a company contracted by the CGS. The datasets were collected at a sampling frequency of 10 Hz using a Scintrex CS-3 Caesium vapour mounted in a wing tip and the instrument sensitivity is 0.0006 nT

Hz ^{½} (AeroPhysix, 2017) as shown in Figure 5-2. The model 539, three-axis fluxgate magnetometer was used to monitor the attitude of the aircraft. The Geometrics G829 caesium vapour magnetometer was used as a base station to monitor temporal variation of the Earth's magnetic field.

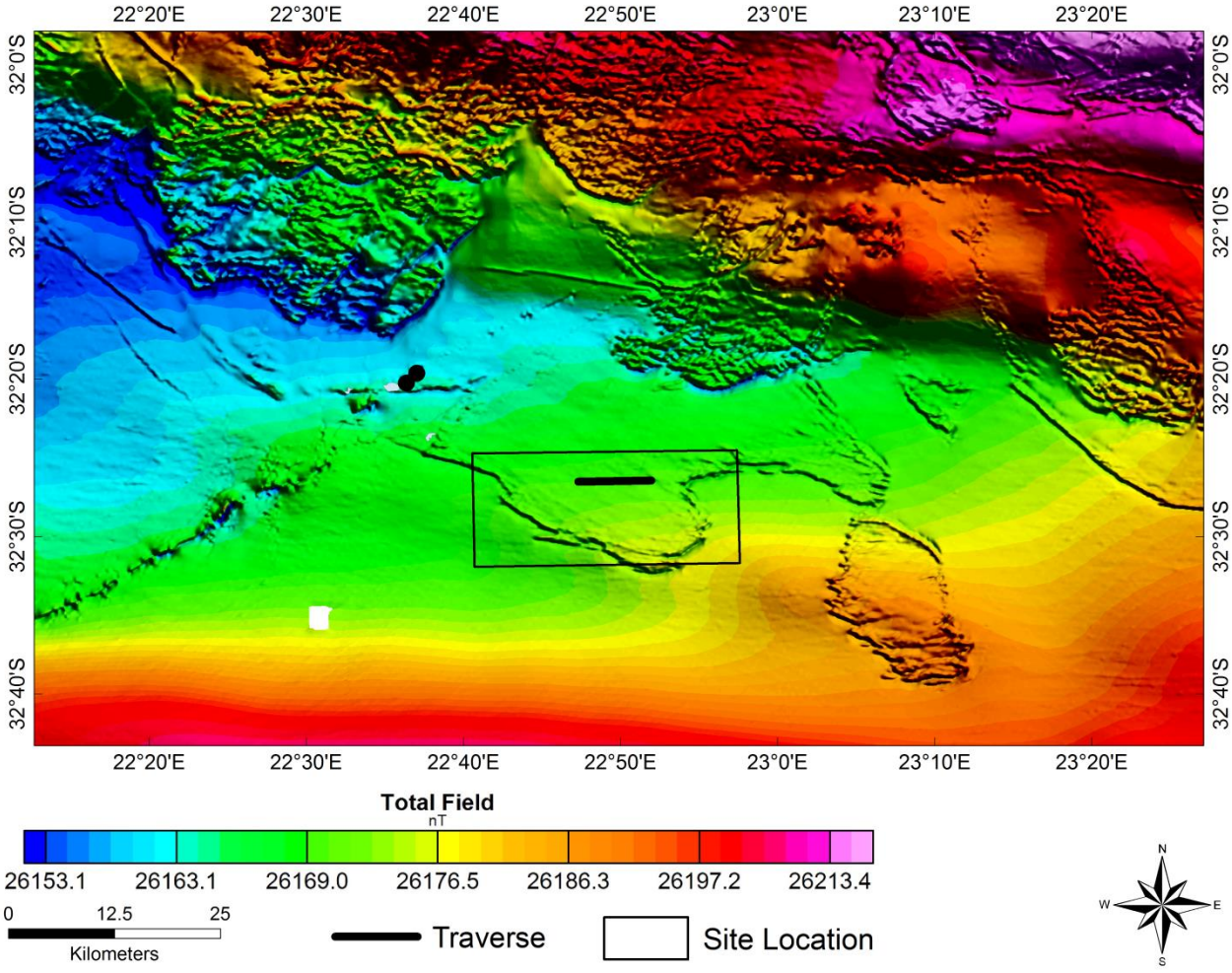

Figure 5-1: Total magnetic field map showing location of magneto telluric survey stations

After acquisition of airborne geophysical data is complete, processing is done by applying several corrections to the data. The presentation of these datasets is normally by profiles, contours and maps. Application of various filtering and transformation processes is necessary prior displaying these datasets to produce secondary products to enhance information content. Airborne geophysical data can be enhanced by a range of linear and non-linear filtering, which normally provides excellent basis for qualitative interpretation from which geological boundaries and lithologies can be inferred (Milligan and Gunn, 1997; Gunn, 1997).

The use of magnetic data to study intrusive rocks depends on various parameters. It is necessary to consider geometry, depth, intensity and direction of magnetization of host and intrusive rocks as well as the contrast between them as a principal factor. An effective approach with interpreting magnetic data is to separate magnetic anomalies into short and long wavelength approach. This is

possible by applying different filtering techniques to enhance the response magnetic signatures into these bodies.

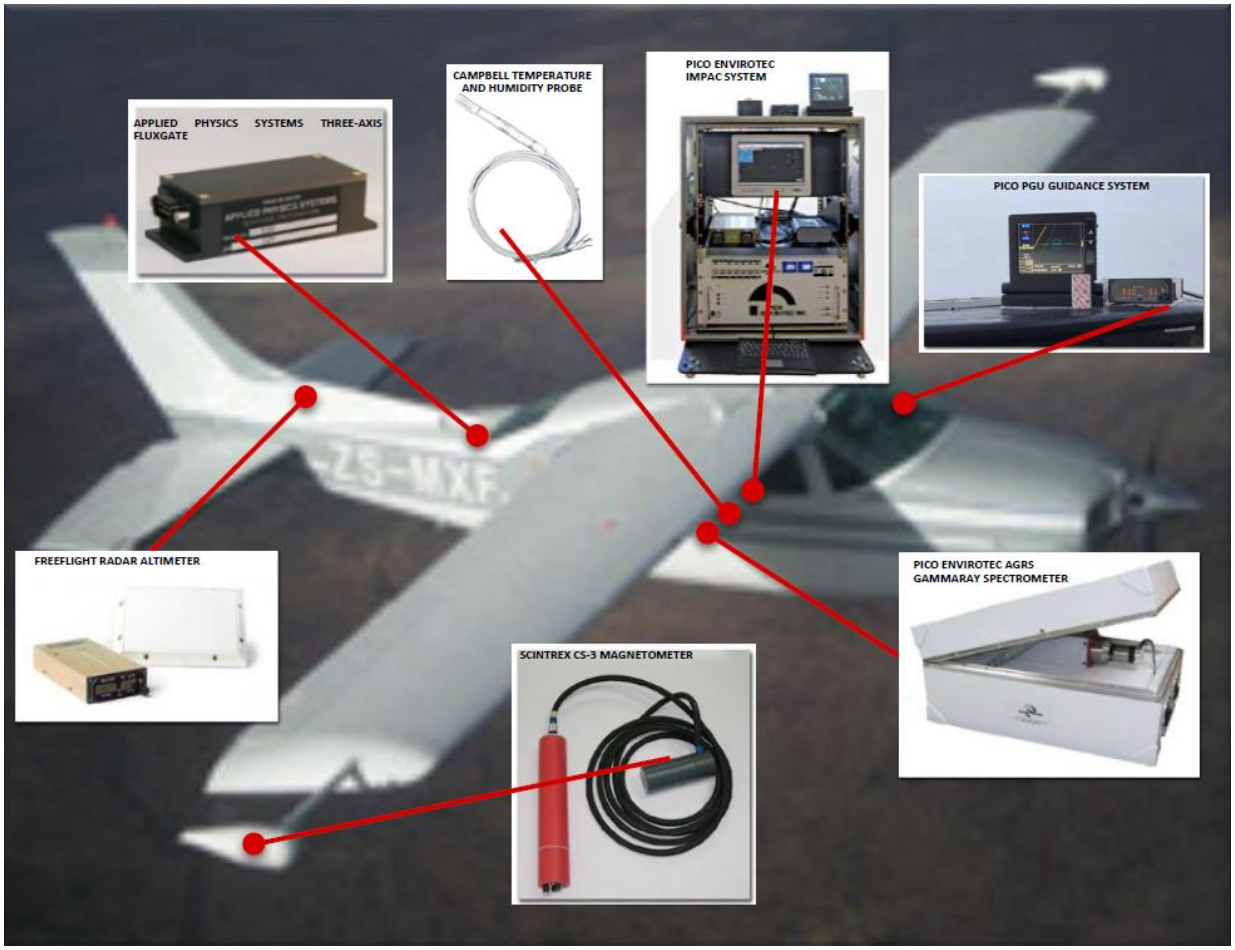

Figure 5-2: Position of instrument on Aircraft (AeroPhysics, 2017)

5.2.2 Ground magnetotelluric geophysical methods

The magnetotelluric data acquisition involves the recording of the time variations of the natural electric and magnetic fields simultaneously. Ideally both the horizontal and vertical magnetic fields can be recorded, but if need be the vertical component can be omitted. The reason for omitting the vertical component is that the vertical electric field at the air-Earth interface is zero, another one can be the logistics of setting up the 100 m vertical electric dipole has proved to be expensive (or challenging on hard ground). But on softer and easier to dig ground the vertical magnetic field can be recorded. For the electric field only the two horizontal components are recorded. To successfully acquire MT data a geological target should be selected, for the current study the primary objective is to delineate aquifer systems beneath the known depth of about 300 m.

There has been an improvement on the instrument to measure MT data. The MT instrument used for the current study was the MTU 5As developed by Phoenix Geophysics in Canada. To begin

with the survey firstly the MTU 5A receivers and all magnetic coils should be calibrated in noisy free area as shown in Figure 5-3.

Figure 5-3: Field crew setting up the MT instrument to begin the calibration of MTU 5A receivers and the coils

The MTU5As receivers are able to record data in the MT range (0.001 s – 50 000 s) and the AMT-MT range (0.0001 s - 50 000 s) respectively. A GPS antenna provides the geographic coordinates and the elevation of the site, and - more importantly - a continuous time signal, that allows accurate recording of the time series to allow synchronization with remote reference stations. The magnetic field sensors used were the 1,44m long MTC-150 induction coils. The specification of the coils indicate the range at which these coils can provide data is between 10 000 Hz to 10 000 s.

For an ideal situation MT data should be recorded away from human interference, electrical noise (e.g., DC train lines, electric fences, power lines and mining activity) and in an area with soft soil that allows the burying of all sensors and cables. Most importantly it is ideal to place the receiver in a shady spot for protection from the sun and overheating. Although the system can be placed in any orientation for measurements, for the current study a “+” shaped configuration was used as shown in Figure 5-4. In the centre of the layout is the recording unit, which consists of a MTU5A powered by 12 V car battery protected in a blue metal box. Four electrodes, to record the variation of horizontal electric fields, are orientated N-S and E-W and are buried typically 50 m away from the ground electrode. The fluctuations of the magnetic field components are recorded by two N-S and E-W oriented horizontal coils and one vertical coil. The GPS antenna provides the MTU5A with the

site geographic coordinates and more importantly with a continuous time signal, which is essential for recording the times series and later for remote reference processing with other sites

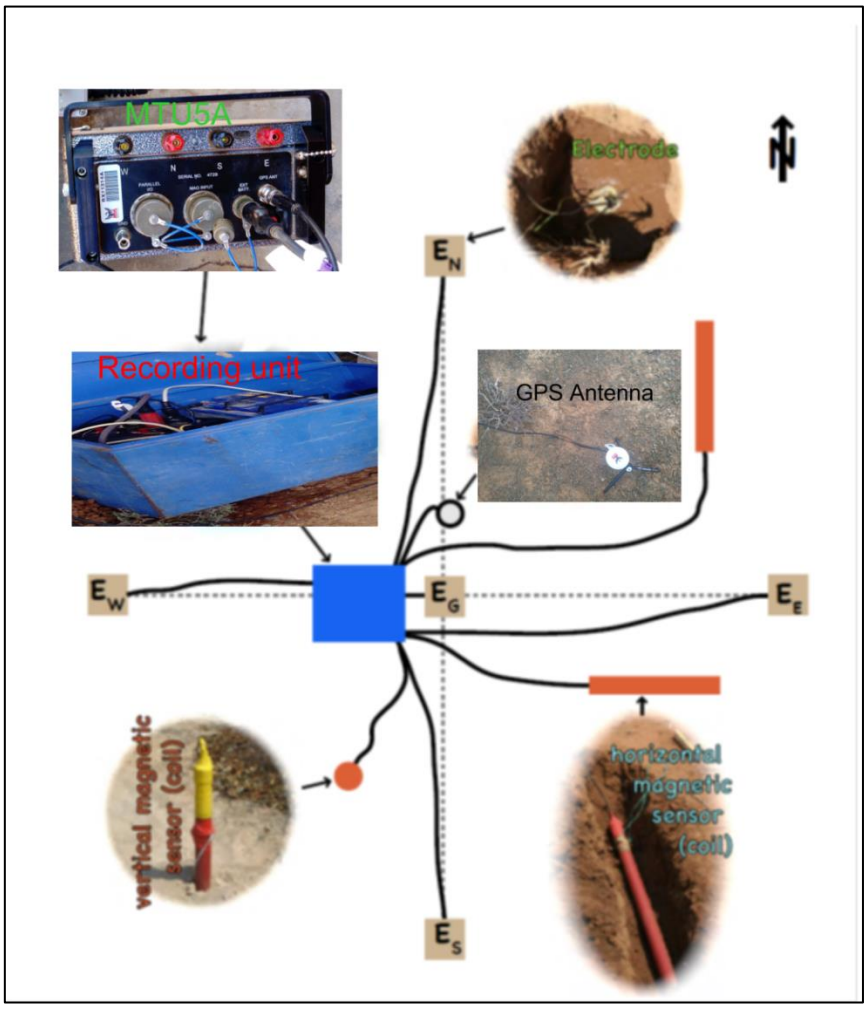

Figure 5-4: A typical survey layout for MT data acquisition using magnetometers and electric lines aligned with the magnetic north-south and east-west. (after Miensopust, 2010)

The recording unit and a ground electrode were at the centre of the layout. Four other electrodes were located in geographical orientation with respect to magnetic north - at 50 m each - north, south, east and west of the ground electrode. To lower the contact resistance with the ground and to keep the electrodes moist for longer in the hot and dry climate, they were put into buckets filled with mud made from local soil and salt water. This electrode-bucket set was buried in the ground. The magnetic sensors were also buried in the ground once they were aligned north-south or east-west (horizontal coils) and levelled (all coils). The sensors were buried to protect them against human and animal interference, avoid movement caused by wind or animals dragging on the cables and to minimize temperature effects.

The survey was conducted using two CGS Phoenix MT data acquisition system placed at 1 km interval, orientated in a west to east direction. The magnetic and electric field time series at all

stations were recorded for over 20 hours. The MTU 5A (Figure 5-5) was programmed to record both AMT and MT data overnight to compensate for best data quality.

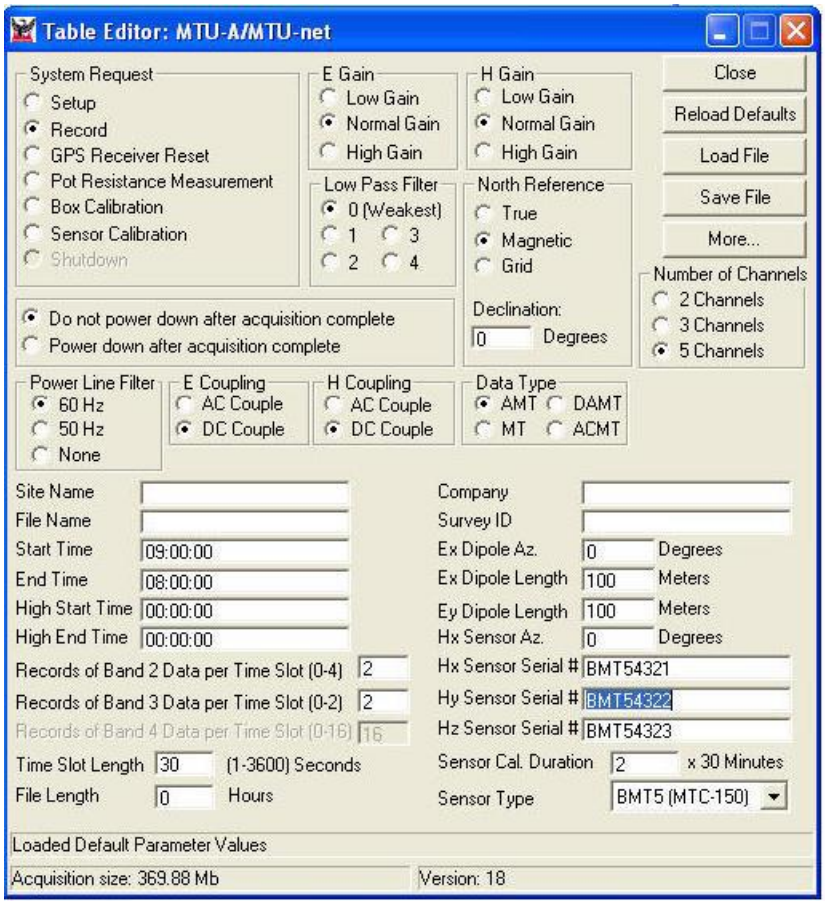

Figure 5-5: MTU5A table editor was programmed to record both AMT and MT overnight

The time series data during the MT survey can easily be recorded to a total of several Gigabytes, depending on the length of the survey and size of the flash card. One time series can contain information about many periods and penetration depths simultaneously. In order to verify if the station did record time series should be displayed to see the spikes (sferics) from the magnetic and electric fields. An example of MT time series collected at a site near Beaufort West is presented in Figure 5-6. The time series present data from the Ex, Ey, Hx and Hy only with sferics highlighted by the orange outline. Hz was not collected as shown by the noisy graph on the picture; however this can be a typical example of malfunctioning magnetic coil. The crew can at this stage take a decision to repeat the station.

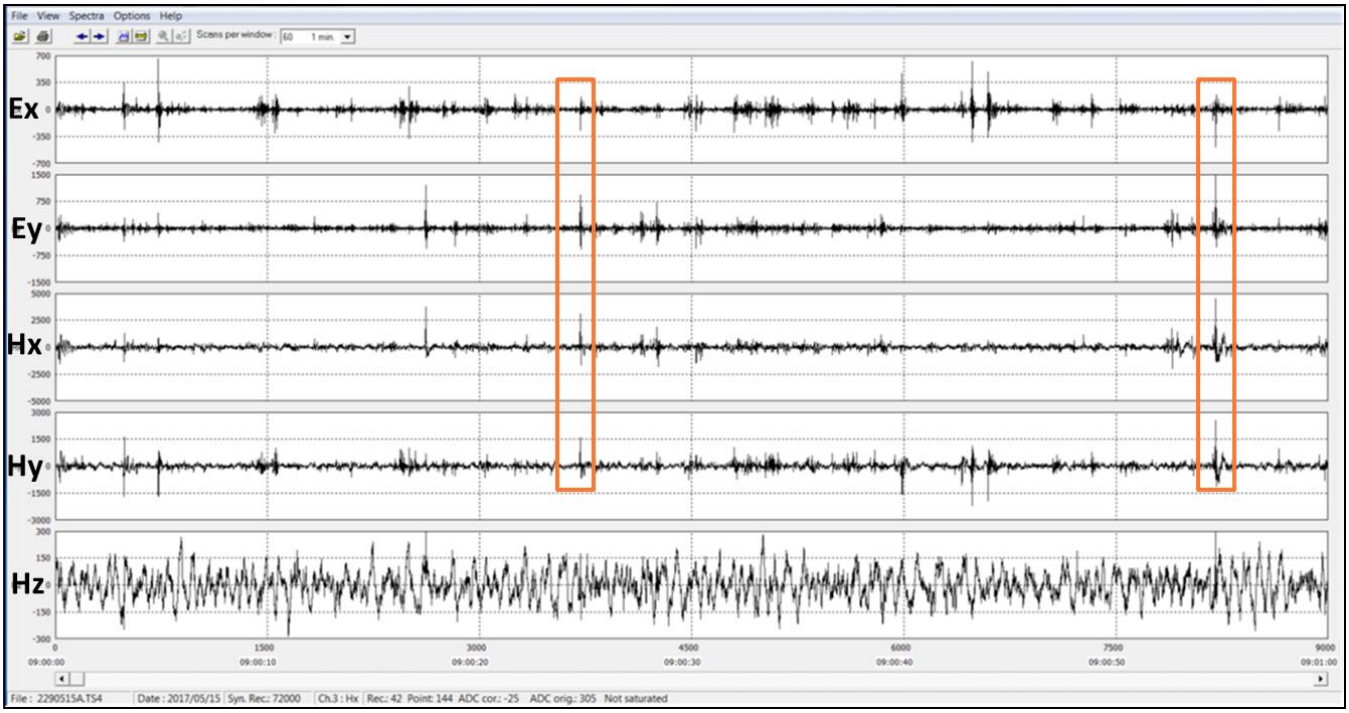

Figure 5-6: Four component MT time series recorded at a site near Beaufort West showing sferics in orange outline

5.3 DATA PROCESSING

5.3.1 Airborne magnetic data

The magnetic method measures anomalies in the Earth's magnetic field produced by magnetic rocks in the crust. Common geological causes of magnetic anomalies are dykes, sills, faults, and lava flow carrying mafic minerals or magnetic rocks (Ledwaba *et al*, 2018). Aeromagnetic data interpretation requires the use of all relevant data enhancement techniques for accurate positioning of geological boundaries and magnetic sources. Furthermore application of these techniques is useful in minimising the noise that might have been influenced by man-made structure. Several filtering including Reduction to pole (RTP), Analytical signal (AS) and vertical derivative (VD) were applied in this study are discussed briefly in following sub-subsections.

5.3.1.1 Reduction to the pole

The original 2D magnetic field data is often difficult to interpret because of the dipole nature of magnetic anomalies. One method of simplification of this problem is to reduce the data to the magnetic pole (RTP), where the presumably vertical magnetisation vector would face in one direction (Oruç and Selim, 2011; Ansari and Alamdar, 2010). RTP results will only be correct if no remanent magnetisation is present and it should therefore be used with care. The inclination and declination affects the shape of any magnetic anomaly of the main magnetic field of the Earth, thus depending on the location and orientation similar magnetic body will produce different anomaly (Mahanyele, 2010). Extreme care should be exercised when dealing with this filtering technique as

it works mostly during induced magnetisation. Pole reduction can be calculated using the following expression shown in Equation 5-1:

$$\mathbf{L}(\boldsymbol{\theta}) = \frac{\mathbf{1}}{[\mathbf{sin}(\boldsymbol{I}) + \boldsymbol{i}\,\mathbf{cos}(\boldsymbol{I})\,\mathbf{cos}(\boldsymbol{D} - \boldsymbol{\theta})]^{\mathbf{2}}} \qquad \text{Equation 5-1}$$

where I = magnetic inclination

$\theta =$ wave number direction

D = magnetic declination

5.3.1.2 Analytical signal

The analytical signal filter was applied to total magnetic field to clearly display anomalous zones and enhance the presents of any near-surface lithological units and linear features. The analytical signal, the function which is not a measurable parameter but interesting in the context of interpretation is related to the magnetic field by the derivative and is expressed in Equation 5-2 (Milligan and Gunn, 1997, as cited in Roest *et al*, 1992):

$$|\boldsymbol{A}(\boldsymbol{x},\boldsymbol{y})| = \left(\left(\frac{\boldsymbol{\partial m}}{\boldsymbol{\partial x}}\right)^{\mathbf{2}} + \left(\frac{\boldsymbol{\partial m}}{\boldsymbol{\partial y}}\right)^{\mathbf{2}} + \left(\frac{\boldsymbol{\partial m}}{\boldsymbol{\partial z}}\right)^{\mathbf{2}}\right) \qquad \text{Equation 5-2}$$

where m = magnetic anomaly

The resulting shape of the absolute value of the analytic signal is independent of the orientation of the magnetisation of the source and is centred on the causative body (Mahanyele, 2010). In simple terms this means that all bodies with the same geometry have the same analytic signal (Milligan and Gunn, 1997). Interpretation of analytical signal maps and images may in principle provide simple easily understood indications of magnetic source geometry, as the peaks of analytic signal functions are symmetrical and occur directly over the edges of wide bodies and directly over the centres of narrow bodies (Milligan and Gunn, 1997). Due to its ability to define the source positions regardless of any remanence in the source and also not subject to the instability occurring in transformations of magnetic fields from low latitudes, the analytic signal maps and images are useful as type of reduction to the pole. (Milligan and Gunn, 1997; as cited in MacLeod *et al*. 1993).

5.3.1.3 Vertical derivative

The first vertical derivative method is one of the most commonly used and effective filters when dealing with shallow source depths and rock types with relatively large contrasts in magnetization. However, in exploration in thick sedimentary cover like the western part of the study area the magnetic responses of shallow sources which are weakly magnetized are often subdued hence

filtering to enhance these low-amplitude anomalies plays an important part of the interpretation process. Both the horizontal and vertical derivatives of potential fields are useful; horizontal derivatives enhance edges, whereas vertical derivatives narrow the width of anomalies and so locate the source bodies more accurately. The higher the order of the derivative used, the more pronounced the effect, but since derivative filters are a form of high-pass filter, noise in the data is enhanced similarly.

5.3.2 Ground magnetotelluric data

Processing of MT data aims at deriving estimates of EM impedances in the frequency domain, from the measured electric and magnetic fields, apparent resistivity information can be derived. Statistical techniques are used in processing time series data to minimise noise and derive resistivity information from the data. Least-square processing techniques which involve isolating components of MT impedance were used to derive transfer functions estimates, with the remainder function assumed to have a Gaussian distribution (Simpson and Bahr, 2005). In case of noise that is not Gaussian distributed, a rigorous and manual screening of the data to remove obvious outliers (Khoza. 2016).

The approach by Jones *et al* (1989) provides excellent summary for deriving transfer function estimates. In general these processing sequences involve three main processes: (a) preconditioning of the data, (b) converting from time to frequency domain and (c) MT transfer function estimation. The steps to be followed in this process as summarized by Khoza (2016) are:

i. Pre-processing of the time series by inspecting the data for inconsistency/null/bad data points and removing any trends in the series.
ii. Fractionalize the recording in segments of equal length
iii. Multiply each segment with a suitable window function
iv. Fourier transforms each segment.
v. Calculate the auto and cross spectra for each segment.
vi. Calculate the resulting impedance from the auto and cross spectra.
vii. Calculate the mean and the error from the various estimates of the transfer function.

These processes are described in more detail in following sub-sections

5.3.2.1 Data pre-conditioning and time-frequency domain conversion

Data preconditioning is employed to reduce the effects of trends and to remove severe noise (spikes), as well as splitting time series into segments of different length, depending on the period

being calculated (Miensopust, 2010). In statistical perspective more segments used the better the results. To reduce spectral leakages a tapering window (such as Parzen or Hamming window) is applied to each segment, this is mostly common in spectral analysis when Fourier Transforms are applied to a time series with finite data length (Khoza, 2016 as cited in Jones, 1977 and Gubbins, 2004). Time series segments are converted to frequency domain once pre-conditioned of the data is done using a (Discrete or Fast) Fourier Transform or a wavelet transform. Calibration of each measured components with respect to the particular instrument's sensitivity is necessary. Application of instrument calibration functions that are either frequency dependent or independent leads to achieving calibration successfully. Calculating auto and cross spectra products of the field components and their complex conjugate is possible when raw power spectra for each time segment for each channel is used. Storage of these spectra is within the SPECTRAL MATRIX:

B_x	B_y	B_z	E_x	E_y	
$B_x \cdot B_x^*$	$B_y \cdot B_x^*$	$B_z \cdot B_x^*$	$E_x \cdot B_x^*$	$E_y \cdot B_x^*$	B_x
	$B_y \cdot B_y^*$	$B_z \cdot B_y^*$	$E_x \cdot B_y^*$	$E_y \cdot B_y^*$	B_y
		$B_z \cdot B_z^*$			B_z
			$E_x \cdot E_x^*$	$E_y \cdot E_x^*$	E_x
				$E_y \cdot E_y^*$	E_y

Several spectral matrices will be stacked and potentially manually edited or weighted using statistical techniques for the same evaluation frequency.

5.3.2.2 Estimating the transfer function

When conversion is complete, the succeeding step is the estimation of the transfer function, the impedance tensor (Equation 5-3 and Equation 5-4) and tipper vector (Equation 5-5):

$$E_x(\omega) = Z_{xx}(\omega) . H_x(\omega) + Z_{xy}(\omega) . H_y(\omega) + \delta Z(\omega) \quad \text{Equation 5-3}$$

$$E_y(\omega) = Z_{yx}(\omega) . H_x(\omega) + Z_{yy}(\omega) . H_y(\omega) + \delta Z(\omega) \quad \text{Equation 5-4}$$

$$E_z(\omega) = T_x(\omega) . H_x(\omega) + T_y(\omega) . H_y(\omega) + \delta T(\omega) \quad \text{Equation 5-5}$$

Where δZ and δT are remainder functions representing uncorrelated noise (in this case electrical noise), this is statistical solution of MT impedance required to minimise a remainder function made by inexact measurement errors and approximation of plane wave source assumption (Simpson and Bahr, 2005). These equations suggest that the recorded electric and magnetic fields are used to estimate the transfer functions. These commonly used least-square and robust processing techniques are examples of statistical processing methods to remove noise from the MT data.

The Phoenix processing software SSMT 2000 (Figure 5-7) implemented heuristic approach by Jones *et al*. (1989) used to process the data, to derive MT impedance estimates that were subsequently converted to apparent resistivities and phases.

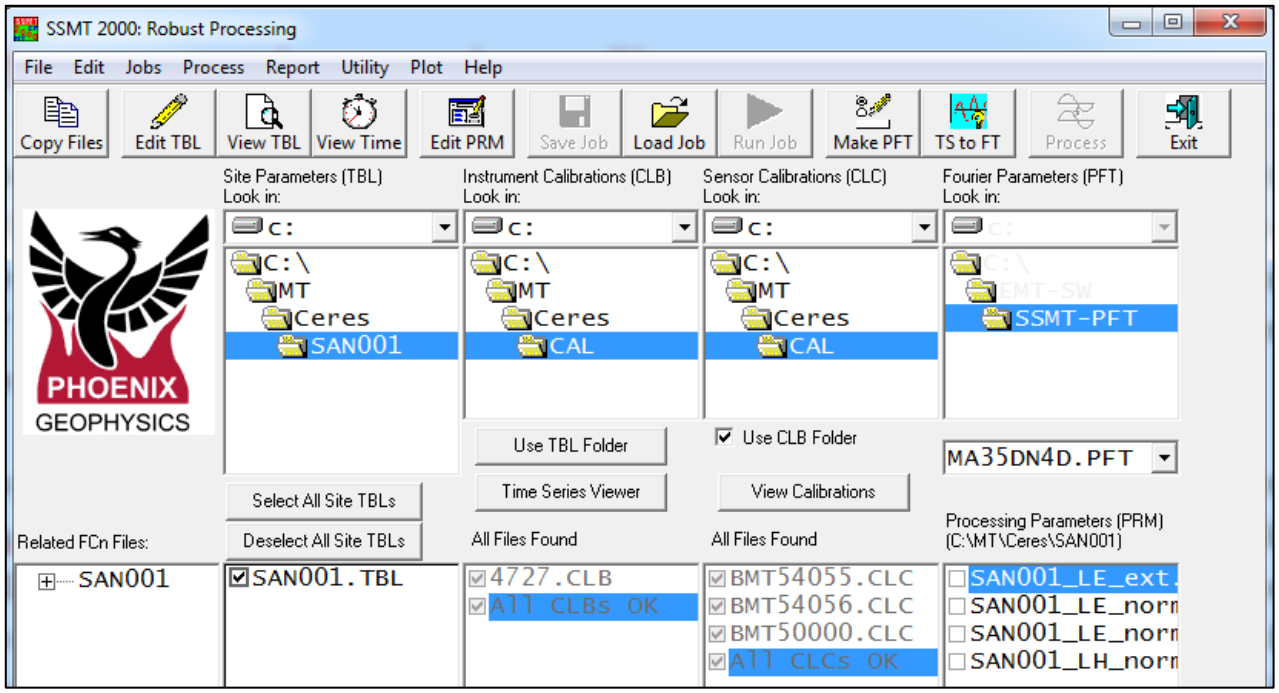

Figure 5-7: SSMT2000 processing software that was used to derive apparent resistivity vs phase curves

High quality data for most sites and some site further data clean-up was required, which involved editing of the cross-power in MTEDITOR software. The presence of underground pipes may have affected the data quality. Figure 5-8 shows examples good quality of MT responses along the BFM.

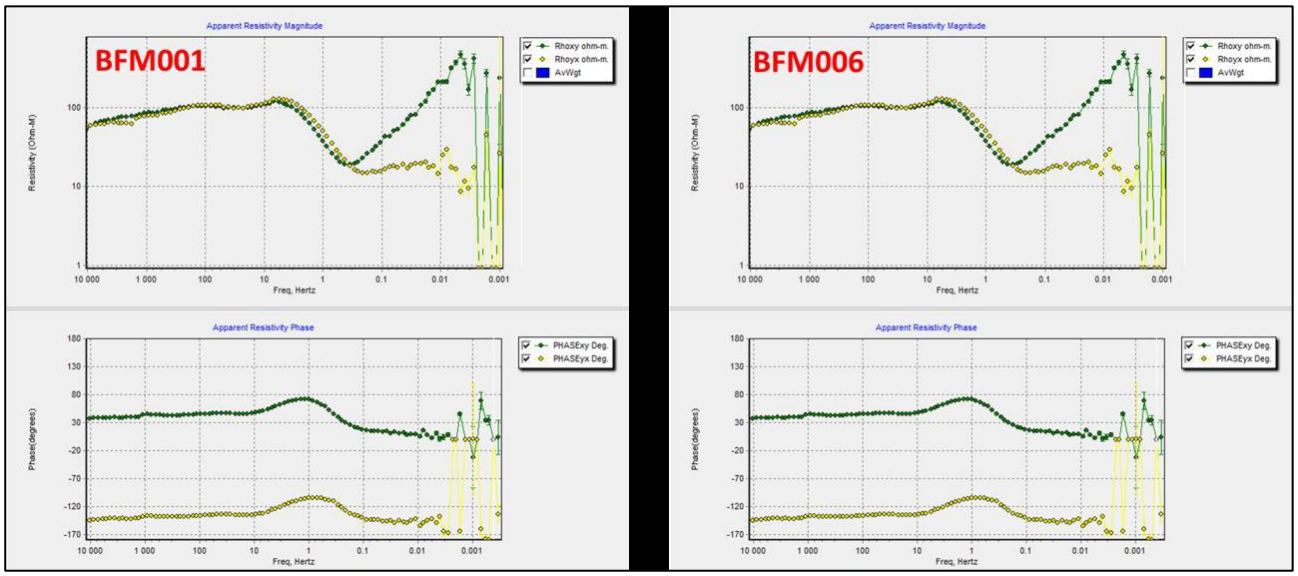

Figure 5-8: Apparent resistivity and phase curves of MT sounding for sites along the BFM profile

5.3.3 Magnetotelluric data modelling and inversion

Once the processing of MT data is complete the next step is to convert to an image of resistivity variation with depth, from which geological interferences can be drawn. The process can be achieved successfully by forward modelling and inversion. The forward and inversion are mostly used to produce a 1D, 2D or 3D model based on the measured data to determine the subsurface conductivity structure. These models help to relate the resistivity structure to geology and other geophysical models to define the current state of the subsurface and potentially provide an indication of Earth processes and Earth history.

The following sections describe the two modelling procedure that shows how Earth modelling showing resistivity variation are developed.

5.3.3.1 Forward modelling

Forward modelling is the procedure of generating synthetic responses for a given conductivity structure. This modelling procedure involves simulation of the electromagnetic induction process by finding geological model that best fit the MT responses using a computer program. The forward modelling is an iterative trial and error process which involves modification of poorly fitted data until a satisfactory fit is achieved. Generally the input conductivity will be discretised into cells or blocks of specific resistivity to solve Maxwell's equations using some form of approximation, from which EM fields everywhere in the mesh can be solved. The resulting synthetic responses, from which apparent resistivity and phases are calculated, can be compared with the observed data and the minimal RMS fit between them can give a confident indication of how close they are (Khoza, 2016).

As suggested by Simpson and Bahr (2005) advantages of doing forward modelling to consider prior to perform inversion of MT data, are: When planning a field campaign a simple model may assist in deriving optimal data acquisition parameters (i.e. site spacing, period required to propagate to a particular depth range). This exercise is cheap and simple compared to the input (human and fiscal) involved in re-designing field survey. Furthermore forward modelling might also benefit on generating a model on already existing dataset. It can also be used to investigate whether features included in a model obtained are constrained by the input data.

Forward modelling can be done in 1D, 2D and 3D, this can be controlled by the desire to simulate the induction process in a layered Earth. For a case of 2D Earth the conductivity varies only in the vertical and horizontal direction. It is time consuming to find a forward model that matches the observed responses reasonably well. This can be supplemented by an inversion process, which is an

automated process that uses the observed data as input and generates a geological plausible (2D or 3D) model.

5.3.3.2 1D and 2D inversion modelling

Inversion modelling is an iterative process which takes the observed data through some automated process reduces the misfit between measured data and forward responses, obtaining a reasonable model. It is a necessary requirement that all inversion problems have the ability to solve forward problems. Thus, this inverse problem is non-linear as it links a set of MT responses to a conductivity model. Inversion provides initial approximations to the Earth's conductivity structure, but the limitations and strengths of MT data become clearly apparent only through forward modelling. This may be because only 1D and 2D inversions are available for standard applications, whereas 3D induction effects are often ignored. When modelling MT data always consider the inherence of non-uniqueness problem.

5.3.3.2.1 1D Inversion

A technique known as 1D OCCAM inversion which allows the determination of the 'minimum structure' of the model and assumes a progressive change in resistivity with depth (Constable et al, 1987) was used. Both OCCAM and BOSTICK models were derived, and are smooth models providing resistivity distribution versus depth. The risk of over-interpreting the data or modelling arbitrary can be reduced by fitting data using smooth model. To obtain meaningful results with1D modelling the need to have aprori information (such as borehole, geological and/or geophysical data) is necessary.

5.3.3.2.2 2D Inversion

The two dimensional (Krivochieva and Chouteau, 2005 cited in Mackie et al, 1997) 2D inversion codes was carried out using the Non-Linear conjugate Gradient scheme, implemented in the WINGLICK software package (IGS, 2018 as cited in Rodi and Mackie 2001). Winglink is very sensitive to the starting model, parameter chosen, data, error floor and modes (TE or TM) used. It is advisable to combine these parameters and settings to obtain a meaningful geological model. The process followed was a systematic inversion to firstly introduce structure in the model. The 2D inversion model was generated using the following five steps procedure outlined:

i. TM phase only inversion – only TM data were used and the apparent resistivity error floor set to a high value (50%). The TM phase error floor was set high (20%), then successively reduced to 10% then 5%.

ii. TE phase was added, with the TE apparent resistivity error floor set to a high value (50%), and the TE phase set high then successively reduced to a value about the same as that of TM phase.

iii. TM apparent resistivity was added and then TM apparent resistivity error floors successively reduced (5% - 20% - 10%) to a value about twice that of the TM phase.

iv. TE apparent resistivity added – then corresponding error floors successively reduces (50% - 20% - 10%) to a value about twice that of TM phase.

v. The statics were set on and the TE and TM apparent resistivity error floor set to same level as TM phase error floor.

The Tipper data was not acquired within these MT stations, therefore within the inversion process the tipper data could not be included. There is an inversion parameter of the WINGLINK programs known as the tau parameter affecting inversion results significantly. This parameter controls the trade - off between data misfit and model smoothness. Multiple inversions were conducted by varying the value of tau and inspecting the resulting RMS misfits. For the subsequent inversion runs the tau value representing the point of maximum curvature was chosen as the most appropriate. A tau of 3 was used to generate the models.

5.4 RESULTS AND INTERPRETATION

5.4.1 Airborne magnetic data

The study area comprises of sedimentary rocks which has been intruded by dolerites mostly in Great Escarpment and on the plateau north of the escarpment. Large amplitude long wavelength positive anomalies are present in the north and south of the area, and are separated by a long wavelength negative anomaly in the middle. Short wavelength anomalies superimposed on these broad anomalies have substantially smaller amplitudes (Figure 5-9).

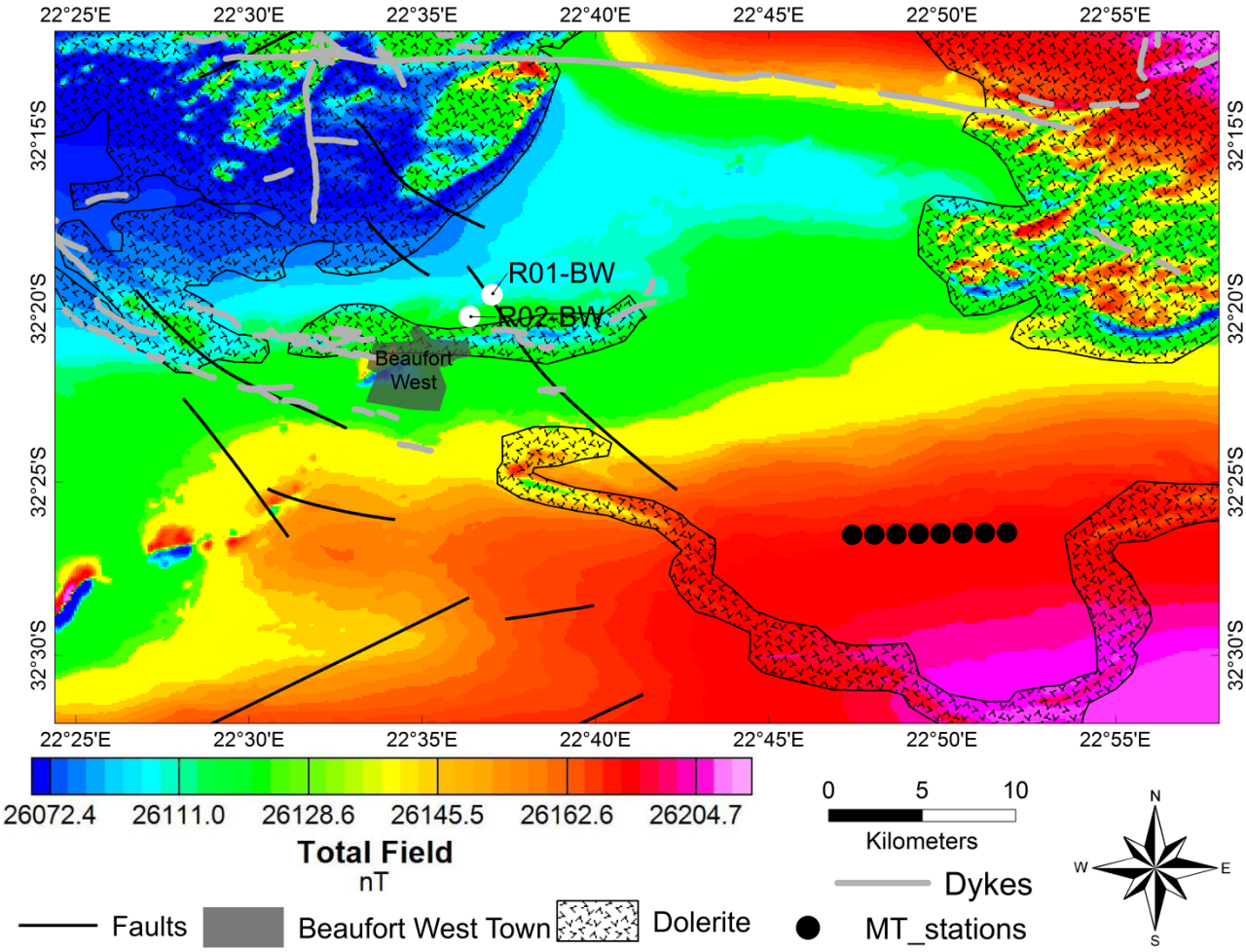

Figure 5-9: Total magnetic field map

5.4.1.1 Reduction to pole

Reduction to the pole (RTP) is used to provide a symmetrical anomaly over a vertically dipping, non-remanent body and is also used to enhance interpretation (Figure 5-10). The RTP has proved to be vital in producing anomaly maps that can be more readily correlated to the surface geology, due to its ability to transform anomalies to lie directly over the causative body (Tessema *et al*, 2010). Features trending northwest to southeast are more clearly delineated on this map, especially on the southern portion of the study area.

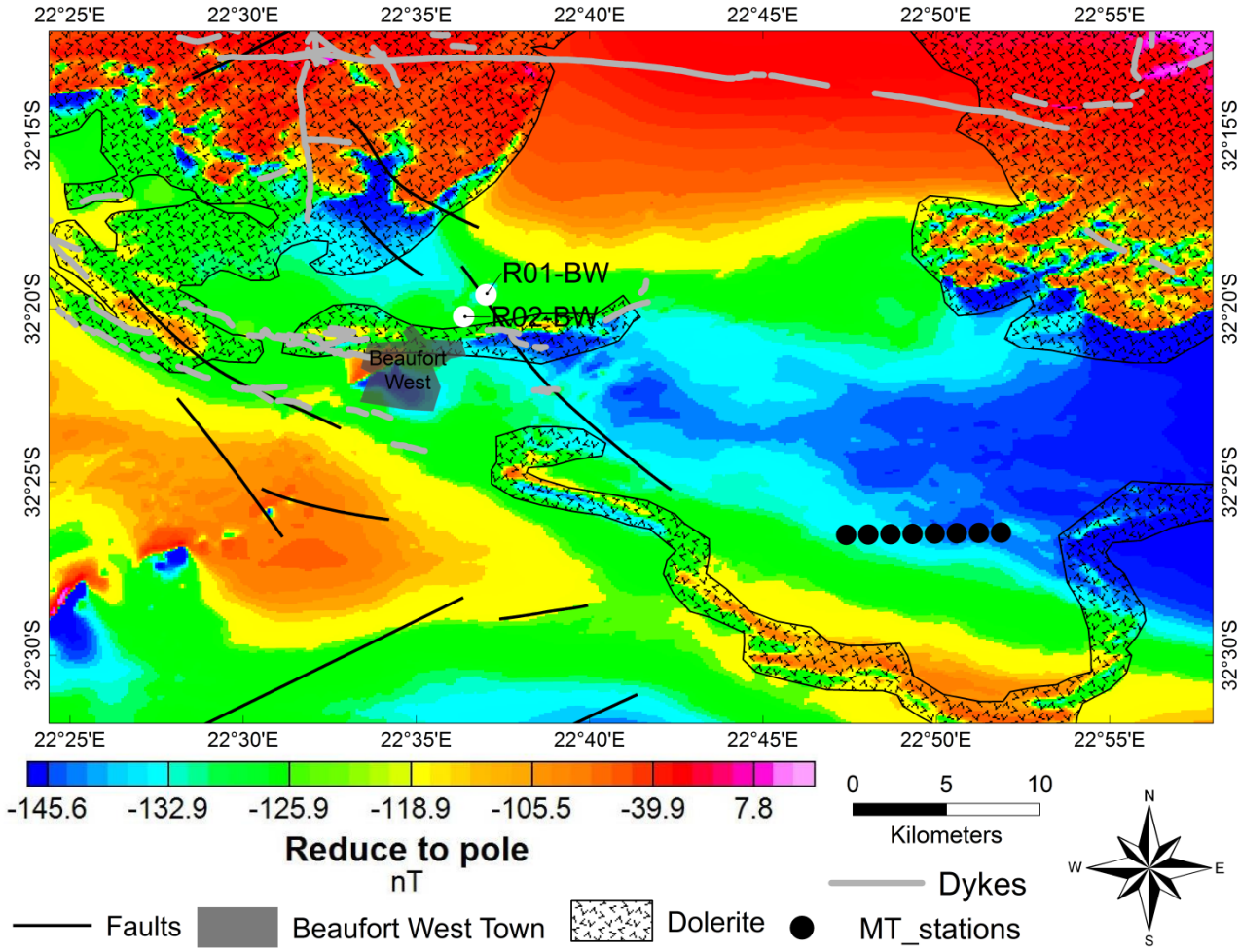

Figure 5-10: Total field data reduced to the magnetic pole

5.4.1.2 Analytical signal

This technique is completely independent to the direction of magnetization and earth's field, i.e. all bodies with the same geometry have the same analytical signal (Milligan and Gunn, 1997). The peaks of the analytical signal are symmetrical and occur directly over the edges of wide and center of narrow bodies. Thus, interpretation of analytical signal map provides simple and easily understood indications of magnetic source geometry. This filtering technique shown in (Figure 5-11) was able to map the edges of the intrusive bodies using the peak values of the analytical signal amplitude. Comparing the results of the analytical signal with the total magnetic field the difference is mostly on the edges of the intrusive bodies.

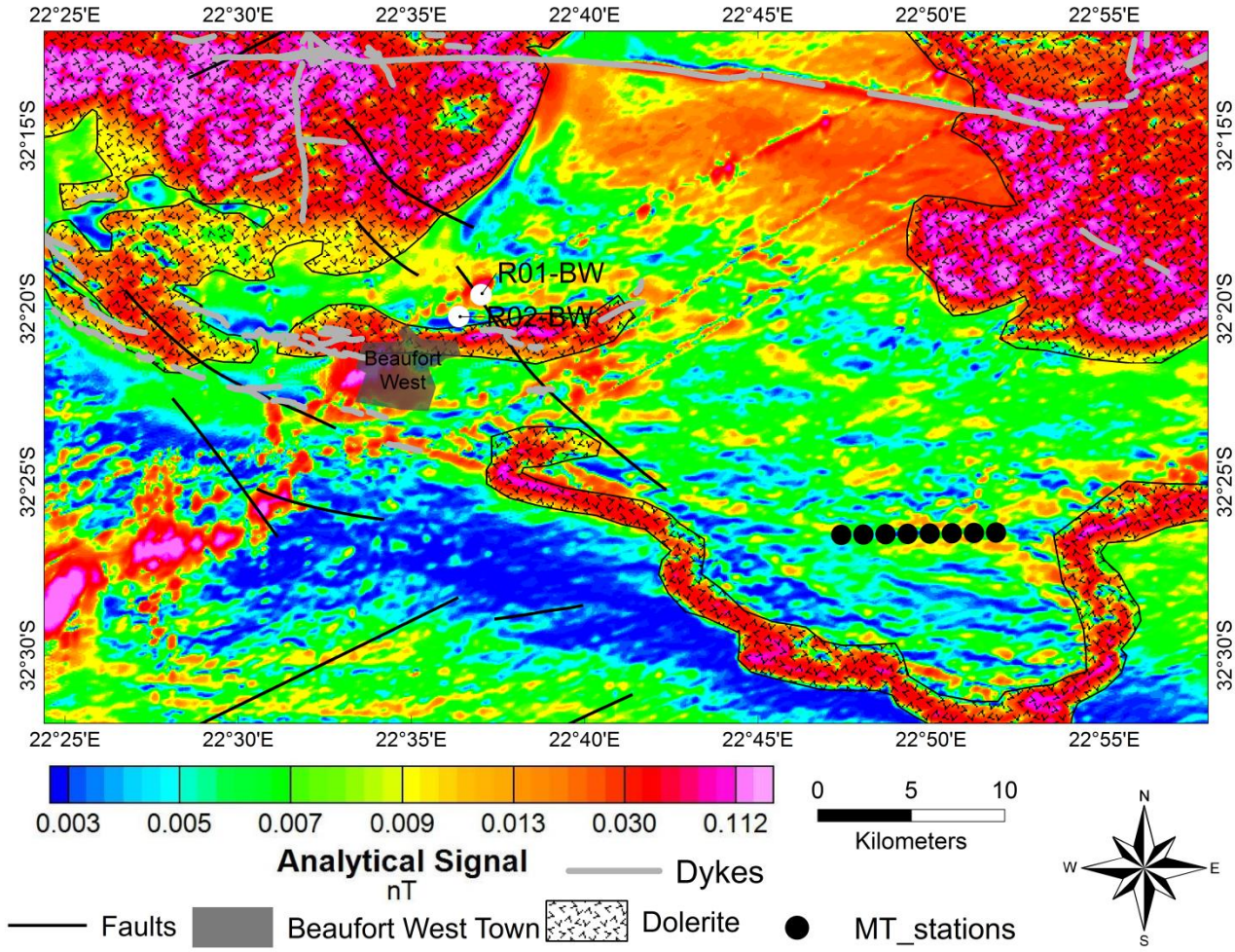

Figure 5-11: Analytical signal

5.4.1.3 Vertical derivative

The results of the analytical signal was supplemented by the first vertical derivative which is physically equivalent to measuring magnetic field simultaneously at two points vertically above each other, subtracting the data and diving the results by the vertical spatial separation of the measurements points (Milligan and Gunn, 1997). Application of this technique enhances high frequency relative to low frequency and this property is the basis for the application of the derivative process which eliminates long wavelength regional effects and resolves the effects of adjacent anomalies. It has become the basic practise to apply first vertical derivative in magnetic interpretation, as it is able to extract linear and structural features.

The first vertical derivative map (Figure 5-12) shows a better resolution on the delineation of high frequency features which were enveloped by large amplitude and low frequency anomalies. As it can be noted on the map the high frequency anomalies were annotated as dolerite dykes and sills. The medium frequency anomalies were inferred as sills. The first vertical method enhances shallow geologic sources and suppresses deeper sources making smaller anomalies more noticeable than on the total field intensity. Furthermore noise in the data produced power lines railways lines will also

be enhanced. The increase visibility of the geological structures such as sills, dykes, faults and the fabric caused by shearing with rocks are more noticeable on the first vertical derivative map when compared with the total field magnetic map. The importance of dolerite dykes orientated north – northwest and east-west, as picked up by satellite imagery interpretation was emphasized by the first vertical derivative. The north-northwest dykes are more visible in the north-western and north-eastern portion of the study area where sills are less dense. The east - west dykes appears to be younger as they are seen cutting into the sills and across the north-northwest striking dykes. The magnetic image suggests new or more extensive lineaments. These lineaments could have gone through various degree of shearing. Interbedded layers of sandstone and mudstone of the Beaufort Group appears to have been cut by brittle faults and intruded by the Jurassic aged dolerite sills dykes (Dhansay *et al*, 2017). These large fault structures shown in the first vertical derivative map (Figure 5-12) variously oriented may have been occurred as a results of reactivation of fractures (Dhansay *et al*, 2017). Jurassic dykes seen to overlie the faults and in some places taking the orientation of the fault, may suggest that they are younger.

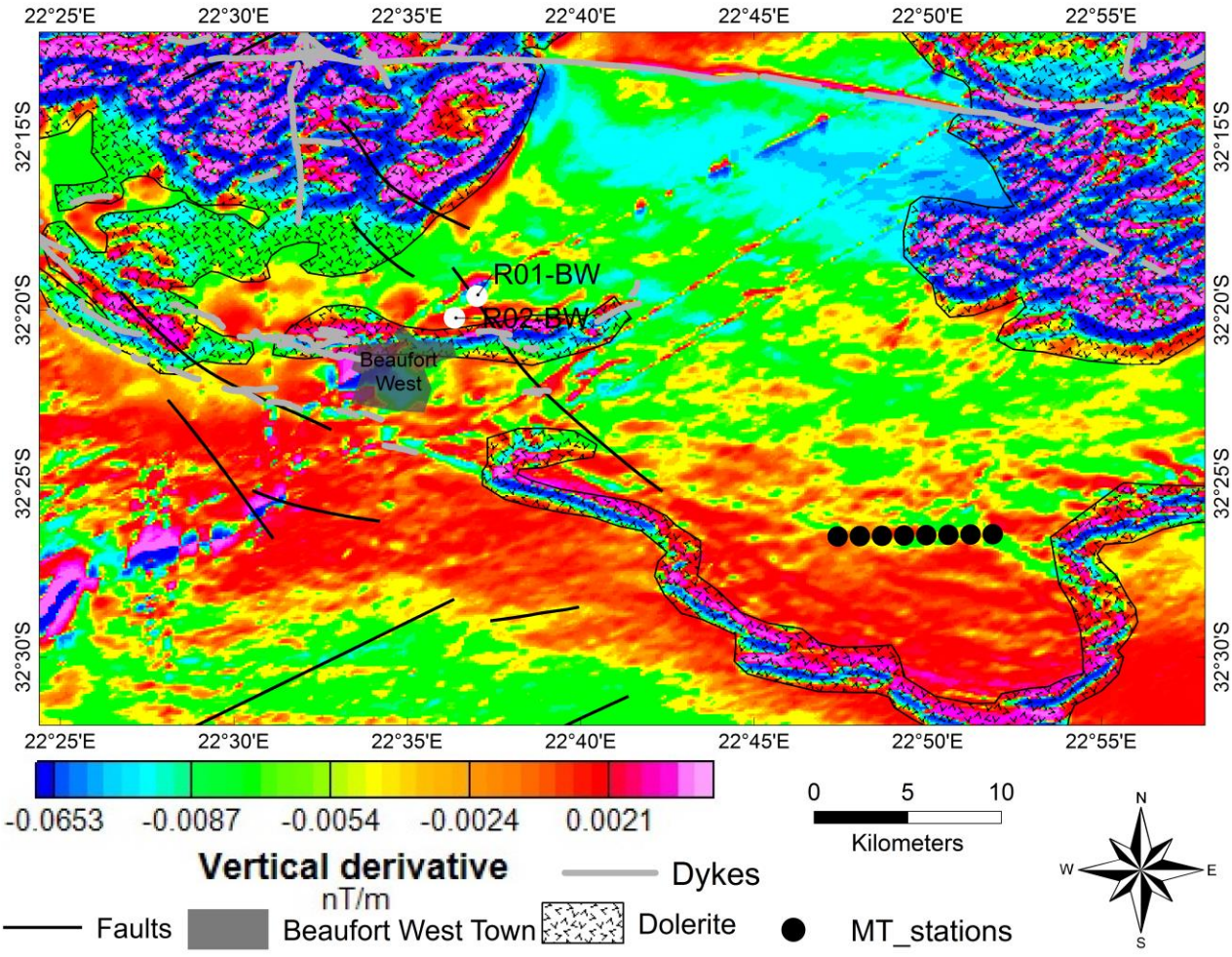

Figure 5-12: Vertical derivative

5.4.1.4 2D Magnetic Modelling

The analytical signal of the magnetic data showing the location of the MT profile (Figure 5-13), suggest the presence of magnetic feature along the profile. The high magnetic field feature might represent a deep seated intrusive magmatic body. The 2D magnetic modelling of the total magnetic intensity data was created using GMSYS-2D software package of the Oasis Montaj. GM-SYS is a program for calculating the potential field methods (gravity and magnetic) response from a geologic model and provides an easy-to-use interface for interactively creating and manipulating models to fit observed data. Modelling of potential field magnetic data is a very ambiguous process, and depends on the susceptibility, remanent magnetization, depths and thicknesses of the bodies. Another factor that affects the results is the selection of a regional field to subtract from the data.

The aim of modelling was created to verify the results obtained from the MT section. The results of the 2D magnetic modelling are presented in Figure 5-14. The magnetic modelling confirms features observed in MT inversion model, in which the resistive layer might be related to dolerite. The results shows the magmatic feature with susceptibility value around 0.012981 SI might represent a slight vertically inclined dolerite to the center at distance ranging between 2 km and 4 km, while to the west and east of the profile appears to be horizontal. These structures may have been connected during their previous formations, as can be seen that it might have been disrupted due to present day erosion. The low magnetic susceptibility values overlying these intrusive bodies might be associated with alluvial. The Poortjie Member might have been heavily intruded by the Jurassic dolerite dykes and sills. The magnetic susceptibility value around 0.000075 SI might be related to Whitehill Formation occurring at depth around 2.4 km and can also be seen that it was heavily intruded by Jurassic dolerite dyke and sill. The magnetic susceptibility value around 0.000138 SI represent rocks of the Ecca Group that appear to have been be suppressed. Dwyka Group occurring at greater depth is represented by magnetic susceptibility value of around 0.000226 SI. The intrusive magmatic bodies might have caused movement within the rocks suggesting the occurrence of faulting. These results enhance the knowledge that aquifers within the Karoo may be occurring beneath the well-studied depth.

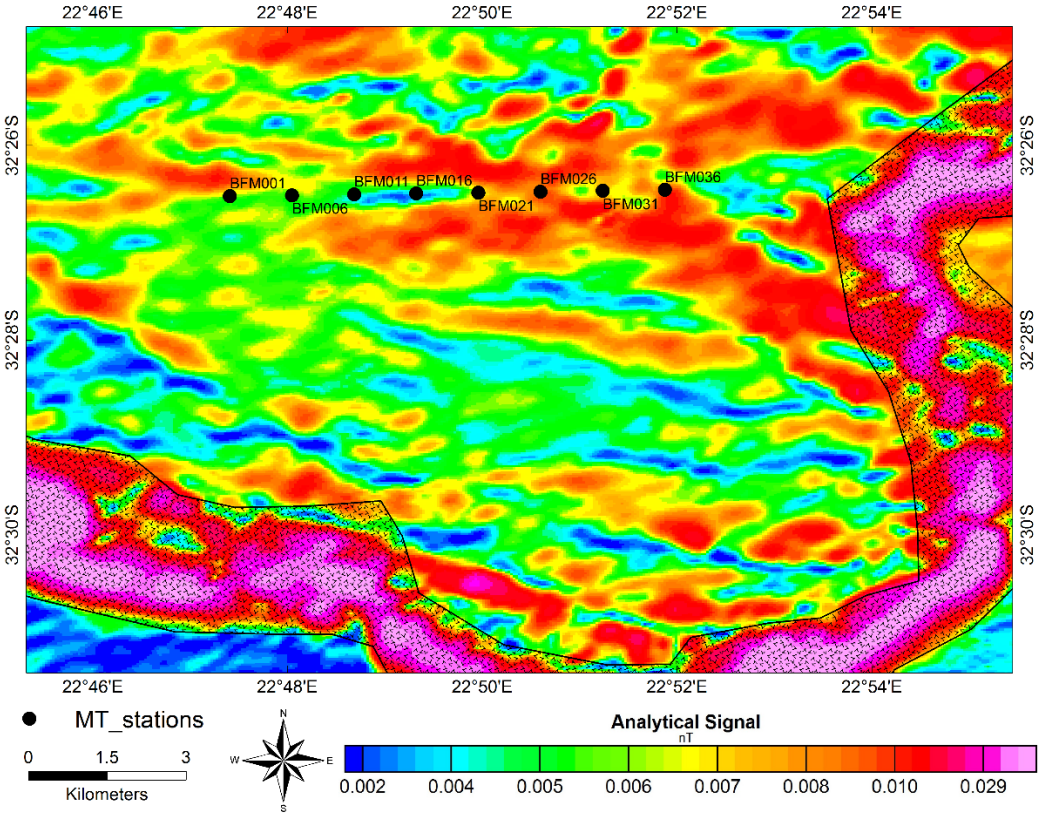

Figure 5-13: Analytical signal of Total Magnetic Intensity data showing location of MT stations

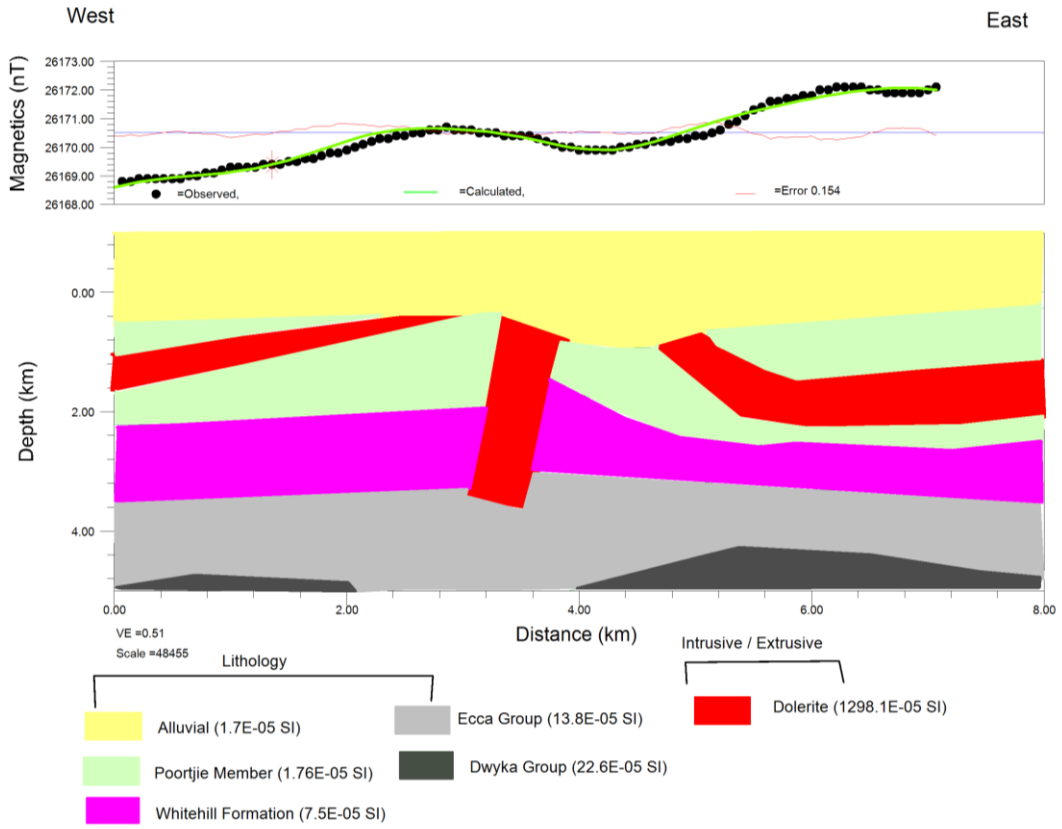

Figure 5-14: 2D magnetic modelling

5.4.2 Ground magnetotelluric data

MT results require investigation of all available geoscience data to infer meaningful geological feature. Geophysical data involving airborne magnetic useful in delineating structural features like intrusive magmatic bodies and faults have been considered in this study (see section 5.4.1). Furthermore 2D magnetic modelling was also created using GMSYS modelling package from Oasis montaj to verify the MT results (see sub-section 5.4.1.4). The 1D and 2D inversion MT results were briefly described in following subsection.

5.4.2.1 1D inversion modelling

Several models were generated along the profile for all the response, where resistivity and phase responses have been calculated. Between the TE and TM mode the invariant curve lies graphically. The OCCAM and BOSTICK model were computed for each station within the MT profile. The OCCAM and BOSTIK models are smooth models with the ability to provide resistivity distribution versus depth. In order to reduce the temptation of over-interpreting the data and eliminate arbitrary discontinuities in simple layered models, a method of fitting using smooth model is recommended. To provide meaning results 1D modelling a-priori information in the form of borehole, geological and/or geophysical information may be used.

To obtain the smoothest model the OCCAM inversion was run with 15 iterations using maximum number of layers. From smooth OCCAM model a sharp boundary model was also computed for 15 iterations to produce a layered model. Furthermore a sharp boundary layered model inversion was also run over 10 iterations with 5% maximum RMS fit to produce layered model from the smooth Occam model. To enhance the match with the Occam models layer thicknesses and resistivities were manually edited and fixed. In the sharp boundary computations the available number of layers is limited to 8 layers. Figure 5-15 illustrate example of 1D inversion model at site BFM0001.

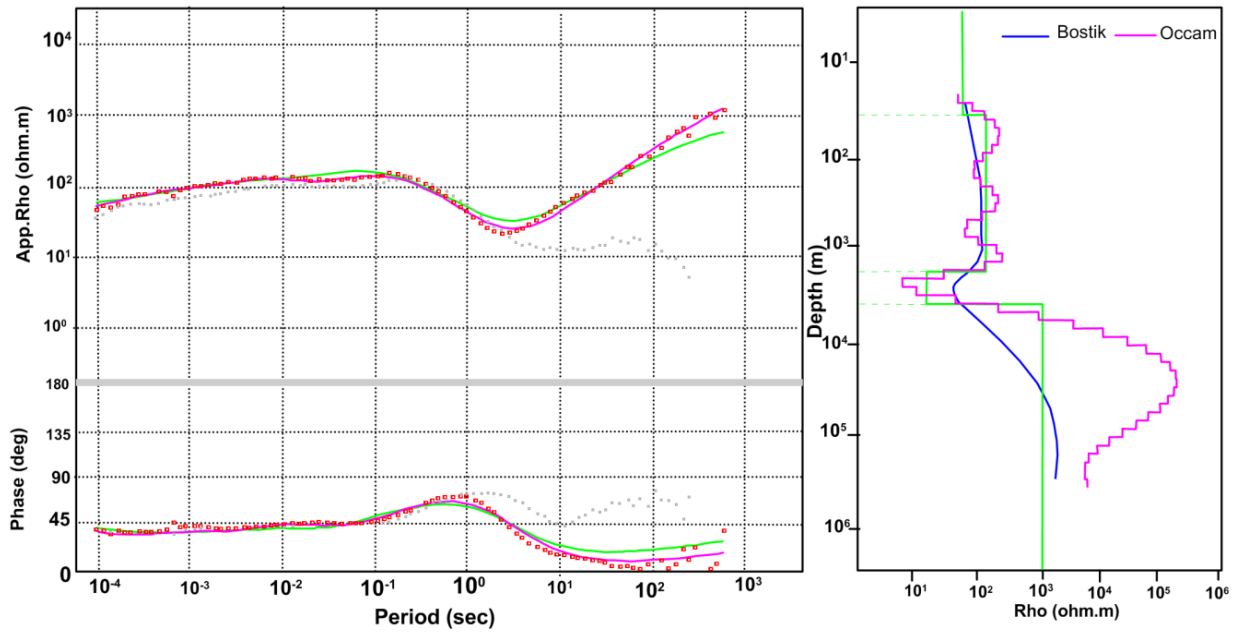

Figure 5-15: 1D layered inversion of sounding curve from MT site BFM0001

5.4.2.2 2D inversion modelling

The 2D model inversion (Figure 5-16) confirm features observed in the 1D layered models individually and present a better data quality. Several model inversion parameters were tested generally producing rather similar models. The TE and TM modes combined produce the best model (Figure 5-17). The 2-D model suggests the presence of strong lateral changes of the subsurface resistivity distribution. The depth extent of the section is about 4 km and no boreholes information was provided in the area. The basement rock units at depth > 3.5 km appears to have been congested by a conductive zone, this may have been caused by strong electrical properties of less resistive obstructing resistive layer.

The relatively conductive zone near the surface at distances around 2800 m, 3000 m and 4200 m thus indicate the presence of highly weathered Poortjie Member sediments. A very high resistive layer seems to have been intruded within the slightly conductive zone might be associated with dolerites. There appears to be a resistive sill-like intrusive body to the west of the section. The resistive substratum reaching a depth of around 2000 m to the east and the inclined resistive layer might be an indication of dolerite sill and dyke respectively. The intrusive bodies may act as the impermeable barrier to the groundwater flow within the study area. It may seem that faulting might also be occurring around the distance 2200 m and 5000m as can be observed by the displacement of conductive zone. The presence of this conductive zone may also be interpreted as the Whitehill Formation.

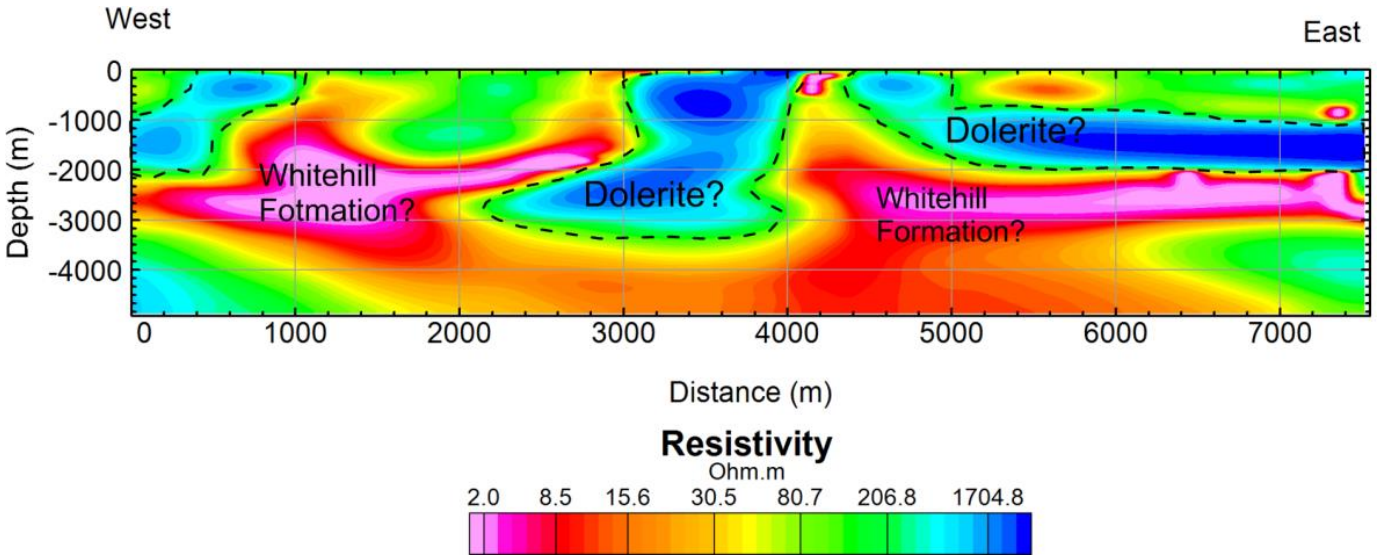

Figure 5-16: 2D inversion model of the BFM profile using both TE and TM modes

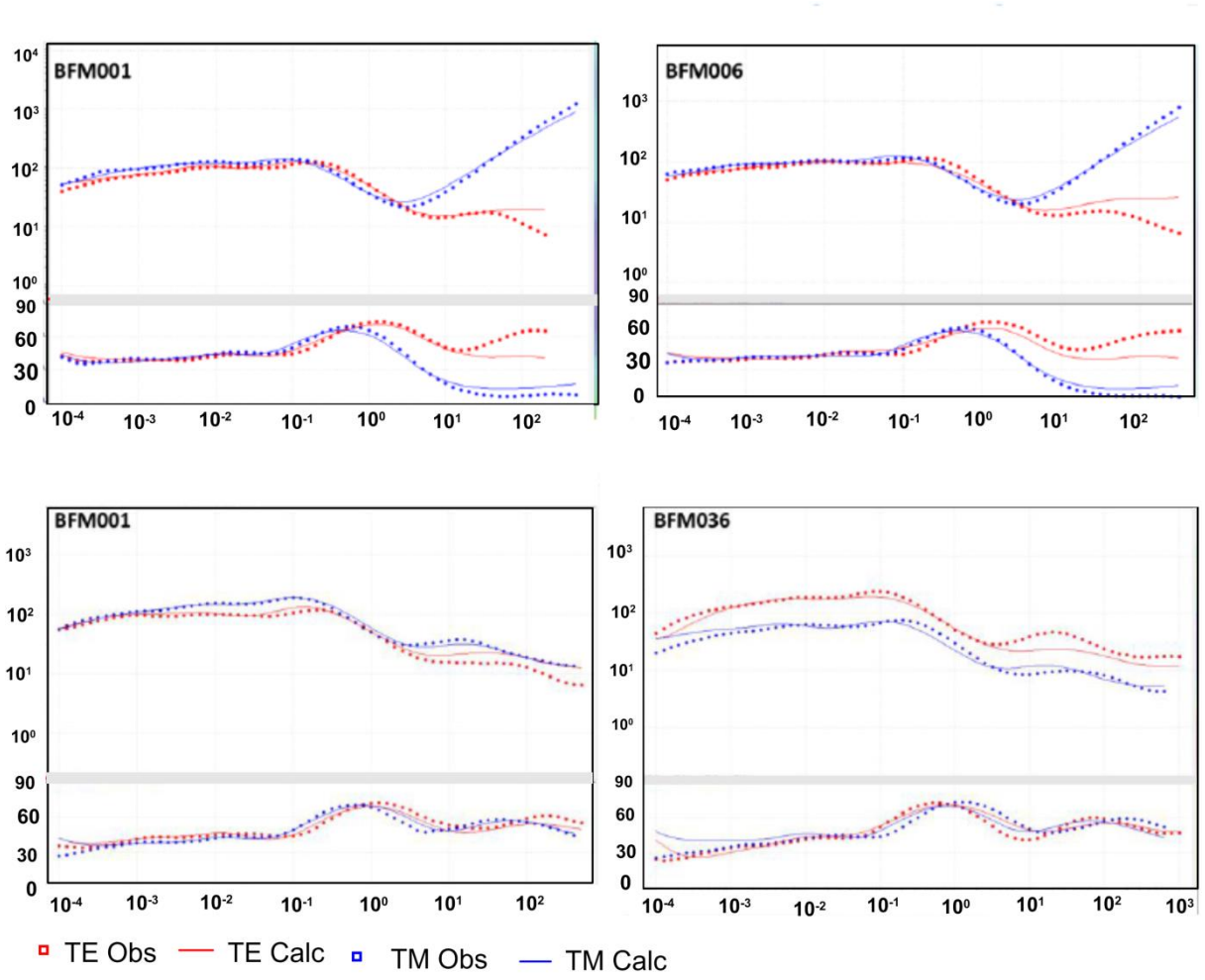

Figure 5-17: 2D inversion model responses compared to the measured data form joint inversion of the TE and TM mode apparent resistivity and phase data

Chapter 6:
DRILLING OF OBSERVATION AND MONITORING BOREHOLES

6.1 INTRODUCTION

As part of the geoscientific investigations, observation and monitoring percussion boreholes were drilled. The purpose of drilling observation holes was to obtain new information on the shallow groundwater, Karoo lithology, stratigraphy and structure. The role of the monitoring boreholes is to monitor properties of possible aquifers when the proposed deep borehole is drilled. The information obtained from the airborne geophysical survey was used to obtained

6.2 PERCUSSION DRILLING

In groundwater exploration percussion drilling method has always been the method used, particularly in hard rock and semi-consolidated formations. This drilling process produces drill cuttings (rock chips) that are removed from the borehole via the annulus between the drill-stem and the wall of the hole by circulating air at high pressure (Malefane, 2016). These rock chips are then arranged at a particular interval from the top to the bottom of the borehole, in order to conduct the geological logging of the borehole. The rock chips produced by percussion drilling are not as easy to interpret like the core logs produced through a core drilling method. One other advantage of the percussion method is the ease with which water can be blown to the surface as soon as a water-bearing zone is encountered. Generally the blowing of water to the surface is referred to as blow yield and usually may provide an indication of the water available supply; although it is an advantage it is only limited in providing the cumulative indication of the yield from an individual fracture during drilling.

Four shallow observation boreholes ranging in depth from 151 to 169 m were drilled within the Beaufort West Municipality grounds (Mosavel and Cole, 2017). These boreholes were drilled with rotary air percussion using the drill rig of the Council for Geoscience. Drilling of the two monitoring boreholes was conducted by Torque Africa, a company contracted by the Council for Geoscience. The monitoring boreholes range in depth between 516 m and 1402 m. The location and distribution of the boreholes is shown in (Figure 6-1).

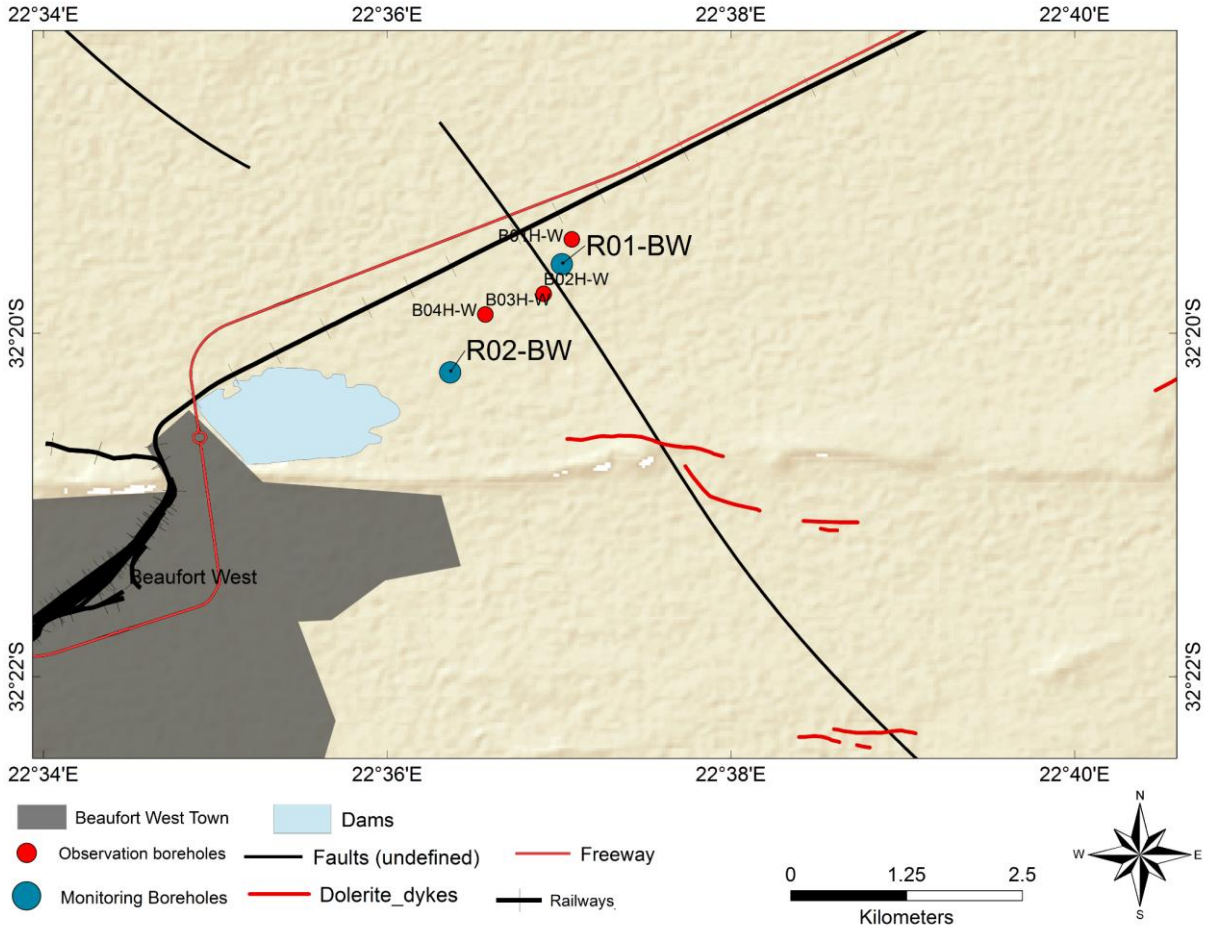

Figure 6-1: Map showing positions of observation and monitoring boreholes drilled within the Municipality grounds of Beaufort West

6.3 GEOLOGICAL LOGS

6.3.1 Observation boreholes

All the boreholes are sited on the Poortjie Member of the Middleton Formation. The Poortjie Member, consisting mostly of sandstone units with subordinate mudstone and siltstone, has an estimated thickness of about 204 m with the Beaufort West area (Nxokwana *et al*, 2018a). A uniform thickness ranging between 49 and 53 m with the predominant sandstone was found in B01H-BW, B03-BW and B04-BW, whereas the intervening borehole (B02-BW) is represented by 15 m of siltstone and shale (Figure 6-2). The Poortjie Member overlies the Abrahamskraal Formation consisting of mudstone and subordinate sandstone and siltstone. Following are the brief discussion of the geological logs.

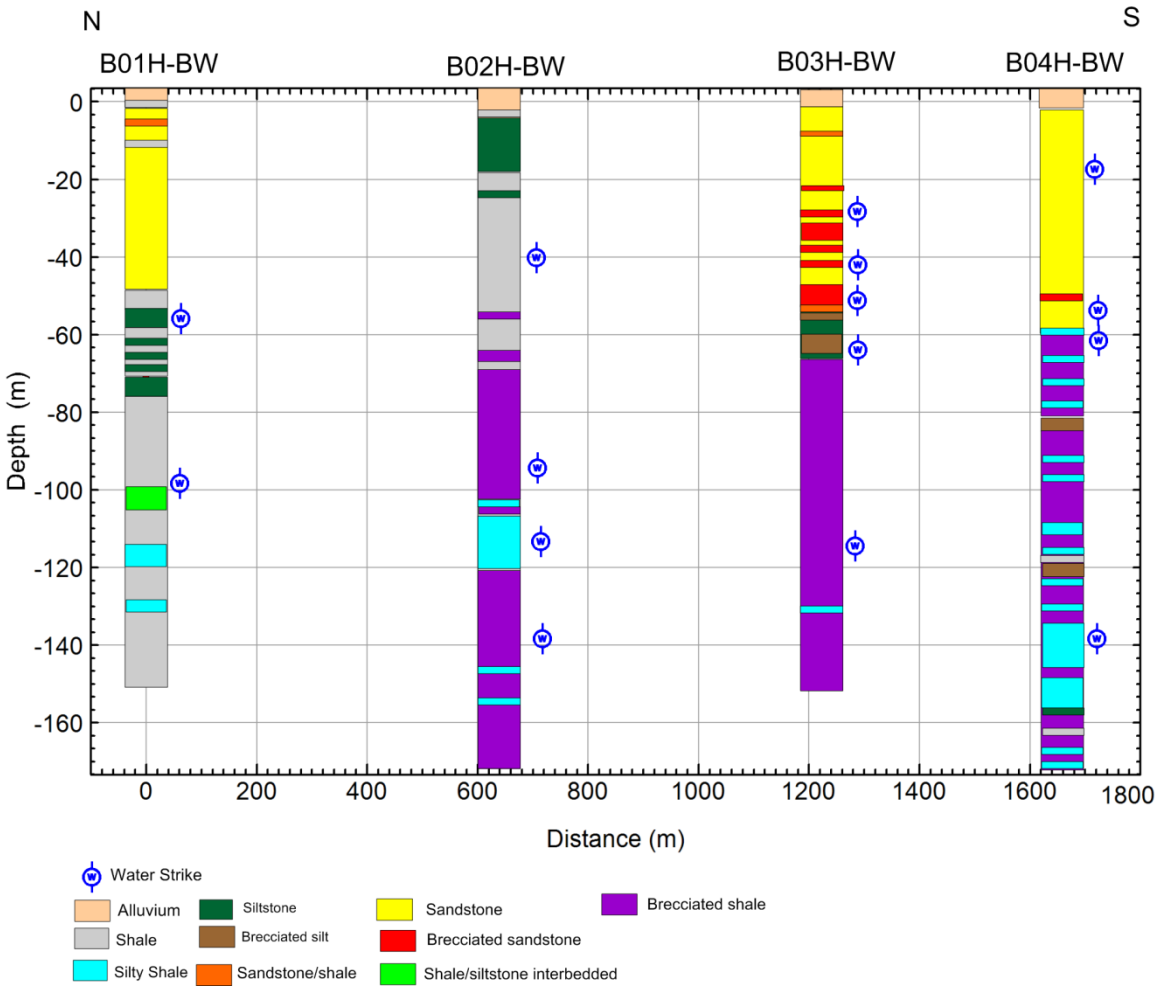

Figure 6-2: Correlation boreholes between B01H-BW, B02H-BW, B03H-BW and B04H-BW (Modified after Nxokwana *et al*, 2018a)

B01H-BW

The borehole drilled to a depth of 151 m intersected 49 m of the Poortjie Member of the Middleton Formation at the surface. The Poortjie Member consisting of shale and very fine-grained sandstone overlies the Abrahamskraal Formation. The formation was intersected below the Poortjie Member to the bottom of the borehole and comprises of shale, siltstone and silty shale. The borehole intersected two water strikes between depths 55 - 56 m and 87 – 88 m. The blow yield was not enough to be considered for pump test.

B02H-BW

The borehole intersecting about 15 m of the Poortjie Member was drilled to a depth of 169 m. Below the Poortjie Member the Abrahamskraal Formation was intersected to the bottom of the borehole. The borehole intersected a water strike and major fracture zone, which may be related to the fault. There were additional six more water strikes intersected throughout the borehole, that may be associated with brecciated shale. Borehole B02H-BW had high yielding blow yield (+ 35 l/s) and was prioritized for pump test.

B03H-BW

The role of this borehole is to monitor future groundwater impacts when the deep borehole (± 4000 m) is drilled. The depth of the borehole is 151 m, intersecting about 53 m of the Poortjie Member beneath alluvial gravel. About 95 m of Abrahamskraal Formation was intersected. There were about six water strikes intersected with the uppermost one occurring at depth between 34 m – 35 m in brecciated zone of very fine grained sandstone. The blow yield was not enough to be prioritized for pump test.

B04H-BW

This borehole drilled to a depth of 169 m intersected about 58 m of Poortjie Member beneath the alluvial gravel. The Abrahamskraal Formation underlying the Poortjie Member consists of 109 m of brecciated shale and silty shale. There were four water strikes intersected within the Poortjie Member and the other in the Abrahamskraal Formation. The borehole was regarded as high yielding from blow yield (+20 l/s) and was prioritized for pump test.

6.3.2 Monitoring boreholes

Two monitoring boreholes were drilled by Torque Africa exploration. The boreholes are positioned at larger distance (± 20 km) from the magnetotelluric traverse, due to the electromagnetic highly influenced by DC powered railway which is near the boreholes site. The boreholes named R01-BW and R02-BW were drilled to a depth of 706 m and 516 m respectively using air rotary percussion drilling method (Nxokwana *et al*, 2018b). The intention initially was to drill borehole R02-BW to a depth of 700 m, but due to greater loss in return chippings at depth 516 m the drilling was stopped. Therefore borehole R01-BW was drilled further to a depth of 1402 m using mud rotary percussion drilling method. The geological logs of the two monitoring boreholes are discussed below.

R01-BW

The borehole drilled to a depth of 1402 m intersecting 57 m of Poortjie Member of the Middleton Formation (Figure 6-3), is positioned around 500 m northeast of the proposed 4000 m deep borehole. The Poortjie Member with an estimated thickness of 204 m in the Beaufort West area consist of sandstone units between 5 and 15 m thick interbedded with subordinate mudstone and siltstone. Below the Poortjie Member is the Abrahamskraal Formation consisting of mudstone and subordinate sandstone and siltstone. The Abrahamskraal Formation intersected at depth between 57 m and 750 m was intruded by dolerite between depths 492 m and 508 m (Figure 6-3, Table 6-1).

At depth between 750 m the boundary between Abrahamskraal Formation and the underlying Waterford Formation of the Ecca Group has been placed. The Waterford Formation is more arenaceous than the Abrahamskraal Formation. The base of the first prominent sandstone above a

shale-dominated succession is defined by the lower boundary of the Waterford Formation within the underlying Tieberg Formation. The argillaceous Tieberg Formation intersected within the lower portion of the borehole to the end is composed of 90 – 95 per cent shale and 5 – 10 per cent siltstone and sandstone.

Table 6-1: Abbreviated log of borehole R01-BW

Depth of unit (m)	**Lithology**	**Stratigraphy**
0 - 56	Shale	Poortjie Member, Middleton Formation
56 - 57	Sandstone	
57 - 89	Shale and siltstone	Abrahamskraal Formation
89 - 115	Sandstone and siltstone	
115 - 162	Shale and siltstone	
162 - 168	Sandstone	
168 - 191	Shale and siltstone	
191 - 196	Sandstone	
196 - 221	Shale and siltstone	
221 - 230	Sandstone	
230 - 237	Shale and siltstone	
237 - 244	Sandstone	
244 - 256	Siltstone and sandstone	
256 - 276	Shale and siltstone	
276 - 492	Siltstone and sandstone	
492 - 508	Dolerite	Karoo dolerite
508 - 554	Siltstone and sandstone	Abrahamskraal Formation
554 - 580	Sandstone	
580 - 582	Siltstone	
582 - 608	Siltstone and sandstone	
608 - 615	Silty shale	
615 - 621	Siltstone and sandstone	
621 - 631	Sandstone	
631 - 633	Shale and siltstone	
633 - 661	Siltstone and sandstone	
661 - 664	Silty shale	
664 - 673	Siltstone and sandstone	
673 - 675	Silty shale	
675 - 680	Siltstone	
680 - 683	Silty shale	
683 - 689	Siltstone and sandstone	
689 - 700	Siltstone and silty shale	
700 - 704	Siltstone and sandstone	
704 - 706	Silty shale	

Depth of unit (m)	Lithology	Stratigraphy
706 - 715	Sandstone, siltstone and shale	Abrahamskraal Formation
715 - 720	Silty shale and siltstone	
720 - 726	Siltstone, sandstone and silty shale	
726 - 731	Silty shale and siltstone	
731 - 750	Siltstone, sandstone and silty shale	
750 - 785	Sandstone, siltstone and shale	Waterford Formation
785 - 798	Siltstone, sandstone and shale	
798 - 810	Siltstone and silty shale	
810 - 823	Siltstone, sandstone and silty shale	
823 - 830	Siltstone and silty shale	
830 - 872	Siltstone, sandstone and silty shale	
872 - 878	Siltstone and silty shale	
878 - 889	Siltstone, sandstone and silty shale	
889 - 892	Siltstone and silty shale	
892 - 900	Siltstone, sandstone and silty shale	
900 - 907	Siltstone and silty shale	
907 - 909	Siltstone, sandstone and silty shale	
909 - 913	Siltstone and silty shale	
913 - 919	Siltstone, sandstone and silty shale	
919 - 937	Siltstone and silty shale	Tieberg Formation
937 - 941	Siltstone, sandstone and silty shale	
941 - 948	Siltstone and silty shale	
948 - 956	Siltstone, silty shale and sandstone	
956 - 975	Siltstone and silty shale	
975 - 983	Siltstone, sandstone and silty shale	
983 - 988	Siltstone and silty shale	
988 - 1015	Siltstone, sandstone and silty shale	
1015 - 1030	Silty shale and siltstone	
1030 - 1034	Siltstone, sandstone and silty shale	
1034 - 1049	Silty shale and siltstone	
1049 - 1063	Siltstone, sandstone and silty shale; clayey	
1063 - 1078	Silty shale and siltstone	
1078 - 1083	Shale, siltstone and sandstone	
1083 - 1088	Silty shale and siltstone	
1088 - 1090	Shale, sandstone and siltstone	
1090 - 1118	Silty shale and siltstone	
1118 - 1136	Siltstone, sandstone and silty shale	

Depth of unit (m)	Lithology	Stratigraphy
1136 - 1141	Siltstone and silty shale	Tieberg Formation
1141 - 1148	Siltstone, silty shale and sandstone	
1148 - 1185	Silty shale and siltstone	
1185 - 1192	Silty shale, siltstone and sandstone	
1192 - 1205	Siltstone and silty shale	
1205 - 1209	Siltstone and sandstone	
1209 - 1213	Siltstone and silty shale	
1213 - 1215	Siltstone, silty shale and sandstone	
1215 - 1228	Silty shale and siltstone	
1228 - 1231	Silty shale, siltstone and sandstone	
1231 - 1256	Silty shale and siltstone	
1256 - 1259	Siltstone, sandstone and silty shale	
1259 - 1266	Silty shale and siltstone	
1266 - 1272	Siltstone and sandstone	
1272 - 1302	Silty shale, siltstone and minor tuffaceous mudstone	
1302 - 1319	Siltstone, silty shale and sandstone	
1319 - 1358	Silty shale and siltstone	
1358 - 1389	Silty shale, siltstone and sandstone; minor tuffaceous mudstone	
1389 - 1396	Silty shale and siltstone	
1396 - 1397	Silty shale, siltstone and sandstone	
1397 - 1402	Silty shale and siltstone	
	END OF BOREHOLE	

Water strikes were obtained at the contact between Poortjie Member and Abrahamskraal Formation and also below the first dolerite at 692 m. However the water strikes intersected at depth between 503 -504 m were in dolerite rock fragments. Foreign water and foam was used during drilling therefore water quality samples could not be taken during the drilling. Water samples were only collected following the in-situ profiling at depth ranging 480 m (above dolerite), 515 m (below dolerite), 930 m (Waterberg Formation) and 1351 m (Tieberg Formation). Steady declines with depth indicating no potential inflow of water from the fractures were obtained from the temperature profile. However, the conductivity profile indicated a sudden decrease at 1350 m within the Tierberg Formation. The yield of borehole R01-BW was found to be not enough to be tested with a pumping test.

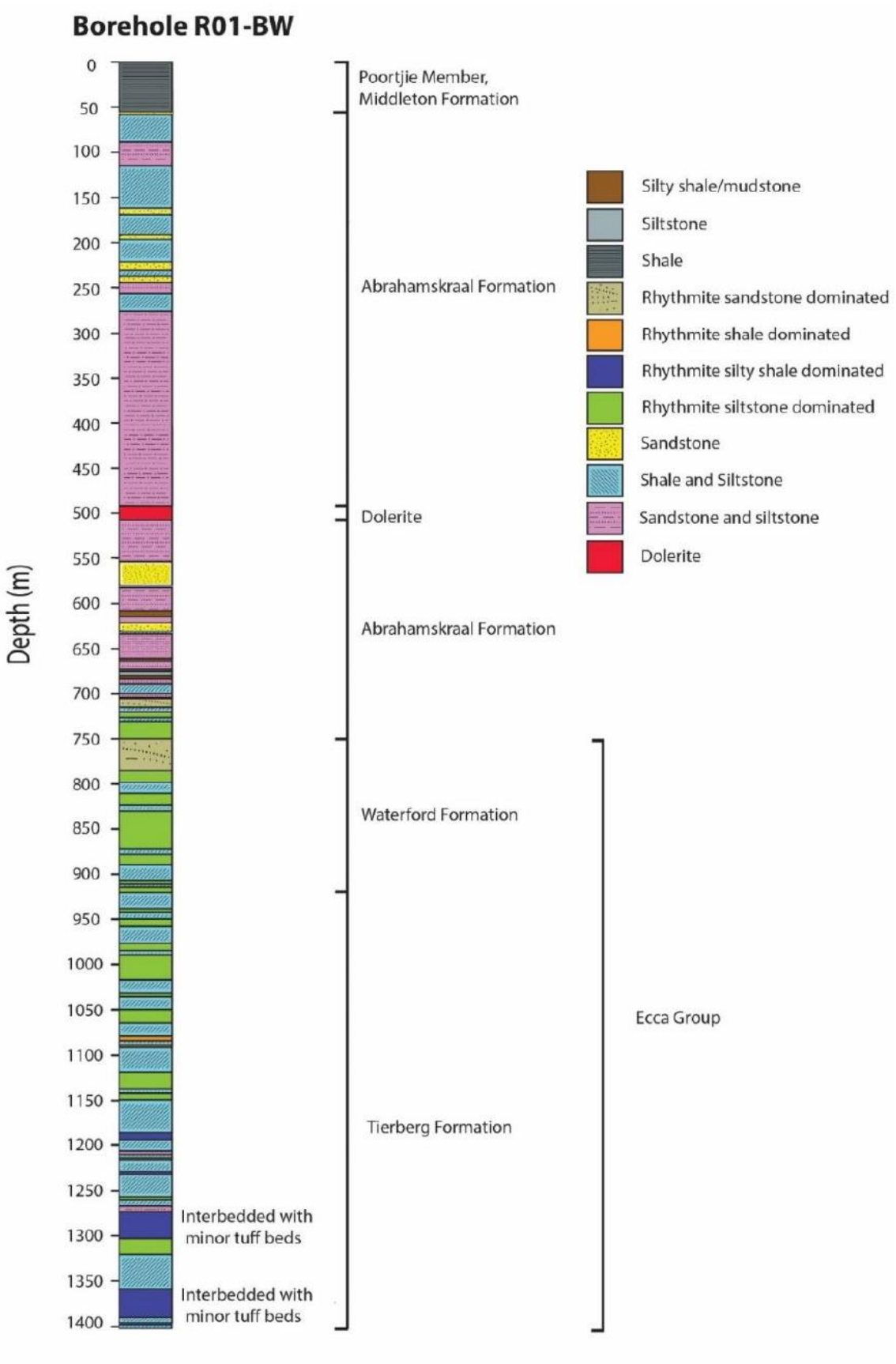

Figure 6-3: Geological log of borehole R01-BW (after Nxokwana *et al*, 2018b)

R02-BW

The borehole drilled to a depth of 516 m intersected 1 m of elluvial gravels at surface underlain by 64 m of Poortjie Member of the Middleton Formation (Figure 6-4). The Poortjie Member mostly consists of sandstone, siltstone and sparse shale. The Member is underlain by the Abrahamskraal Formation composed of mudstone and subordinate sandstone and siltstone. The Abrahamskraal Formation intruded by dolerite at depth between 161 m ad 178 was intersected from depth 66 m to the end of the borehole (Figure 6-4; Table 6-2).

Table 6-2: Abbreviated log of borehole R02-BW

Depth of unit (m)	**Lithology**	**Stratigraphy**
0 - 1	Eluvial gravels and soil	
1 - 4	Siltstone and sandstone	Poortjie Member, Middleton Formation
4- 11	Sandstone	
11 - 13	Shale	
13 - 40	Sandstone and siltstone	
40 - 42	Siltstone and silty shale, clayey	
42 - 59	Sandstone and siltstone, clayey	
59 - 65	Sandstone and siltstone	
65 - 73	Siltstone, sandstone and shale	Abrahamskraal Formation
73 - 88	Sandstone	
88 - 100	Shale, siltstone and sandstone	
100 - 106	Sandstone, siltstone and silty shale	
106 - 109	Silty shale and siltstone	
109 - 146	Sandstone and silty shale	
146 - 161	Siltstone, sandstone and silty shale	
161 - 178	Dolerite and rock fragments	Dolerite
178 - 179	Sandstone and shale	Abrahamskraal Formation
179 - 188	Siltstone, sandstone and shale	
188 - 193	Sandstone and shale	
193 - 195	Sandstone, siltstone and shale	
196 - 230	Fine-grained to very fine-grained sandstone (mudstone?) and very fine-grained shale.	
230-317	Fine-grained to very fine-grained siltstone and very fine-grained shale.	
317-375		
375-474		
474-505		
505-517		
End of borehole		

The water strike at depth around 39 m recovered only muddy chips may be associated with unsaturated zone. More significant water strike which may be related to fracture zone was intersected at depth between 57 m and 58 m within the Poortjie Member and the blow yield was measured at 6.67 L/s. Furthermore, smaller water strikes were encountered at the brecciated zones. Due to strong hydrostatic pressure drilling was completed to a depth 516m and no further drilling was recommended. The borehole yield increased with depth with a final blow yield of 16.3 L/s recorded.

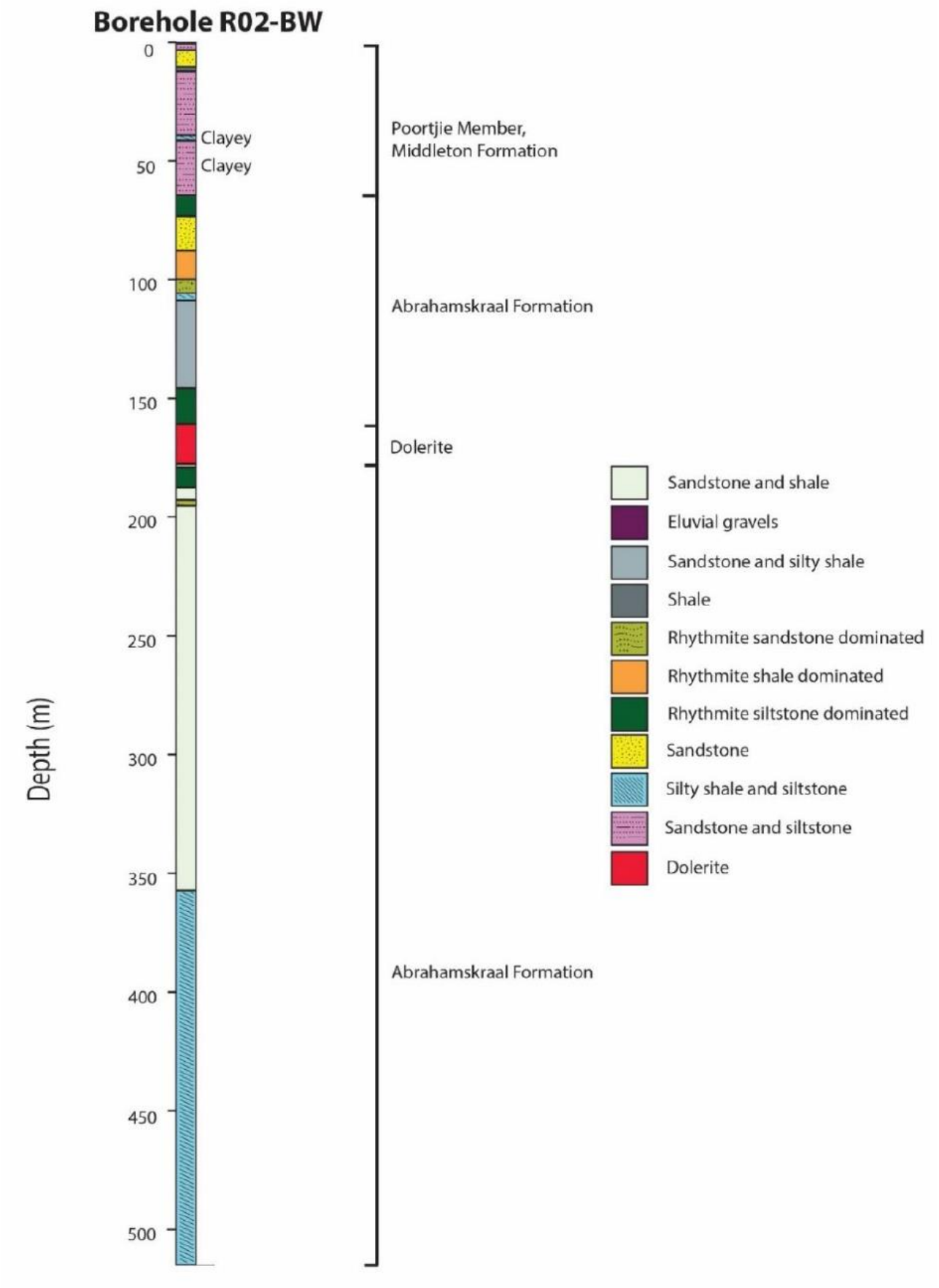

Figure 6-4: Geological log of borehole R02-BW (after Nxokwana *et al*, 2018b)

6.3.3 Identification of lithology using downhole geophysical log

Due to the challenge of interpreting rock chips during geological logging as may be mixed during drilling, the downhole geophysical was conducted on the two monitoring boreholes (Nxokwana *et al*, 2018b). The surveys were aimed on obtaining in-situ geotechnical and structural information of rock formations that were intersected by the two boreholes. The downhole geophysical survey was conducted by Wireline Africa in association with Wireline Alliance. The tools used for downhole geophysical survey includes 3-Arm caliper, Acoustic (ATV) and Optical (OTV) Televiewer, Neutron, Density, Resistivity, Gamma, Temperature, Conductivity and flowmeter. The lithological identification and aquifer delineation logs for borehole R01-BW are shown in Appendix A – C, while for logs borehole R02-BW are shown in appendix D - F.

6.3.3.1 Lithology identification and anomalies linked to aquifer delineation for Borehole R01-BW

The geological logs suggested the presence of dolerite between depths of 492 and 508 m (Appendix A). The suggestion corresponds to very low gamma ray values, high density values and high resistivity values on the geophysical log between depths of 489 and 508 m (Appendix A). At depth between 489 m and 492 m intersection of very fine grained sandstone with the absence of dolerite might be due to rock chips not reaching the surface immediately. The very low gamma ray, high density and resistivity identified another lithology at depth between 690 m and 692 m as dolerite. the geophysical log results was of great assistance as the geological log only showed silty shale and siltstone, this may be probably due to that dolerite chips been missed during sampling.

The low gamma ray and high resistivity values with correlation from the rock chips could be associated with sandstone, but identifying such from geophysical log was not always assured. However some sandstone units identified from the percussion chips, did not give the low gamma ray/ high resistivity signature on the geophysical log at depth between 221 m – 229 m, 332 m – 342 m, 367 m – 372 m and 646 m – 649 m (Appendix A). Inference of sandstone between depths of 311 m and 315 m from the low gamma ray value and high resistivity value, whereas the rock chips identified a mixture of sandstone, siltstone and shale.

The interpreted dolerite lying between depths of 492 and 508 m identified from the rock chips, may be associated with very low gamma ray values, high density values and high resistivity values between depths of 490 and 508 m (Appendix A). For about 15 m above and below the dolerite the resistivity indicates an increase and decrease, this may be due to contact metamorphism of the intruded sedimentary rocks (Appendix A). Another dolerite at depth around 690 m and 692 m was identified by very low gamma ray values and high density and resistivity values, but the geological log missed it. A thin (~ 1 m) dolerite also missed by geological logging at depth 700 m was

identified by a very low gamma ray and high density/resistivity signature. Beneath the 700 m depth there was no other dolerite signatures were found in the geophysical log, as much as it was not present in the geological log.

The possibility of identifying sandstone from the low gamma ray and high resistivity, could mostly be applicable to sandstone in the Abrahamskraal Formation and the Waterford Formation above 750 m-depth. However, the geological log identified a mixture sandstone, siltstone and shale, as opposed to the low gamma ray value and high resistivity value which inferred it as eight sandstones within the Abrahamskraal and Waterford Formations around depths 888 and 890 m. below the 919 m in the Tierberg Formation the twelve sandstones inferred from the low gamma ray value and high resistivity value, was found to be a mixture of siltstone, silty shale and sandstone from the geological log. No other lithologies could be identified from the geophysical log. However, one of the four tuffaceous mudstone units between depths of 1374 m and 1376 m; coincides with a high gamma ray value.

The geophysical logs identified anomalies that may be linked to aquifer delineation using an acoustic televiewer (ATV) as shown in Appendix B. The hydrological analysis log (Appendix C) was challenging to interpret, however it may also assist in delineating aquifers. Most of these anomalies are associated with fracturing. Of all fractures that were identified from shallow depth to greater depth, others coincided with the water strikes and others did not. An open fracture of an aperture of 72.68 mm was identified at depth around 11.51 m and no water strike was observed (Figure 6-5). A minimum fracture at depth between 67.45 – 67.82 m coincided with the water strike at depth 67 – 68 m (Figure 6-6). The water strike at depth between 131 – 132 m might be associated with an open fracture of an aperture around 5.77 mm at depth 130.18 m (Figure 6-7). The water strike at depth between 503 – 504 m coincided with a fracture at depth 503.49 m (Figure 6-8). Other water strikes that did not coincide with the identified fractures might be associated contact zones. An open fracture of an aperture of 77.88 mm identified at depth around 779.01 m did not coincide with water strike was observed (Figure 6-9).An open fracture of an aperture of 14.47 mm was identified at depth around 1105.73 m and no water strike was observed (Figure 6-10).

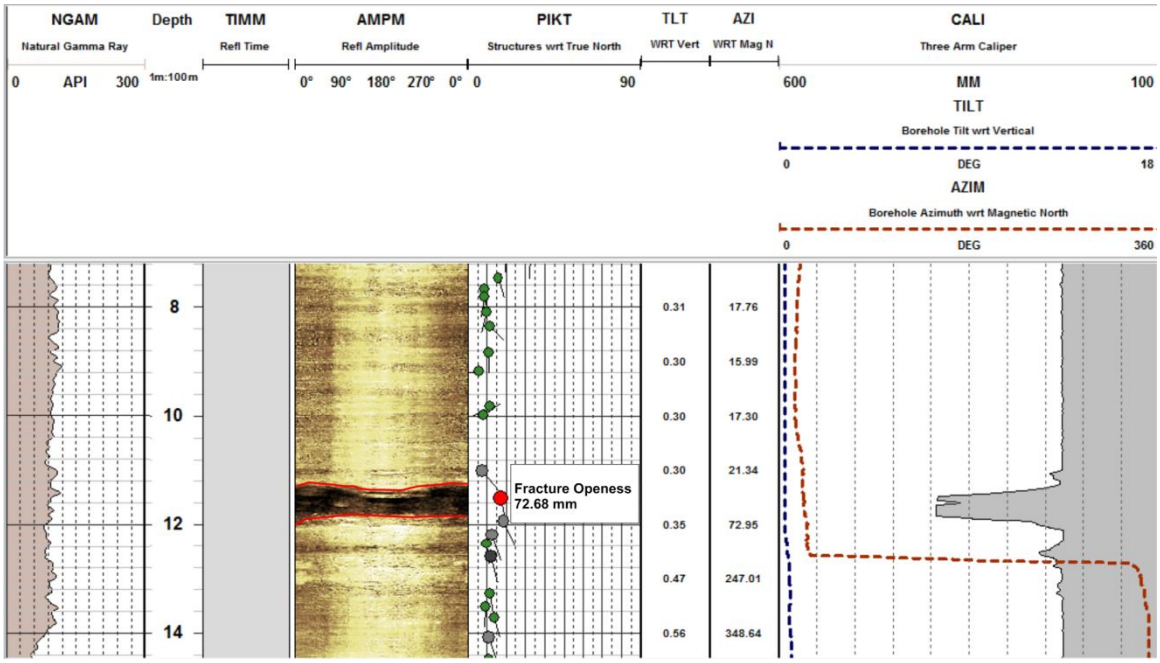

Figure 6-5: Open fracture identified at depth 11.51 m

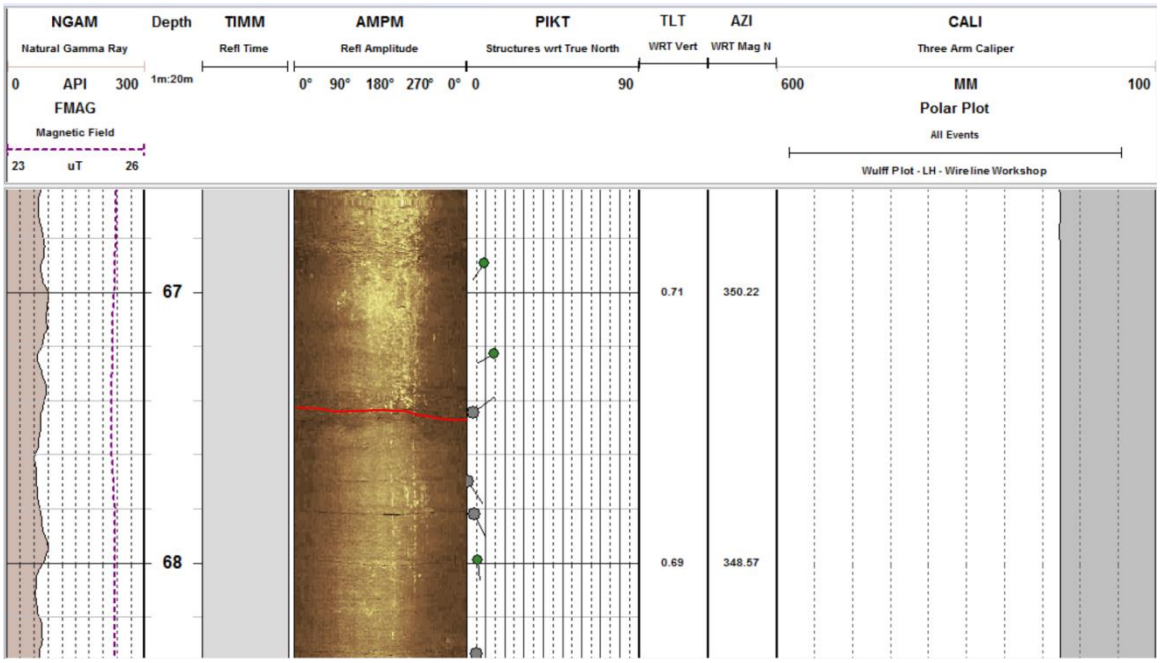

Figure 6-6: Minimum fracture identified at depth 67.49 m

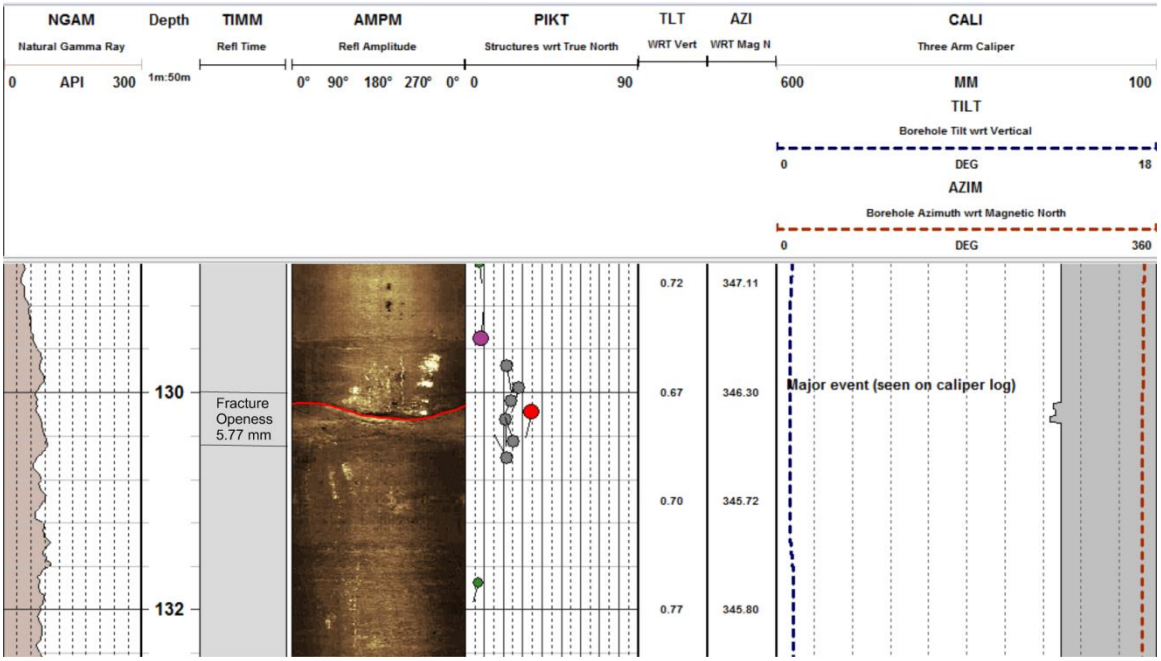

Figure 6-7: Open fracture identified at depth 130.18 m

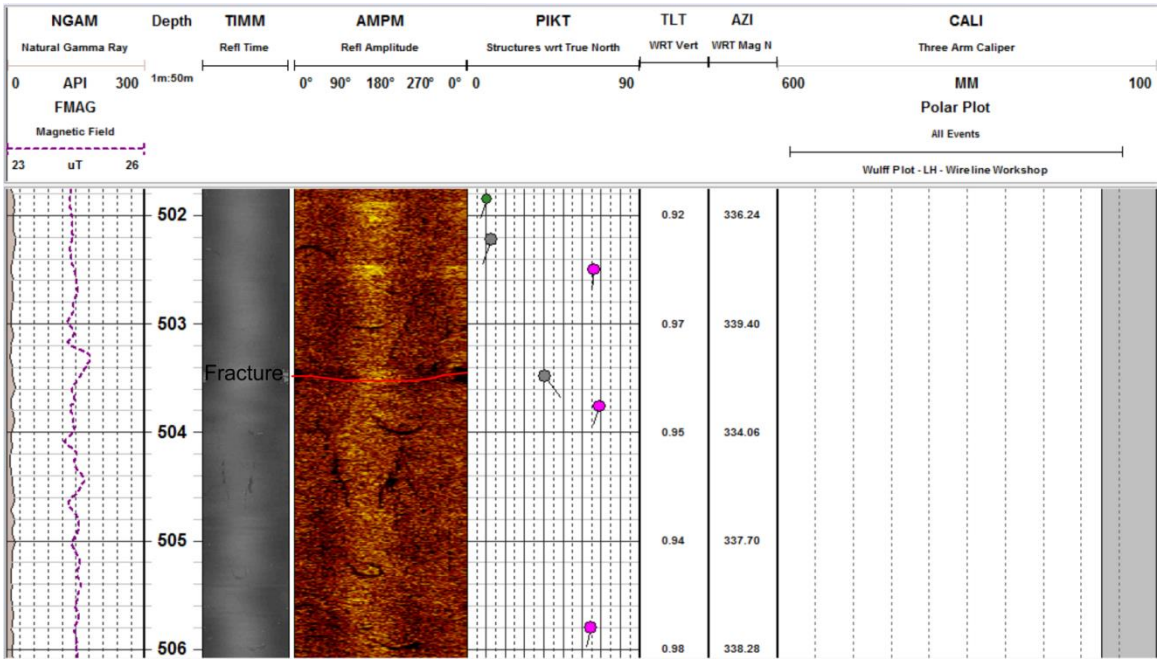

Figure 6-8: Minimum fracture identified at depth 503.49 m

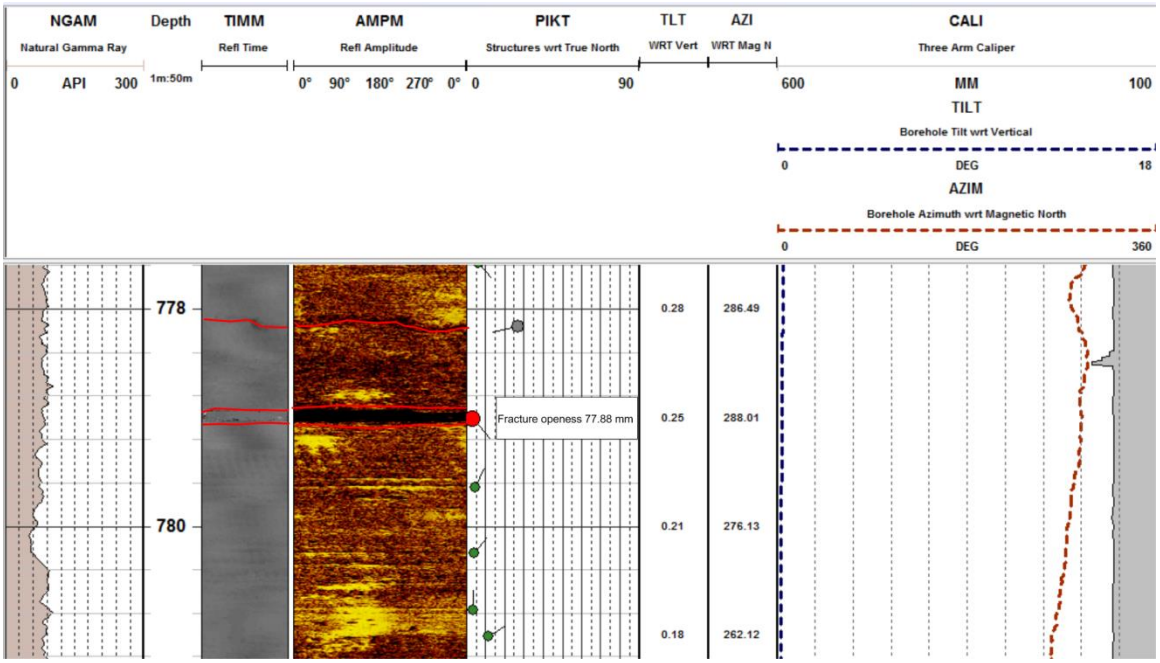

Figure 6-9: Open fracture identified at depth 779.01 m

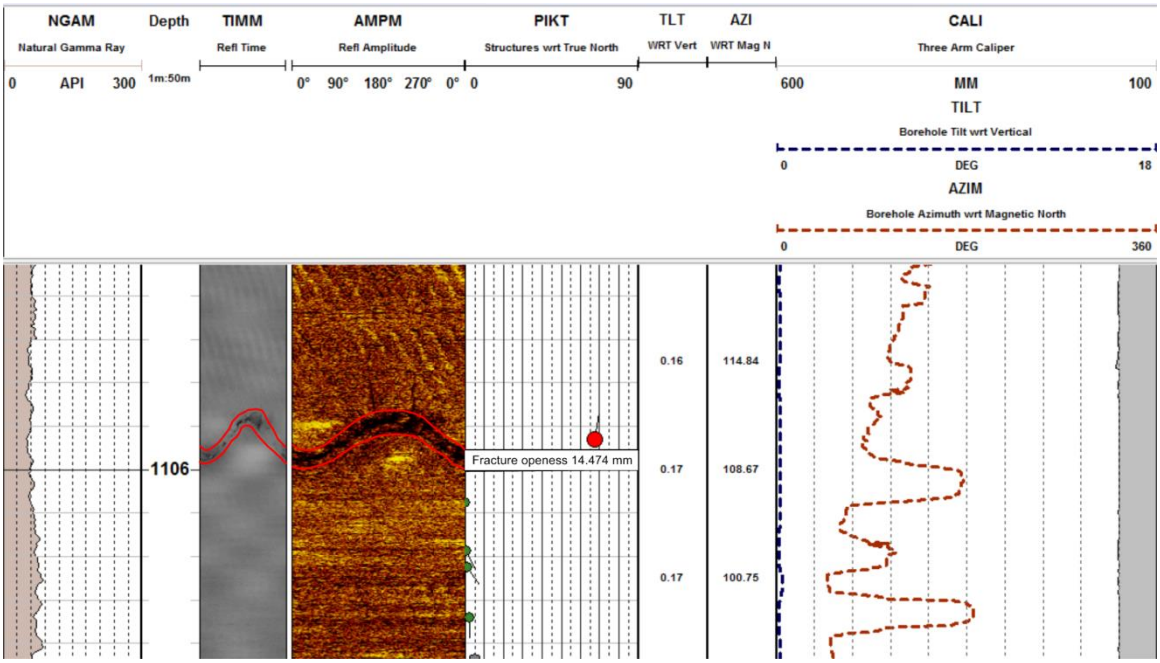

Figure 6-10: Open fracture identified at depth 1105.73 m

6.3.3.2 Lithology identification and anomalies linked to aquifer delineation for borehole R02-BW

The downhole geophysical survey for this extended to a depth up to 508 m. Similar to borehole R01-BW the dolerite may clearly be identified from the geophysical logs. Geological log results indicate the presence of dolerite between depths of 161 and 178 m. This correlated to geophysical log results characterized by very low gamma ray values, high density values and, generally, high resistivity values at depths ranging around 159.5 m and 176.5 m (Appendix D).

Geophysical log may have identified sandstone below depth 186 m, but without good correlation from the geological log. Low gamma ray value and high resistivity value may be related to sandstone and correlation was made between three sandstones in the Poortjie Member and upper part of the Abrahamskraal Formation. Sandstone with minor inter-bedded siltstone, silty shale and shale between depths of 4 m and 11 m gave a good correlation with interpreted sandstone from the geophysical log at depths between 4 m and 10 m (Appendix D). A good correlation can be observed between sandstone with siltstone and shale in places between depths of 73 m and 88 m and the interpreted sandstone from the geophysical log, at depth between 77 m and 78 m (Appendix D). The interpreted sandstone from the geophysical log (Appendix D) at depths between 111 m and 116 m corresponds to the geological log sand sandstone at depths between 111 m and 114 m. Siltstone and shale between 114 m and 115 m coincides with an interval of average gamma ray and resistivity on the geophysical log. Thirteen sandstones with low gamma ray high resistivity values were identified from the geophysical log below 186 m-depth (Appendix D). The absence of abundant sandstone in the percussion chips below 186 m-depth cannot be explained, but might be related to a strong water flow from the 17 water strikes that were intersected. No other lithologies could be identified from the geophysical log.

The acoustic televiewer was used to identify possible anomalies linked to aquifers and were also correlated with the water strikes observed during drilling (Appendix E). The hydrological analysis log (Appendix F) was challenging to interpret, however it may also assist in delineating aquifers. An open fracture identified at depth around 32.29 m with an aperture of 276.887 mm did not yield water strike, however the water strike observed at depth of 39 m might be associated with minimum fracture at depth 38.85 m (Figure 6-11). An open fracture at depth 57.27 m with aperture of 96.440 mm correlates very well with the significant water strike at depth between 57 and 58 m (Figure 6-12). Factures at depth between 81.40 and 81.97 m and have apertures 25.692 and 15.540 mm respectively might be related to water strikes intersected at depth between 65 and 163 m (Figure 6-13).

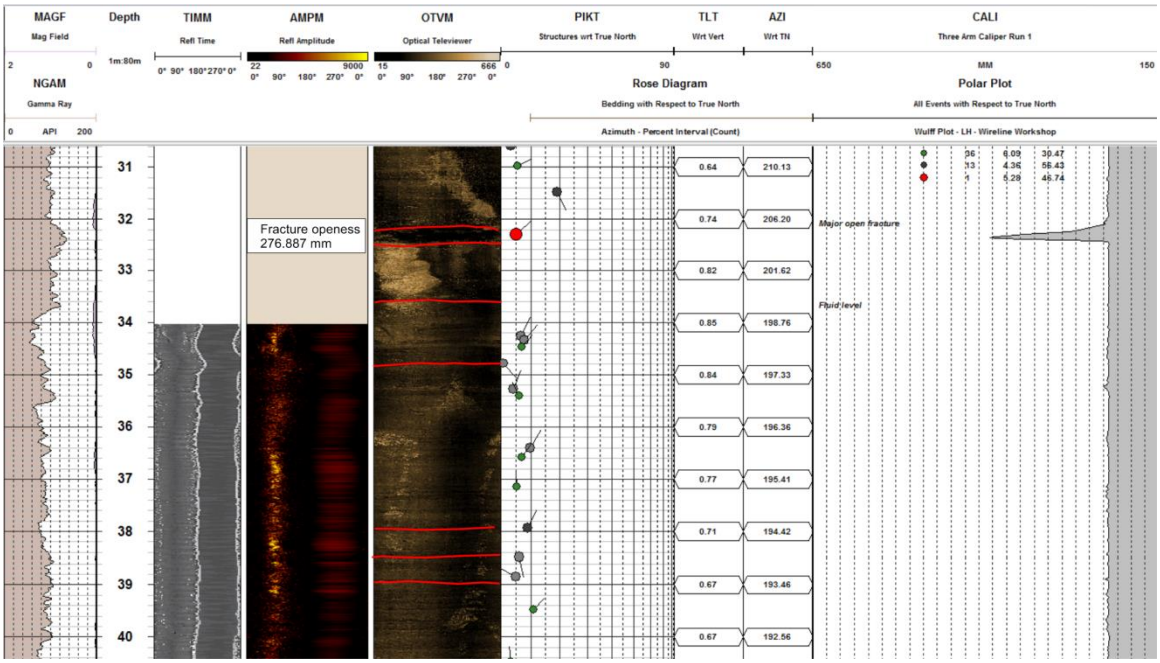

Figure 6-11: Open fracture identified at depth 32.29 m, with other five minimum fractures identified

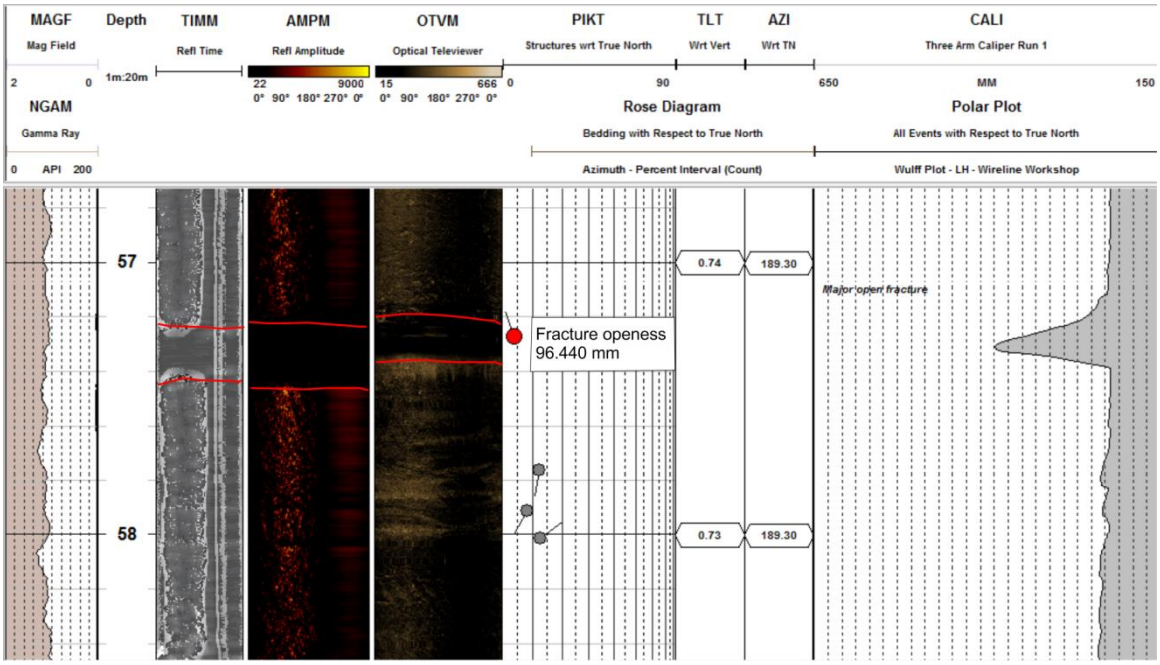

Figure 6-12: Open fracture identified at depth 57.27 m

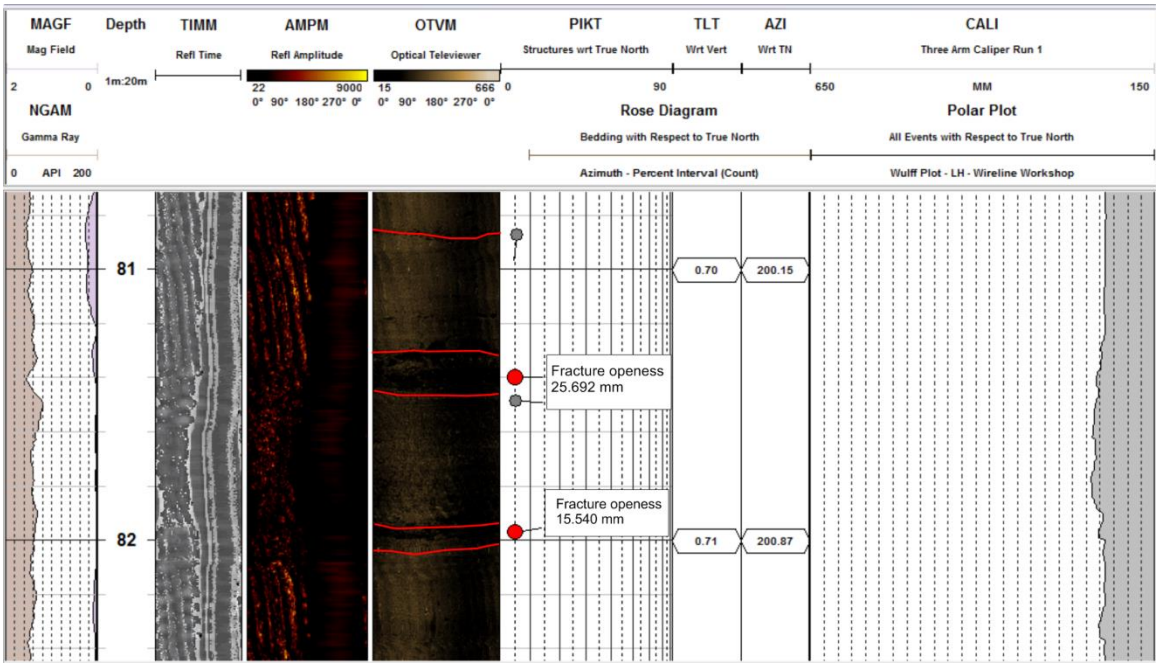

Figure 6-13: Open fracture identified at depth 81.40 and 81.97 m

Chapter 7:
DISCUSSION

7.1 INTRODUCTION

This chapter discusses the results of the current investigations in particular the information obtained from the ground and airborne geophysical data, along with the geological data recorded at the two monitoring boreholes, to detect and delineate the deep aquifer system. The study involves a multidisciplinary approach to science of which ground and airborne geophysical surveys forms the major part.

7.2 SUMMARY OF GEOPHYSICAL RESULTS

The geophysical approach used in this study played a major role in characterising and delineating aquifer system. Airborne magnetic data was used as an aid in delineating dolerite that does not appear to the surface and mapping structures of regional extent. Interpretation of the results depicted that airborne magnetic is effective in mapping major structures and intrusive magmatic bodies. Using enhanced filtering techniques features of high magnetic field may be inferred as intrusive magmatic body. The intrusive magmatic body correlates clearly with mapped dolerite dykes and sills. It may be fair to associate the high magnetic field intensity with the intrusive dykes and sills. The dolerites have a great influence on the groundwater dynamics, especially in the fracture zones as they provide pathways for groundwater. It was vital to understand their locality and orientation to enable to assist the planning of the two monitoring boreholes and deep borehole.

Some of these magnetic anomalies exhibit strong positive magnetic amplitudes and some show strongly negative amplitudes when compared to the surrounding areas. Other magnetic anomalies possesses dipolar signature (where the anomaly exhibits both magnetic negative and positive amplitudes). The dipolar anomalies were interpreted as due to sills or intrusive bodies. Interpreted magnetic bodies extracted from the magnetic data are shown in Figure 7-1. The interpretation of lineaments and magnetic bodies can be helpful in updating the geology map and for groundwater exploration.

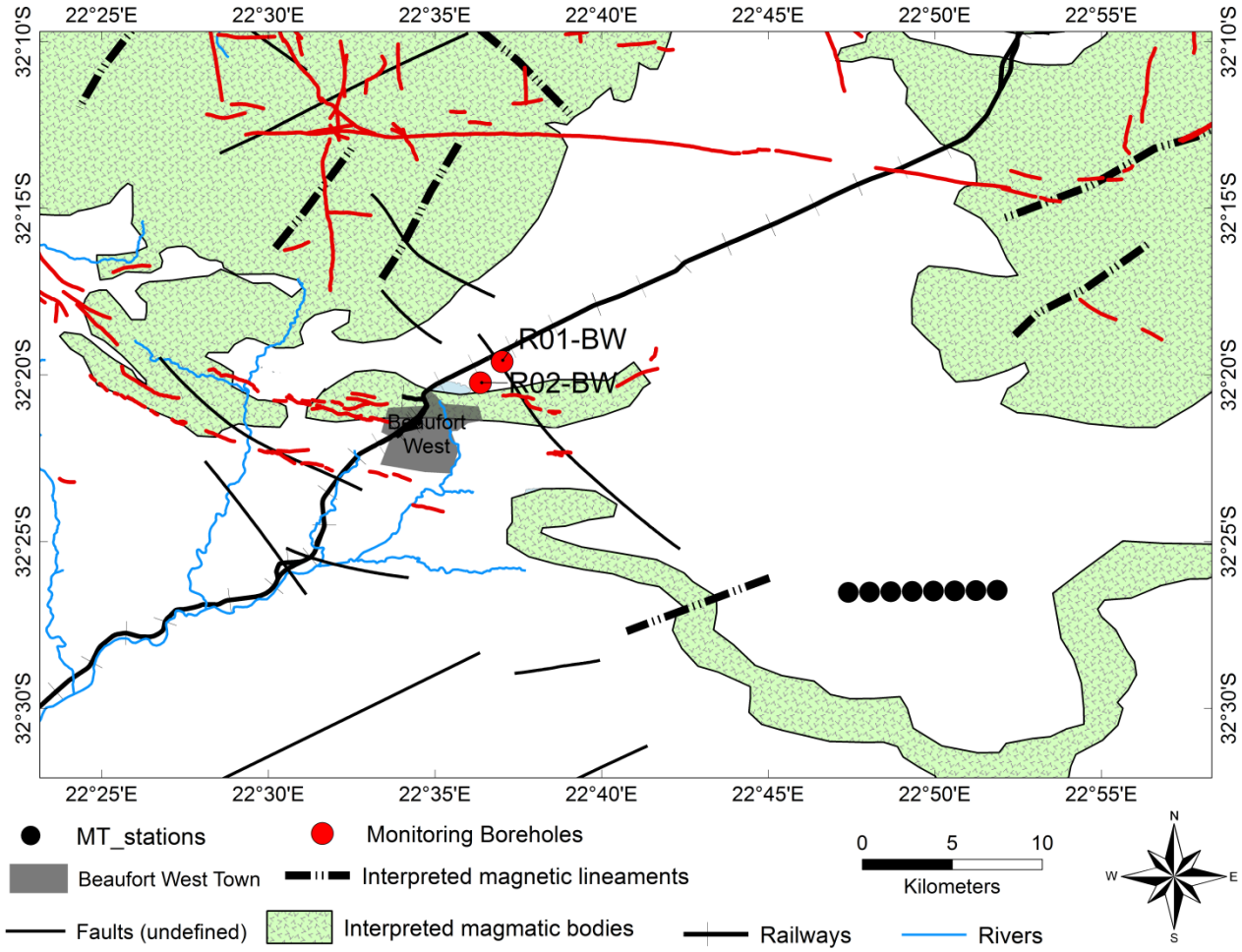

Figure 7-1: Magnetic interpretation highlighting intrusive magnetic bodies and lineaments

The 3D perspective view (Figure 7-2) identified from the analytical signal a circular or irregular shape feature which may be interpreted as deep-seated intrusive magmatic. The MT section identified very high resistive body. Due to its strong electrical properties correlation to aquifer properties, the resistive body of average resistivity values of around 1705 ohmm may be associated with the intrusive magmatic body. On both sides of the intrusive feature are the conductive features which may be associated with possible Whitehill Formation. The 2-D model suggests the presence of strong lateral changes of the subsurface resistivity distribution. The resistive substratum to the east of section and the inclined resistive layer might be an indication of dolerite sill and dyke respectively. Based on this results it may fair to note that magnetotelluric geophysical method is a non-intrusive tool that played a major role in obtaining information of the subsurface at great depth. The depth extent of the section is about 4 km and no boreholes information was provided in the area. Due to lack of borehole information the interpretation was limited to airborne and ground geophysical datasets. The high magnetic field intensity corresponds very well with the high resistive feature mapped in the resistivity section.

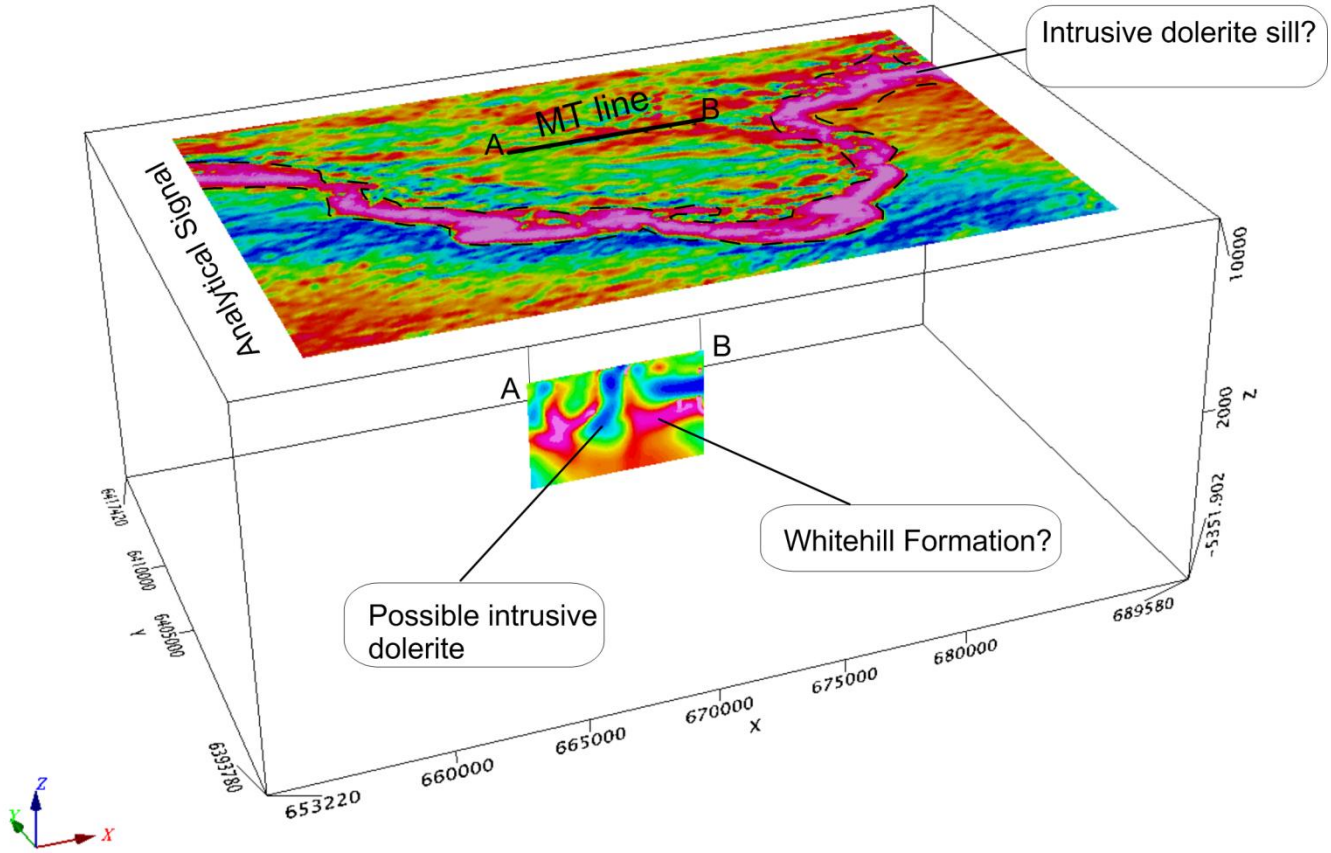

Figure 7-2: The MT section shown in 3D perspective, together with high resolution airborne magnetic data set

7.3 DRILLING AND DOWNHOLE LOGGING

Two monitoring boreholes (R01-BW and R02-BW) were drilled to a depth 1402 m and 516 m respectively. The boreholes were drilled at a larger distance (± 20 km) from the magnetotelluric traverse, due to the electromagnetic highly influenced by DC powered railway which is near the boreholes site. Magnetotelluric results may not be constrained with confidence with the borehole information due to the larger distance separation. Drilling of the boreholes was aimed on determining the lithology and stratigraphy of the Beaufort Group and underlying Ecca Group, and the properties of shallow groundwater. Borehole R01-BW drilled to a depth of 1402 m intersected from surface downwards shale and sandstone, 57 m thick, of the Poortjie Member (Middleton Formation), siltstone, shale and sandstone, 677 m thick, of the Abrahamskraal Formation, sandstone, siltstone and shale, 169 m thick of the Waterford Formation, and siltstone and shale, 483 m thick, of the Tierberg Formation. Dolerites 16 m and 2 m thick, intrude the Abrahamskraal Formation. Borehole R02-BW drilled to a depth of 516 m intersected from surface downwards sandstone, siltstone and subordinate shale, 64 m thick, of the Poortjie Member (Middleton Formation), and sandstone, siltstone and shale, 434 m thick, of the Abrahamskraal Formation. A dolerite 17 m thick, intrudes the Abrahamskraal Formation.

Due to the challenge of interpreting rock chips during geological logging as may be mixed during drilling, the downhole geophysical was conducted on the two monitoring boreholes in order to obtain in-situ geotechnical and structural information. Borehole R01-BW gave a good correlation with the identification of dolerite at depth between 489 and 508 m. a great assistance can be observed at depth between 690 and 692, where the geophysical identified dolerite which was missed by geological logging. Borehole R02-BW, the identification of dolerite at depth between 159.5 and 176.5 m gave a good correlation with the geological log. Geophysical log may have identified sandstone below depth 186 m, but without good correlation from the geological

7.4 CONCEPTUAL GEOLOGICAL AND HYDROGEOLOGICAL MODEL

Information obtained from the six boreholes (four observation (150m) and the two deep monitoring (1400m and 500m)) have been used to draw a cross section at the site. Another borehole used was G2 drilled by a consultant for the municipality north of the dolerite ridge. The section extends from the dolerite ridge in the South to the Northern observation borehole BO1H-BW. The dolerite sill has been intercepted by G2 (60m), RO2-BW (160 to 176 m) and RO1-BW (492-508m). The resulting cross section shows that the dolerite sill observes a sudden up-stepping from 350 m elevation in the North to 700 m elevation in the South (Figure 7-3).

Several water strikes were intercepted during drilling of monitoring boreholes. Many of the high yielding strikes are concentrated at the contact of Poortjie Member and Abrahamskraal Formation. Very few water strikes were intercepted below the dolerite sill. These are also low yielding as compared to the strikes at the contact of the formations. A possible conclusion could be that the fractured aquifer below the sill is compacted and semi-confined

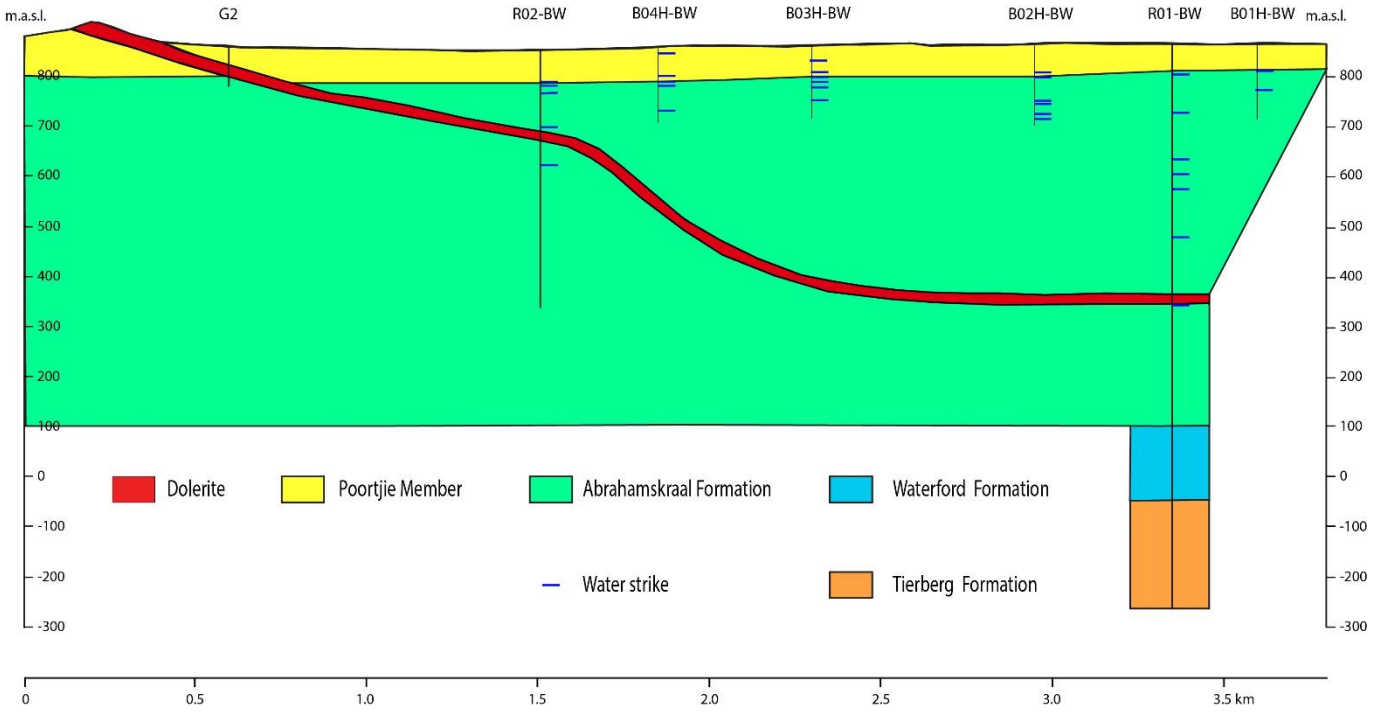

Figure 7-3: South to North Cross section showing the up stepping of the dolerite sill. Note the concentration of water strikes at the bottom or below the Poortjie formation

Chapter 8:
CONCLUSIONS AND RECOMMENDATIONS

The potential of geophysical methods to derive properties and state variables that are critical to aquifer has played a major role in many studies to characterise and delineate the aquifer system. The use of geophysics has been and still is the best practise for groundwater studies to avoid the risk of drilling dry borehole and cost implication associated with poor groundwater production.

The current research study focuses on using the magnetotelluric method, in conjunction with airborne magnetic methods, to investigate the deeper aquifer systems in the vicinity of Beaufort West. High resolution aeromagnetic data is necessary in mapping dolerite sills and dykes that are not exposed at surface. Magnetotelluric is an electromagnetic method that is useful in obtaining information at greater depth that shallow drilling could not reach. The possibility of shale gas exploration has triggered the need to better understand the aquifer system and groundwater dynamics in the Main Karoo Basin.

The high resolution airborne magnetic survey was undertaken in order to upgrade the geology map and reveal presence of hidden geological features such as dolerite dykes or sills, faults and magnetic lineaments. The results showed that magnetic method can play a significant role in generating mineral and groundwater targets. The total magnetic field showed positive anomalies that exceed the local magnetic field of the area as recognized by a steep gradient, while negative anomalies are below the local magnetic fields. The high-resolution data clearly mapped dyke, sills, faults, geological contacts, magnetic lineaments and intrusive bodies. These lineaments could be an indication of foliation in the area in response to shearing. The development of the foliation within the Beaufort Group sediments is restricted to the finer grained sandstone, mudrock and siltstone.

Magnetotelluric results displays very high resistive layers that appear to have been intruded within the slightly conductive zone might be associated with dolerites. The displacement of a conductive zone around distance 2200 m and 5000 m might be an indication of faulting. The resistive substratum reaching a depth of around 2000 m to the east and the inclined resistive layer might be an indication of dolerite sill and dyke respectively. Based on this results it may be fair to note that geophysics is a non-intrusive tool that played a major role in obtaining information of the subsurface at great depth.

The 2D magnetic modelling was created using GMSYS modelling package from Oasis montaj to verify the MT results. The magnetic modelling confirms the resistive layer observed in MT inversion model might be related to dolerite. The results shows the magmatic feature with

susceptibility value of around 0.012981 SI unit might represent a slight vertically inclined dolerite to the center at distance ranging between 2 km and 4 km, while to the west and east of the profile appears to be horizontal. These structures may have been connected during their previous formations, as can be seen that it might have been disrupted due to present day erosion. The Poortjie Member might have been heavily intruded, whereas the Ecca and Dwyka Groups appear to be suppressed. These intrusive bodies have been covered by younger alluvial. These results enhance the knowledge that aquifers within the Karoo may be occurring beneath the well-studied depth.

The monitoring borehole (R01-BW) has revealed that the Ecca Group sediments are located shallower than initially predicted from the preliminary models, with the dark shales of the Tieberg Formation intersected at the depth of 930m. This borehole has intersected seven water strikes with the upper two strikes found to be the strongest. The water strikes intersected at depth between 503-504 m were in dolerite rock fragments. The result confirms the occurrence of aquifers beneath the well-known depth.

The positions of the two monitoring boreholes were removed by a large distance from the positions of the magnetotelluric survey. Although the combined use of airborne and ground geophysical surveys was of a great assistance in understanding of the subsurface geological and geohydrological conditions, the information obtained from the boreholes cannot be used with confidence to constrain the geophysical interpretation. Considering this and also the ambiguity and none uniqueness in geophysical interpretation, it is therefore highly recommended that geophysical results be constrained through drilling.

REFERENCES

AeroPhysX. (2017). Council for geoscience ST-2016-1250 Karoo Blocks Magnetic and Radiometric Field Survey Final Report.

Araffa, S.A.S., Pek, J., (2014). Delineating groundwater aquifer and subsurface structures using integrated geophysical interpretation at the Western part of Gulf of Aqba, Sinai, Egypt. International journal of water resources and arid environments 3(1): Pg. 51-62.

Araffa, S.A.S., Sabet, H.S., Al Dabour, A.M., (2015). Intergrated geophysical interpretation on the groundwater aquifer (at the norsth western part of Sinai, Egypt). International Journal of Innovative Science, Engineering & Technology, Vol. 2. Issue 12.

Beaufort West Municipality., 2013. Intergrated development plan. Annual review 2012/2013.

Bera, P., Rao, C.K., (2012). Magnetotelluric: A tool for deep crustal study. 9th Biennial international conference and exploration on petroleum geophysics.

Botha, J.F., Verwey, J.P., Van der Voort, I., Vivier, J.J.P., Buys, J., Collinston, W.P., Loock, J.C., (1998). Karoo Aquifers, their geology, geometry and physical properties. WRC report no: 487/1/98.

Botha, W.F., Combrinck, M., Botha, F.S., van Rooy, J.L., (2001). An integrated multi-disciplinary geophysical approach to groundwater exploration in the Nebo granite, Northern Province. WRC Report No. 862/1/01. WRC project K5/862/0/1.

Botha, J.F., Cloot, A.H., (2004). Karoo Aquifers, deformation, hydraulic and mechanical properties. Draft report of the Water research commission on the project: Flow and transport characteristics of groundwater in Karoo Formation.

Bratus, A., Santarato, G., (2009). The characterization of aquifers by means of resistivity investigations. Bollettino di Geofisica Teorica ed Applica. Volume 50, n 1, Pg. 15-28.

Bubnov, V.P., Yakovlev, A.G., Aleksanova, E.D., Yakovlev, D.V., Berdichevsky, M.N., Pushkarev, P.Yu., (2007). Regional magnetotelluric exploration in Russia. In Spichak, V.V. (ed) Methods in Geochemistry and Geophysics. Volume 40.

Burger, C.A.J., Hodgson, F.D.I., and Van der Linde P.J., (1981). Hidrouliese eienskappe van akwifere in die Suid-Vrystaat. Die ontwikkeling en evaluering van tegnieke vir die bepaling van die ontginninspotensiaal van grondwaterbronne in die Suid-Vrystaat en in Noord-Kaapland, Volume 2, Instituut vir Grondwaterstudies, Oranje Vrystat Universiteit.

Catuneanu, O., Wopfner, H., Eriksson, P.G., Cairncross, B., Rubidge, B.S., Smith, R.M.H., Hancox, P.J., (2005). The Karoo basins of south-central Africa. Journal of African Earth Sciences Vol 43, Pg. 211 – 253

Chandler, V. W., (1994). Gravity investigation for potential ground-water resources in rock county, Minnesota. Report of investigation 44. University of Minnesota.

Chave, A.D., Weldeit, P., (2012). The theoretical basis for electromagnetic induction In: Chave, A.D., Jones, A.G., (eds). The magnetotelluric method, Pg. 19 – 47.

Cham Polteau, S., Ferre, E., Planke, S., Neumann E.R. and Chevallier L., (2008). How are saucer-shaped sills emplaced? Constrains from the Golden Valley sill, South Africa. Journal of Geophysical Research, vol. 113, Pg. 12104.

Chevallier, L., Woodford, A., (1998). Morpho-tectonics and mechanism of emplacement of the dolerite rings and sills of the western Karoo, South Africa. S.Afr.J.Geol., volume 102, Pg. 43-54.

Chevallier, L., Goedhart, M. and Woodford, A. C., (2001). The influence of dolerite sill and ring complexes on the occurrence of groundwater in Karoo fractured aquifers: a morpho-tetconic approach. Water Research Commission No 937/1/01, Pg.165.

Chevallier, L., Gibson, L.A., Nhleko, L.O., Woodfor, A.C., Nomquphu, W. and Kippie, I. (2004). Hydrogeology of fractured-rock aquifers and related ecosystems within the qoqodala dolerite ring and sill complex, great Kei catchment, Eastern Cape. WRC report 1238/1/04, Pg. 127.

Chevallier, L., (2012). Hydrogeology and ecology. In: Planke, S., Svensen, H. (eds). Field Guide – Karoo Basin. LASI V: Physical geology of subvolcanic systems: Laccoliths, Sills, and Dykes, Pg. 55 – 63.

Cole, D.I., Robey, K., Chevallier, L., Viljoen, J., (2011). The geology of shales with a gas potential in the Main Karoo Basin of South Africa and impact of hydraulic fracturing on groundwater. In Council for Geoscience Report 2011-0142, Pg. 43.Council for Geoscience Western Cape Regional Office (Bellville).

Cole, D., Mosavel, H., Browning, C., Chevallier, L., Mitha, V., Dhansay, T., Musekiwa, C., Maya, M., (2016a). Environmental baseline modelling and observed changes during drilling of a deep stratigraphic borehole in the Karoo: Results of a geological investigation around Beaufort West. Report, Council for Geoscience, Number 2016-0093, Pg. 55.

Cole, D.I., Johnson, M.R. and Day, M.O., (2016b). Lithostratigraphy of the Abrahamskraal Formation (Karoo Supergroup), South Africa. South African Journal of Geology, Vol. 119, Pg. 415-424.

Danielsen, J.E., Dahlin, T., Owen, R., Mangeya, P., Auken, E., (2007). Geophysical and hydrogeologic investigation of groundwater in the Karoo Stratigraphic sequence at Sawmills in Northern Matabeleland, Zimbabwe: a case history. Hydrogeology journal, volume 15, Pg. 945-960.

De Wit, M.J., (2011). The great shale debate in the Karoo. South African Journal of Science 107.

Dhansay, T., Navabpour, P., De Wit, M., Ustaszewski, K., (2017). Assessing the reactivation potential of pre-existing fractures in the southern Karoo, South Africa: Evaluating the potential for sustainable exploration across its Critical Zone. Journal of Earth Sciences., vol 134, Pg. 504 – 515.

Duncan, R.A., Hooper, P.R., Ehacek, J., and Marsh J.S., (1997): The timing and duration of the Karoo igneous event, Southern Gondwana. J. Geophys.Res., 102. Pg. 18127 - 18138.

Du Toit, A.L. (1905). Geological survey of Glen Grey and parts of Queenstown and Woodehouse, including the Indwe area. Geological Commission of the Cape of Good Hope, tenth annual report, Pg. 95-140.

Du Toit, A.L. (1920). The Karoo Dolerites- a study in Hypabyssal Intrusion. Trans. Geol. Soc. S. Afr., vol. 23, Pg. 1-42.

EPA., (1997). Surface geophysical methods. In: Expedited site assessment tools for underground storage tank site. A guide for regulators. Cited: 20 January 2017. http://www.epa.gov/oust/pubs/esa-ch3.pdf, 510-B-97-001.

Ernstson, E., (2006). Magnetic, geothermal, and radioactivity metods. In: Kirsch, R., (Ed), Groundwater geophysics a tool for hydrogeology, Pg. 275 – 294.

Fatti, L. J, (1970). The use of seismic reflection techniques in the Karoo Basin. Unpublished MSc Dissertation submitted to the Department of geophysics, University of the Witwatersrand, Johannesburg South Africa

Fatti, L.J., (1987). Reflection seismic surveys in the Karoo Basin by Soekor. Unpublished SAGA yearbook.

Fourie, F.D., (2003). Application of electro-seismic techniques to geohydrological investigations in Karoo rocks. Unpublished PhD thesis, University of the Free State, Bloemfontein.

Fitch, F.J. & Miller, J.A. (1984): Dating Karoo igneous rocks by the conventional K-Ar and 40Ar/39Ar age spectrum methods. In: A.J. Erlank (Ed), Petrogenesis of the volcanic rocks of the Karoo Province. Geol. Soc. South Afr. Spec. Publ., No 13, Pg. 247-256.

Heath, R.C., (1983). Basic ground-water hydrology, Pg. 84.

Hoover, D.B., Klein, D.P., Campbell, D.C., (1995). Geophysical methods in exploration and mineral environmental investigations.

Integrated Geoscience Solution, (2018). Magneto-telluric baseline in Ceres and Beaufort West areas. A report for the Council of Geoscience.

Johnson, M.R[1]., Van Vuuren, C.J[1]., Hegenberger, W.F[2]., Key, R[3]., Shoko, U[4]., (1996). Stratigraphy of the Karoo Supergroup in southern Africa: an overview. Journal of African Earth Science Vol 23, No 1, Pg. 3 – 15.

Johnson, M.R., van Vuuren, C.J., Visser, J.N.J., Cole, D.I., Wickens, H. de V., Christie, A.D.M., Roberts, D.L., Brandl, G., (2006). Sedimentary rocks of the Karoo Supergroup. In: Johnson, M.R., Anhaeusser, C.R., Thomas, R.J. (Eds), The geology of South Africa, Johannesburg/Council for Geoscience, Pg. 461 – 499.

Jones, A., Chave, A., Egbert, G., Auld, D., Bahr K., (1989). A comparison of techniques for magnetotelluric response function estimation, Journal of Geophysical Research, 94, Pg. 14,201–14,213.

Khoza, T.D., (2016). Magnetotelluric studies across the damara orogeny and Southern Congo craton. Unpublished PhD Thesis, University of the Witwatersrand and Dublin Institute of Advanced studies.

Krivochieva, S., Chouteau, M., (2002). Integrating TDEM and MT methods for characterization and delineation of the Santa Catarina aquifer (Chalco Sub-Basin, Mexico). Journal of applied geophysics 52 (2003), Pg. 23-43.

Kruseman, G.P., de Ridder, N.A., (1992). Analysis and Evaluation of Pumping Test Data. Second Edition. International Institute for Land Reclamation and Improvement. Wageningen. Netherlands.

Leketa, K.C., (2011). Flow characteristics of groundwater systems: An investigation of hydraulic parameters. Unpublished MSc Dissertation submitted to the Institute of groundwater studies, University of the Free State, Bloemfontein South Africa.

Mahanyele, P.J., (2010). Interpretation of airborne magnetic data over selected areas of Witbank coalfield, South Africa: An aid to mine planning. Unpublished MSc Dissertation submitted faculty of agricultural and natural science, University of Pretoria, Pretoria South Africa.

Makhokha, D., (2016). A systematic approach to the interpretation of conducting anomalies across intrusive dolerite dykes and sills in the Karoo Supergroup. Unpublished MSc Dissertation submitted to the Institute of groundwater studies, University of the Free State, Bloemfontein South Africa.

Malefane, L., (2016). Groundwater resource assessment for town water supply in Steynsrus in the Free State Province of South Africa. Unpublished MSc Dissertation submitted to the Institute of groundwater studies, University of the Free State, Bloemfontein South Africa.

Miensopust, M.P., (2011). Multidimensional magnetotellurics a 2D case study and a 3D approach to simultaneously invert for resistivity structure and distortion parameters. Unpublished Phd Thesis, National University of Ireland, Galway.

Milligan, P.R., Gunn, P.R., (1997). Enhancement and presentation of airborne geophysical data. Journal of Australian geology and Geophysics, Vol. 17(2), Pg. 63-75.

Mohamed, A.K., (2002). Application of magnetotelluric and transient electromagnetic methods in groundwater and engineering studies. Submitted for doctor of philosophy thesis.

Mokgatle, T., (2016). Assessment of groundwater resource in the Tsineng area, Northern Cape: a geophysical survey perspective. Unpublished MSc Dissertation submitted to the Institute of groundwater studies, University of the Free State, Bloemfontein South Africa.

Molaba, L.G., (2017). Investigating the possibility of targeting major dolerite intrusives to supplement Municipal water supply in Bloemfontein: a geophysical approach. Unpublished MSc Dissertation submitted to the Institute of groundwater studies, University of the Free State, Bloemfontein South Africa.

Mosavel, H., Cole, D., Chevallier L., 2016. Cenozoic Isopachs and Bedrock Topography near Beaufort West for drilling project ST- 2016-1250. CGS Report No 2016- 0132, Pg. 30.

Mosavel, H., Cole, D., (2017). Report from the drilling of five shallow percussion boreholes in the Beaufort West Municipality area. in unpublished Counci for Geoscience report. Number 2017-0190, Pg. 62.

Naidu, G.D., (2012). Deep crustal structure of the Son-Narmada-Tapti Lineament, Central India. Springer Theses, DOI: 10.10007/978-3-642-28442-7_2.

Nhleko, O.L., (2008). Implications of the geological structure of the Qoqodala dolerite ring complex for groundwater dynamics. Unpublished MSc Dissertation submitted to the Department of earth science, Faculty of natural science, University of the Western Cape, Cape Town, South Africa.

Nhleko, L., Dondo, C., (2008). The hydrogeology of the Beaufort West. Report no. 2008-0050. Project no. ST-2008-0974.

Nimmo, J.R., Healey, R.W., Stonestrom, D.A., (2005). Aquifer Recharge, in Anderson, M.G., and Bear, J., eds., Encyclopedia of Hydrological Science: Part 13. Groundwater: Chichester, UK, Wiley, v. 4, Pg. 2229-2246, doi:10.1002/0470848944.hsa161a.

Nimmo, J., Stonestrom, D.A., Healy, R.W., (2008) Aquifers: Recharge, Encyclopedia of Water Science, DOI: 10.1081/E-EWS2-120010040.

Nyathi, N., (2014). Stratigraphy, sedimentary facies and diagenesis of the Ecca Group, Karoo Supergroup in the Eastern Cape, South Africa.

Nxokwana, N., Musetsho, M., Mosavel, H., Daniels, W., (2018a). Karoo deep drilling and geo-environmental baseline. Council for Geoscience. Number 2012-0202. Pg. 68.

Nxokwana, N., Cole, D., Mosavel, H., Mahlatji, M., Lenong, S., Ngobeni, D., (2018b). Karoo deep drilling program: 2018-19 Q1 & Q2 quarterly report. In unpublished Council for Geoscience report. Number 2012-0140, Pg. 354.

Pacome, A.D., (2010). Fracture characterization of Karoo Aquifers. Unpublished MSc Dissertation submitted to the Institute of groundwater studies, University of the Free State, Bloemfontein South Africa.

Planke, S., Svensen, H., Myklebust, R., Bannister, S., Manton, B., Lorenz, L., (2014). Geophysics and remote sensing. In: Breitkreuz C., Rocchi S. (eds) Physical Geology of Shallow Magmatic Systems. Advances in Volcanology (An Official Book Series of the International Association of Volcanology and Chemistry of the Earth's Interior). Springer,

Reynolds, J. M., (2011). An introduction to applied and environmental geophysics. Second edition. The Atrium, Southern Gate, Chichester, West Sussex. John Wiley and sons, Pg. 696.

Richardson S.H. (1984): Sr, Nd and O isotope variation in an extensive Karoo dolerite sheet, Southern Namibia. In: A.J. Erlank (Ed), Petrogenesis of the volcanic rocks of the Karoo Province. Geol. Soc. South Afr. Spec. Publ., No 13, Pg. 289-293.

Rosewarne, P., Woodford, A., Goes, M., Talma, S., O'Brien, R., Tredoux, G., Esterhuyse, C., van Tonder, G., Visser, D., (2003). Recent developments in understanding of Karoo aquifers and the deeper underlying formations. Groundwater: A New Paradigm.

Rosewarne, P.N., Woodford, A.C., O'Brien, R., van Tonder, G., Goes, M., Talma, A.S., Tredoux, G., Visser, D., (2013). Karoo Groundwater Atlas volume 2.

Rubidge, B.S., Erwin, D.H., Ramezani, J., Bowring, S.A. and De klerk, W.J., (2013). High-precision temporal calibration of late Permian vertebrate biostratigraphy: U-Pb zircon constraints from the Karoo Supergroup, South Africa. Geology, Vol. 41, Pg. 363 – 366.

Sakala, E., Sekiba, M., (2017). National hydrogeological and water quality mapping: exploratory borehole sitting in the shire basin using geophysical methods. In unpublished Council for geoscience report. Number 2017-0125.

Scheiber-Enslin, S.E., Webb, S.J., Ebbing, J., (2014). Geophysically plumbing the main Karoo Basin South Africa. South African Journal of Geology. Vol 117.2, Pg. 275 -300.

Smith, R.M.H., (1990). A review of stratigraphy and sedimentary envirnements of the Karoo Basin of South Africa. Journal of African Earth Sciences. Vol. 10, Pg. 117-137.

Steyl, G., van Tonder, G.J., (2013). Hydrochemical and hydrogeological impact of hydraulic fracturing in the Karoo, South Africa. Dr. Rob Jeffrey (Ed), InTech, DOI: 10.5772/ 56310. Available from: http://www.intechopen.com/books/effective-and-sustainable-hydraulic-fracturing/hydrochemical-and-hydrogeolocal-impact-of-hydraulic-fracturing-in-the-karoo-south-africa.

Svensen, H., Planke, S., Chevallier, L., Malthe-Sorenssen, A., Corfu, F., Jamtveit, B., (2007). Hydrothermal venting of greenhouse gases triggering Early Jurassic global warming. Earth Planet. Sci. Lett. 256, Pg. 554–566.

Svensen, H., Corfu, F., Polteau S., Hammer, Ø., Planke, S., (2012). Rapid magma emplacement in the Karoo Large Igneous Province. Earth and Planetary Science Letters 325–326 1–9.

Tessema, A., Chirenje, E., Sekiba, M., Sethobya, R. M., (2010). The Relationship between Lineaments density and Borehole yield in the Northwest Province: Results from Geophysical Studies. Council for Geoscience. Number 2010-0051. Pg. 101.

Turner, B. R., (1981). Revised stratigraphy of the Beaufort Group in the southern Karoo Basin. Palaeont, afr., Pg. 24.

Van Tonder, G.J., Kirchner, J., (1990). Estimation of natural groundwater recharge in the Karoo Aquifers of South Africa. Journal of hydrology, vol 121, Pg. 395-419.

Van Wyk, Y., (2010). Transport mechanisms of uranium and thorium in fractured rock aquifers. Unpublished MSc Dissertation submitted faculty of agricultural and natural science, University of Pretoria, Pretoria South Africa

Van Wyk, Y., Withueser, K., (2011). A force-gradient tracer test on the Hansrivier Dyke: Beaufort West, South Africa. Water South Africa Vol. 37 No. 4.

Vereecken, H., Kemna, A., Münch, H.M., Tillmann, A., Verweerd, A., (2005). Aquifer characterization by geophysical methods. In M. G. Anderson (eds), Enclypedia of hydrological sciences. Chapter 148.

Vermeleun, P.D., (2012). A South African perspective on shale gas hydraulic fracturing. In: C.D. McCullough, L.A. Lund and L. Wyse (eds), International Mine Water Association Annual Conference, Institute for Groundwater Studies, University of the Free State, Bloemfontein South Africa, 2012, Pg. 149 – 146.

Vozoff, K., (1990). Magnetotelluric: Principles and Practice. Proc. Indian Acad. Sci. (Earth Planet. Sci.), Vol. 99, No 4, Pg. 441 – 471.

White R.S. (1997): Mantle plume origin for the Karoo and Ventersdorp flood basalts, South Africa. S.Afr.J.Geol., 100 (4), Pg. 271 - 282.

Woodford, A.C., Chevallier, L., (2002a). Regional characterization and mapping of Karoo Fractured aquifer systems – an integrated approach using geographical information system and digital image. WRC report no. 653/1/02.

Woodford, A.C., Chevallier, L., (2002b). Hydrogeology of the Main Karoo Basin: current knowledge and future research needs. WRC report no. TT 179/02.

ABSTRACT

A geoscientific research project of which the current study forms part is underway in the Karoo Basin, near Beaufort West in the Western Cape, South Africa. The aim of the research is to better understand the potential impact of the geo-resource exploration activities on the Western Karoo Basin. The current study strongly emphasis the use of airborne and deep-probing magnetotelluric (MT) geophysical techniques to better understand geological structures and deep aquifer systems. The need to understand the deeper aquifer systems arose from the possibility of shale gas exploration in the Main Karoo Basin.

The high resolution airborne magnetic survey was undertaken in order to upgrade the geology map and reveal the presence of hidden geological features such as dolerite (dykes or sills), faults or other magnetic lineaments. The results showed that magnetic method can play a significant role in generating groundwater targets. The total magnetic field showed positive anomalies that exceed the local magnetic field of the area as recognised by a steep gradient, while negative anomalies are below the local magnetic fields. The high-resolution data clearly mapped dykes, sills, faults, geological contacts and intrusive bodies. These lineaments could be an indication of foliation in the area in response to shearing. The development of the foliation within the Beaufort Group sediments is restricted to the finer grained sandstone, mudrock and siltstone.

Magnetotelluric results suggested that the very high resistive layers that appear to have been intruded within the slightly conductive zone might be associated with dolerites. The displacement of a conductive zone around distance 2200 m and 5000 m might be an indication of faulting. The resistive substratum reaching a depth of around 2000 m to the east and the inclined resistive layer might be an indication of dolerite sill and dyke respectively. Based on this results it may be fair to note that magnetotelluric method is a non-intrusive tool that played a major role in obtaining information of the subsurface at great depth.

The 2D magnetic modelling confirms the resistive layer observed in MT inversion model might be related to dolerite. The results shows the magmatic feature with susceptibility value of around 0.012981 SI might represent a slight vertically inclined dolerite to the center at distance ranging between 2 km and 4 km, while to the west and east of the profile appears to be horizontal. These structures may have been connected during their previous formations, as can be seen that it might have been disrupted due to present day erosion. The Poortjie Member might have been heavily intruded, whereas the Ecca and Dwyka Groups appear to be suppressed. These intrusive bodies have been covered by younger alluvial. These results enhance the knowledge that aquifers within the Karoo may be occurring beneath the well-studied depth.

Two monitoring boreholes (R01-BW and R02-BW) were drilled to a depth 1402 m and 516 m respectively. The boreholes were drilled at a larger distance (± 20 km) from the magnetotelluric traverse, due to the electromagnetic highly influenced by DC powered railway which is near the boreholes site. Magnetotelluric results may not be constrained with confidence with the borehole information due to the larger distance separation. Drilling of the boreholes was aimed on determining the lithology and stratigraphy of the Beaufort Group and underlying Ecca Group, and the properties of shallow groundwater. Borehole R01-BW drilled to a depth of 1402 m intersected from surface downwards shale and sandstone, 57 m thick, of the Poortjie Member (Middleton Formation), siltstone, shale and sandstone, 677 m thick, of the Abrahamskraal Formation, sandstone, siltstone and shale, 169 m thick of the Waterford Formation, and siltstone and shale, 483 m thick, of the Tierberg Formation. Dolerites 16 m and 2 m thick, intrude the Abrahamskraal Formation. Borehole R02-BW drilled to a depth of 516 m intersected from surface downwards sandstone, siltstone and subordinate shale, 64 m thick, of the Poortjie Member (Middleton Formation), and sandstone, siltstone and shale, 434 m thick, of the Abrahamskraal Formation. A dolerite 17 m thick, intrudes the Abrahamskraal Formation.

Due to the challenge of interpreting rock chips during geological logging as may be mixed during drilling, the downhole geophysical was conducted on the two monitoring boreholes in order to obtain in-situ geotechnical and structural information. Borehole R01-BW gave a good correlation with the identification of dolerite at depth between 489 and 508 m. a great assistance can be observed at depth between 690 and 692, where the geophysical identified dolerite which was missed by geological logging. Borehole R02-BW, the identification of dolerite at depth between 159.5 and 176.5 m gave a good correlation with the geological log. Geophysical log may have identified sandstone below depth 186 m, but without good correlation from the geological.

The positions of the two monitoring boreholes were removed by a large distance from the positions of the magnetotelluric survey. Although the combined use of airborne and ground geophysical surveys was of a great assistance in understanding the subsurface geological and geohydrological conditions, the information obtained from the boreholes cannot be used with confidence to constrain the geophysical interpretation. Considering this and also the ambiguity and none uniqueness in geophysical interpretation, it is therefore highly recommended that geophysical results be constrained through drilling

Appendices

Appendix A: Lithology log for Borehole R01-BW

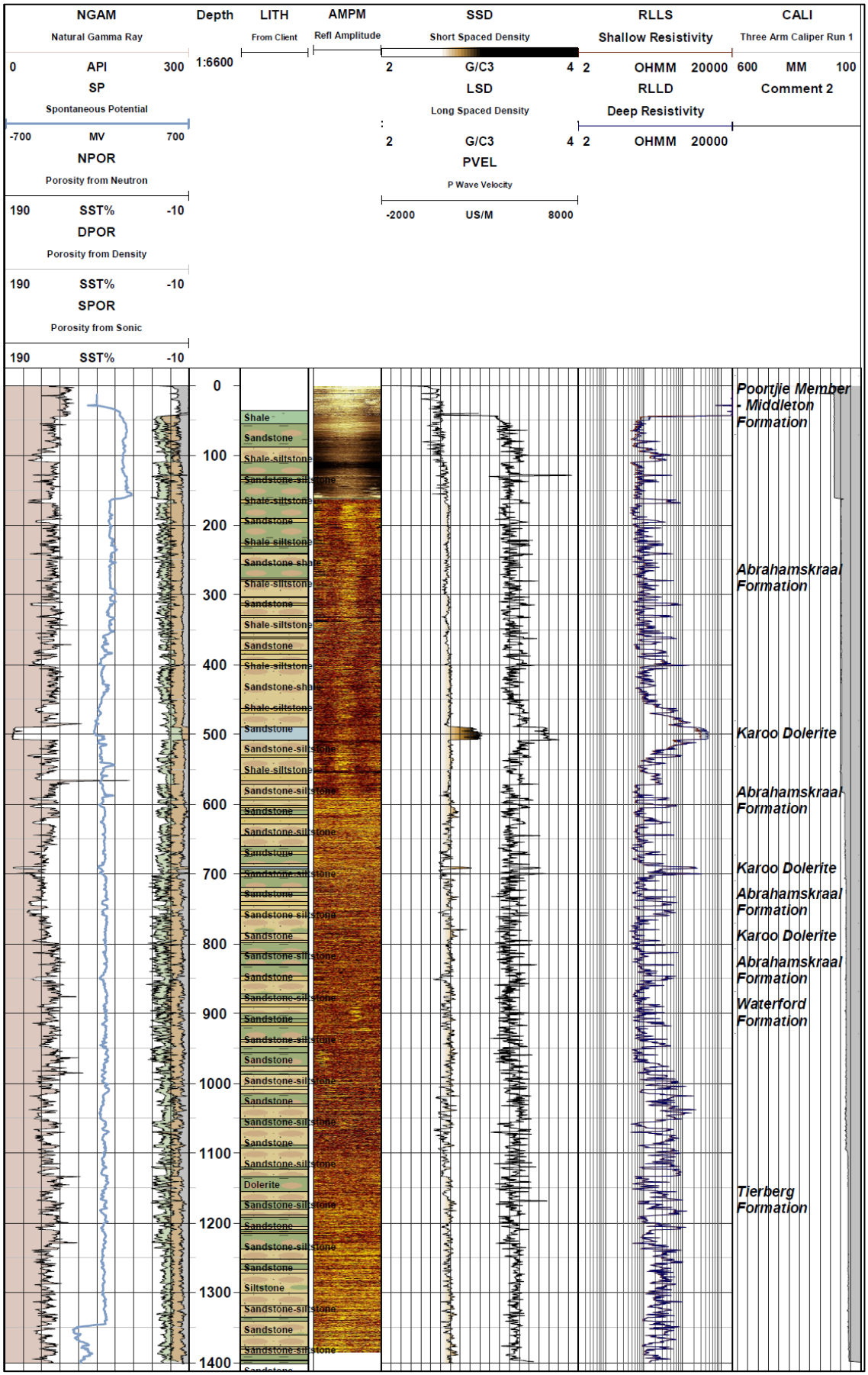

Appendix B: Structure log for borehole R01-BW

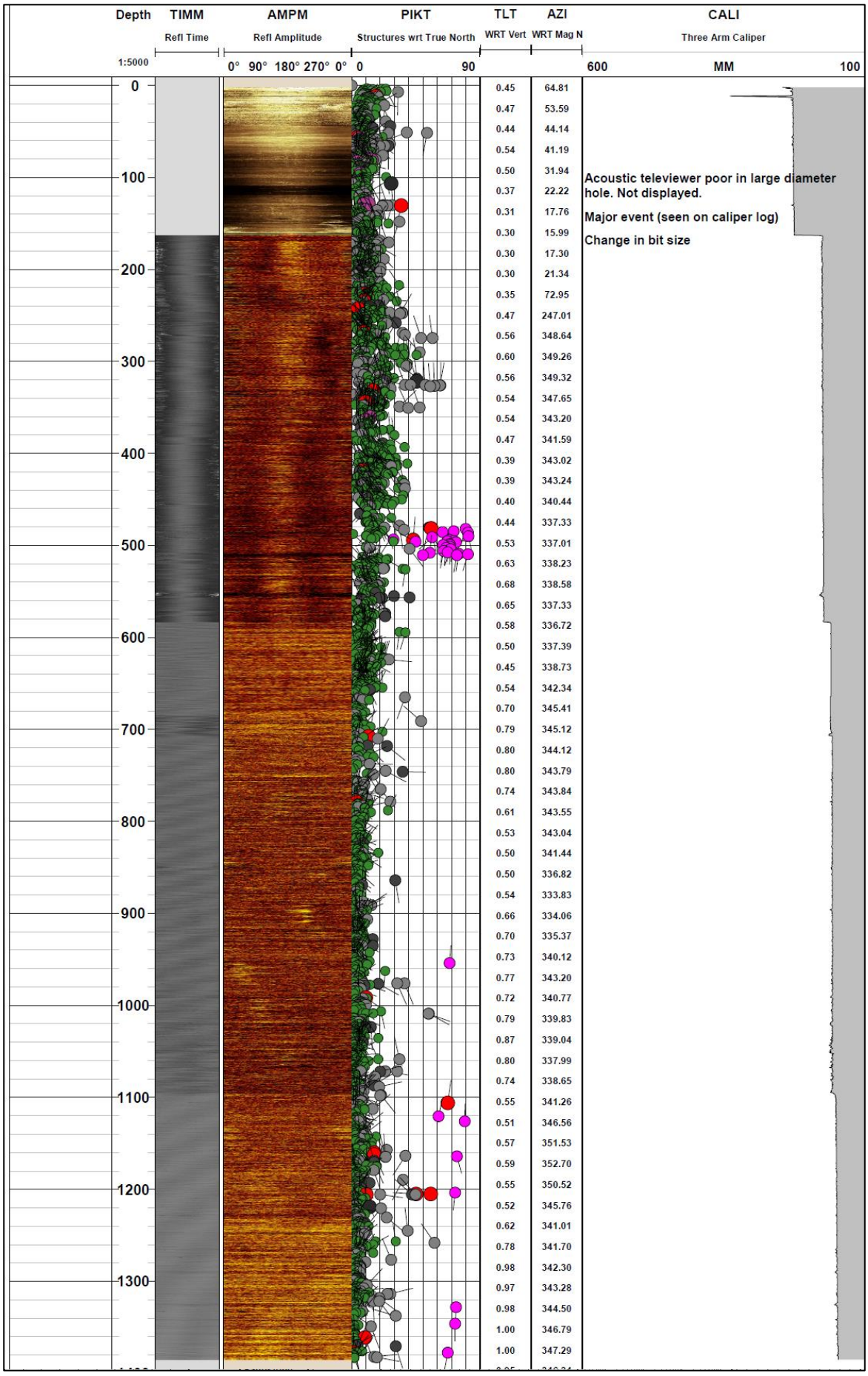

Appendix C: Hydrology log for borehole R01-BW

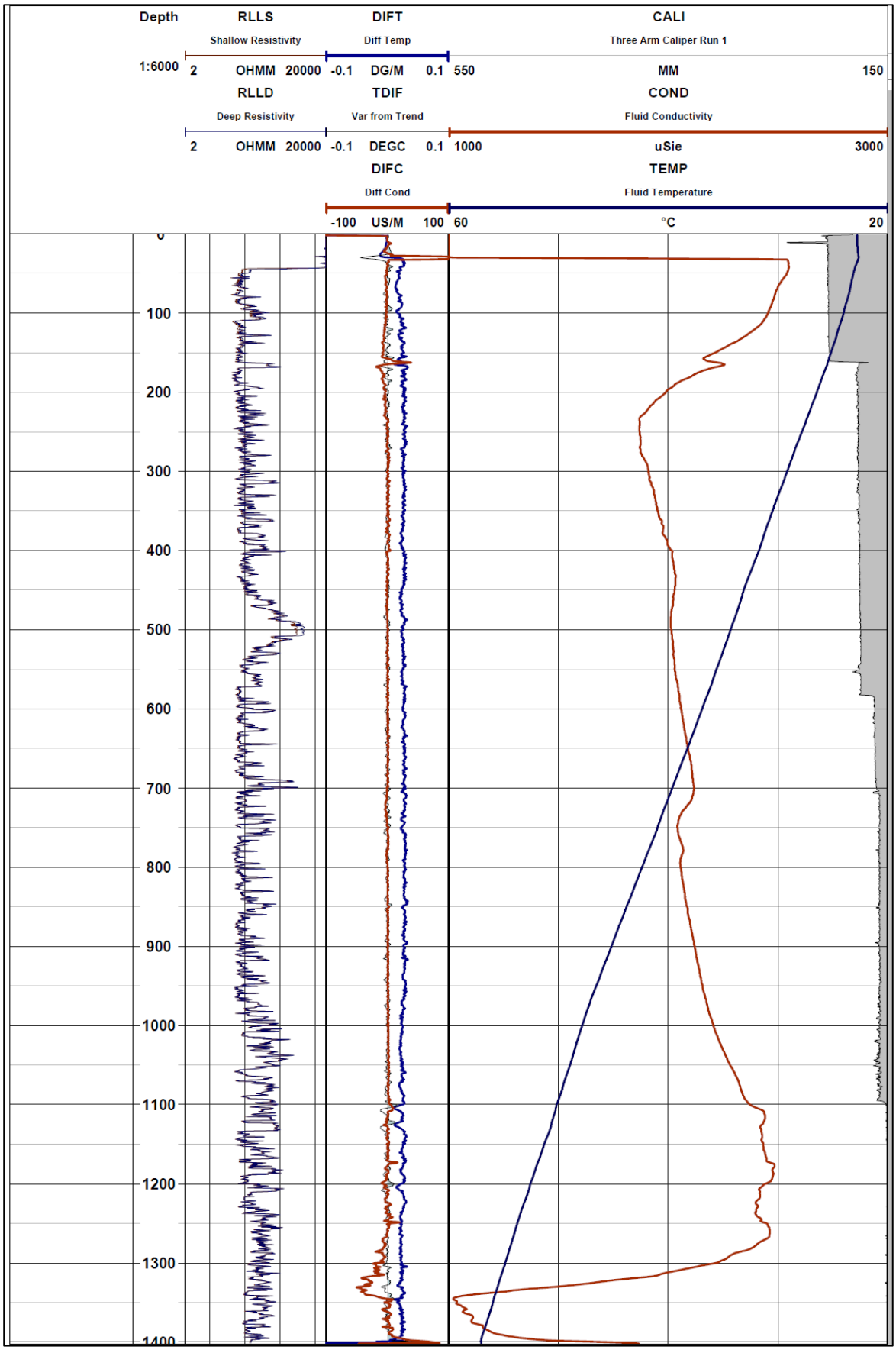

Appendix D: Lithology log for borehole R02-BW

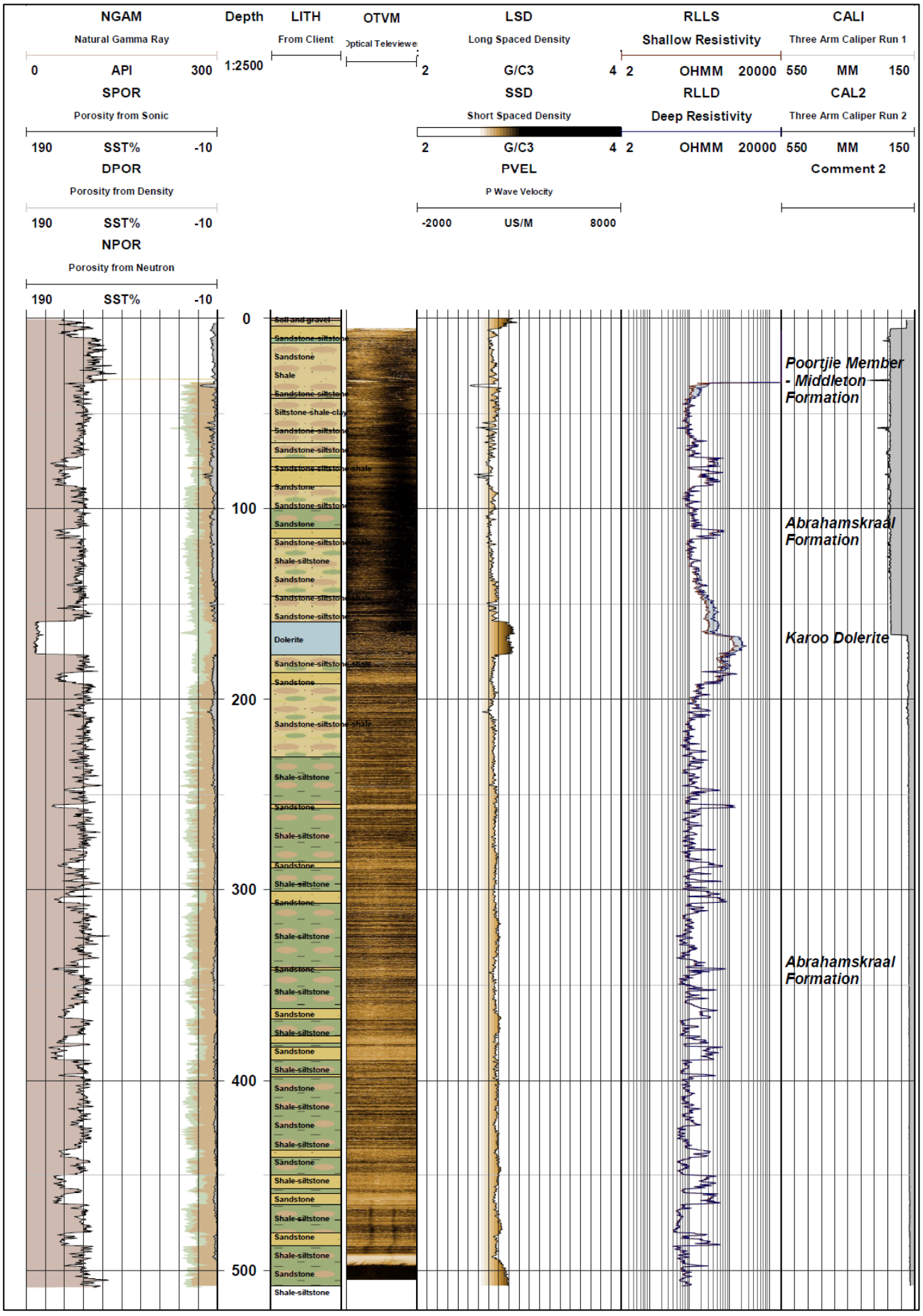

Appendix E: Structure log for borehole R02-BW

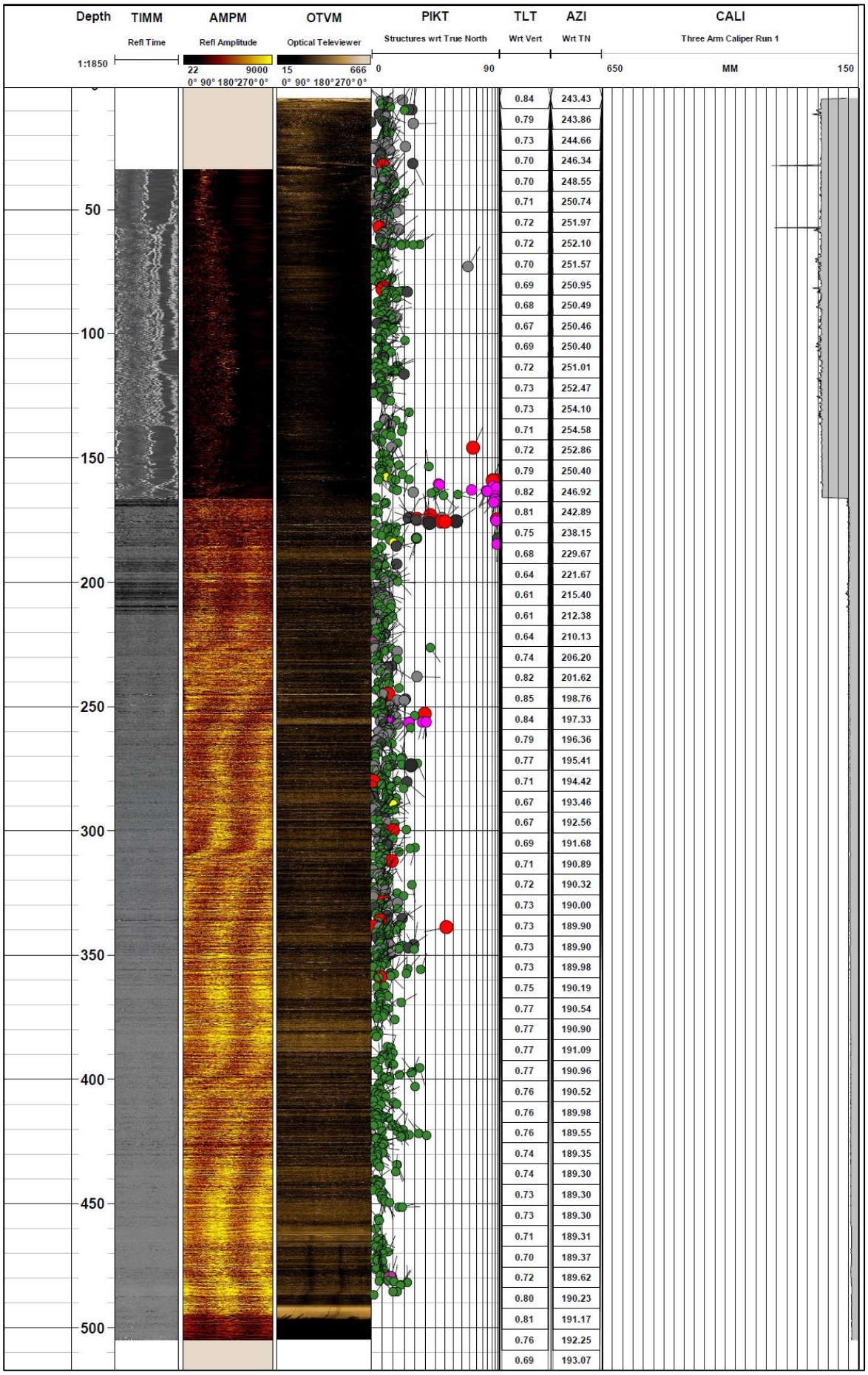

Appendix F: Hydrogeological log for borehole R02-BW